ANNEXURE –VIII

PROFORMA FOR SUBMISSION OF INFORMATION AT THE TIME OF SENDING THE FINAL REPORT OF THE WORK DONE ON THE PROJECT

1.	Name and Address of the Principal Investigator	:	Dr.G.Madhurambal Associate Professor of Chemistry, A.D.M.College for Women, (Autonomous) Nagapattinam.
2.	Name and Address of the Institution	:	A.D.M.College for Women, (Autonomous) Nagapattinam.
3.	UGC Approval No. and Date	:	F.No.38-2/2009(SR)
4.	Date of Implementation	:	February 2010
5.	Tenure of the Project	:	Three Years
6.	Total Grant Allocated	:	Rs.13,55,800/-
7.	Total Grant Received	:	
8.	Final Expenditure	:	Rs. 13,56,100/-
9.	Title of the Project	:	"Isolation and Characterization of bioactive Metabolities from the medicinal plant tribulus terrestris and its therapeutic activity on nephrolothesis and urolothesis"
10.	Objectives of theProject	:	Annexure – (a)
11.	Whether Objectives were achieved	:	Yes, the Objectives were achieved. Annexure – (b)

12. Achievements from the Project : Annexure – (c)

13. Summary of the Findings (in 500 words): Annexure – (d)

14. Contribution to the Society
(Give Details) :

15. Whether any Ph.D enrolled/Produced : Yes. The Co-Investigator
Out of the Project Mrs.N.Prabha submitted the thesis.

16. No.of Publications out of the project : Three

(Principal Investigator) (Registrar / Principal)

(Co – Investigator)

ANNEXURE – a

OBJECTIVES OF THE PROJECT

The development of bio-technological techniques and medicinal inquisitiveness, drive the interest towards the field of biological crystals. The increasing incidents of renal calculi and the current interest in treating without surgery urged to considerable research. Cystein, Calcium Oxalate mono hydrate, Octa calcium phosphate, Ammonium Magnesium Phosphate hexa hydrate, Uric acid are known to occur often as constituents of urinary stones. The methodological research relating to the food habits for the formation of various types of urinary stones leads a better way to investigate the medicines.

Many parameters influence nucleation and growth of urinary stones. The stones in the kidney or the bladder of vata origin, because the vitiation of vayu leads to the accumulation of bio-chemical substances around the nucleus of urinary salts, which take the shape of stones. The systematic investigation of the food habits, life cycle and tospography relating to the formation of various types of urinary stones are surveyed. The study of constituents of urinary stones along with the food habits is carried out. The phytochemical investigation of the plant extract and the inhibitor effect of the metabolites for the nephrolothesis and urolothesis were investigated. The study has aided to develop suitable medicinal forms of ayurvedic doctrine suggestions.

ANNEXURE –b

WHETHER OBJECTIVES WERE ACHIEVED

Objectives	Research and Design	Work done and Achievement activities schedule	Publication
I YEAR 1.The systematic investigation of the food habits life cycle topography relating to various stone formation survey.	Questionnaire was prepared and given to two different region Chennai and Thanjavur. The study was made in different hospitals. The data was collected from the patients' survey.	Statistical Correlation on the epidemiological study was carried out based on the Questionnaire collected and fruitful conclusions were achieved and elaborate discussion was in chapter I	1. Epidemiology of Urinary Stones, IEEE-ICAESM, 2012, 146-151. 2. Epidemology of kidney stones – an attempt to discuss in terms of Mathematical Epidemic Modelling, IJCET, Vol.I(1) Jan-2013, 98-105.
2. The Collected stones from the patients were characterized.	10 samples were characterized by Qualitative analysis, ICP,UV,FTIR, XRPD,SEM,DSC analysis.	The type of stones were investigated from the analysis and it was concluded that most of the stones were the variety of mixed stones of COM, COD and Hydroxy apatite crystals. Cystine and Xanthine variety of crystals was not found.	3. Thermal, UV, FTIR and XRD studies of Urinary Stones, J. Thermal Analysis and Calorimetry, Vol.112, No.2 (2013), 1067-1075.
II YEAR 3. The medicinal plant was collected and all fractions were extracted. The perseverated was investigated by	As the plant is a seasonal grown plant and this will be available only during winter season, the plant is collected; air dried	The following metabolities Glycoside,Saponins, Phenolic compound and Tannins. The constituents were separated and the	

its physical and chemical constituents. The Chemical analysis was undertaken for its constitution.	and extracted with ethanol and phytochemical investigation was done by TLC, GCMS and NMR spectroscopy. The analysis and as well as separation was done by TLC for its constitution.	individual constituents were named.	
III YEAR 4.The effect of added plant extract on the decrystallisation of urinary stones was studied.	The crystals are grown in vitro by Gel method. Calcium oxalate dihydrate, Hydroxy apatite, Cystine and Xanthine crystals are grown in the U-tube by gel method and characterization was done by UV,FTIR,NMR analysis. The individual constituents were added in different concentration and the ability to dissolve the stones was tested.	All the constituents were added and the order of dissolving capacity of the different constituents were investigated by the dissolve in length of the crystal column and it was found that saponins are very good solvent for the all types of crystals. Hence using the saponins the drug design can be formulated.	

ANNEXURE – c

ACHIEVEMENTS FROM THE PROJECT

1.From the Epidemology study of kidney stones, the stones are more common in men than in women. Stone formation in renal systems in one of the oldest and the most common form of crystal deposition. Populations that consume diets rich in animal protein have a higher risk of stones than those with a more vegetarian diet. The risk of forming a stone is increased further by a high intake of refined sugar, salt and oxalate-rich foods. Living and working in a hot environment or engaging in regular vigorous exercise can increase the risk of forming stones by decreasing urine volume as a result of dehydration from sweating. Obesity results in increased urinary excretion of stone formation. Forty six samples are collected from various Hospitals with survey of various factors in the form of questionnaire from the patients. From the questionnaire, a detailed statistical study on the Epidemiology of the kidney stones. The study is based on the on the basis of Age, Symptoms, Food habits, Occupation, Obesity, Sexual correlation and Recurrence is discussed with in the study. Stones are removed surgically, ureterscopy and 'crushing and evacuation' method. Though a large number of crystals are collected, only ten samples are measurable in size due to surgical operation and the rest of them are removal by laparoscopy. The seasonal variation plays an important role in the formation of kidney stones.

2. From the chemical analysis of kidney stones only the mixed variety of COD,COM and Hydroxy apatite with elements like Si, Al, Fe, etc.,are seen in the stones. This may be due to the intake of food prepare through utensils and hence the aluminum usage may be avoided.

3. The plant Tribulus terrestris is a seasonal plant and grown only in rainy and winter season and the plant extract in ethanol may be separated and its constituents are preserved for its potency.

Phytochemical investigation of Tribulus terrestris was done by TLC,GCMS and NMR. Glycoside,Saponins,Phenolic compound and Tannins fractions are found to be pure.

The total work was classified into the following Chapters.

CHAPTER - 1

EPIDEMIOLOGY OF URINARY STONES

INTRODUCTION

Disease of renal calculi is known to be one of the oldest, diseases leading to hospitalization and surgery. In India it affects nearly 2 million people every year and the life time risk is about 20% in those having this disorder. Northern part of India is defined as the stone forming belt and the incidence is low in Southern part. In 1980, the percentage of population, which had the incidence of stones in USA, Sweden, Germany, Italy and UK was found to be 12.0, 9.5,6.8, 3.1 and 1.5 respectively. In the United States the probability of formation of the renal calculi in the adult population is 2%. The pediatric problem of bladder stone was found to be a continuous problem in Southeast Asia. Urolithiasis is found to be a multifactor disorder, among the fluid intake, geographical location, climate etc., In many countries, the geographical distribution of renal calculi is uneven. So a precise knowledge of the epidemiological factors and composition of the urinary stones with respect to the geographical location is essential for suggesting a better method of treatment and also to avoid the factors which could influence their recurrence.

Regarding costs, urinary stone disease is increasingly treated on an outpatient basis; the number of inpatient discharges for a diagnosis of urolithiasis has been declining gradually. Nevertheless, in 2007, the Nationwide inpatient sample recorded 155,860 urinary stone inpatient discharges. The actual cost for treatment of urinary stone disease would probably be several orders of magnitude greater if outpatient procedures were included. Proper acute and long-term management of such patients is therefore essential.

There is no recent epidemiological study from Chennai city and old Thanjavur district area. In order to have an idea of the prevalence of the stone disease in Chennai and Thanjavur district an investigation was made on the patients who were admitted for the treatment of urinary calculus disease in Stanley

Medical College Chennai and SP Hospital Thanjavur with survey of various factors in the form of questionnaire. The work presented here is a consolidated report of the data collected during March 2010 to January 2011.

DATA COLLECTION

There are no population based data on the incidence or prevalence of kidney stones in Tamil nadu. Estimates of the incidence of first kidney stones between the ages of 30 and 70 years vary between approximately 100-300/100000/year in men and 50-100/100000/year in women.[1-4] Overall, the prevalence of kidney stones is approximately 6-9% in men and 3-4% in women and this appears to be increasing.[2-7]

In the study, a series of 46 cases of urinary stone disease was documented. By analyzing the case histories, the distribution of stone incidence in different sex, age and occupation was studied. The symptoms, food habits, heredity and recurrence of the disease in each patient were noted. The details the stones such as location of the stones, mode of stone removal, and number of stones, size and weight of the stones, colour and appearance of surface of the stones were observed. These are tabulated in Table.1

TABLE.1 Data Collection for Patients

Case	Sex	Age	Occupation	Symptoms	Duration of symptoms	Recurrence
1	M	36	Coolie	Loin Pain	6 Months	-
2	M	42	Coolie	Irritation	2 Months	-
3	M	39	Coolie	Loin Pain	4 Months	-
4	M	65	Coolie	Irritation	8 Months	-
5	M	45	Coolie	Irritation	1 Year	-
6	M	50	Coolie	Loin Pain	8 Months	1
7	M	36	Coolie	Irritation	6 Months	-
8	M	39	Coolie	Irritation	4 Months	-
9	M	48	Coolie	Irritation	5 Months	-
10	M	42	Coolie	Loin Pain	3 Months	-
11	M	38	Coolie	Irritation	6 Months	-
12	M	40	Coolie	Irritation	2 Months	-
13	M	38	Coolie	Irritation	4 Months	-
14	M	39	Coolie	Irritation	6 Months	-
15	M	41	Coolie	Irritation	4 Months	-
16	M	36	Coolie	Irritation	8 Months	-
17	M	45	Coolie	Loin Pain	8 Months	-
18	M	36	Coolie	Loin Pain	1 Year	-
19	F	42	Coolie	Irritation	1 and half Years	-
20	F	65	Coolie	Loin Pain	9 Months	-
21	M	38	Farmer	Irritation	1 Year	-
22	M	46	Farmer	Irritation	8 Months	-

Case	Sex	Age	Occupation	Symptoms	Duration of symptoms	Recurrence
23	M	56	Farmer	Loin Pain	6 Months	-
24	M	48	Farmer	Irritation	1 Year	-
25	M	52	Farmer	Loin Pain	7 Months	-
26	M	37	Clerk	Irritation	1 Year	-
27	M	56	Typist	Loin Pain	1 Year	-
28	F	39	Junior Assistant	Loin Pain	8 Months	-
29	M	42	Driver	Irritation	8 Months	-
30	F	40	Business	Loin Pain	9 Months	-
31	M	36	Business	Irritation	1 Year	-
32	M	43	Business	Irritation	8 Months	-
33	M	52	Business	Irritation	4 Months	-
34	M	46	Business	Irritation	6 Months	-
35	F	35	House Wife	Loin Pain	4 Months	-
36	F	36	House Wife	Irritation	6 Months	-
37	F	52	House Wife	Irritation	8 Months	1
38	F	47	House Wife	Loin Pain	2 Months	-
39	F	50	House Wife	Loin Pain	9 Months	-
40	F	49	House Wife	Irritation	7 Months	-
41	F	37	House Wife	Irritation	8 Months	-
42	F	49	House Wife	Loin Pain	9 Months	-
43	F	47	House Wife	Loin Pain	1 Year	-
44	F	10	Student	Irritation	6 Months	-
45	M	14	Student	Irritation	4 Months	-
46	M	58	Coolie	Irritation	1 Year	-

The details of the analyses are as described below.

SEX

Men are at greatest risk of developing kidney stones with incidence and prevalence rates between two and four times that of women.[2,3] The ratio has decreased from 3:1 male to female predominance to less than 1.3:1 and this is due in part to lower testosterone levels providing protection for women and children against developing oxalate stones, as testosterone may increase hepatic oxalate production.

A 15 year retrospective study by Baker et al.[8] found that the peak age for the development of calcium oxalate stones was between 50 and 60 years. Men were at greater risk of producing Calcium oxalate stones and uric acid stones. Women were at greater risk of infection stones. In a separate study by Gault and Chafe in Canada, women were also found to be more likely to produce calcium phosphate stones than men.[9]

Our analysis of the distribution of the disease in different sex has shown that, out of the 46 cases, 70% were males and 30% were females. The diagram is shown in Figure.1

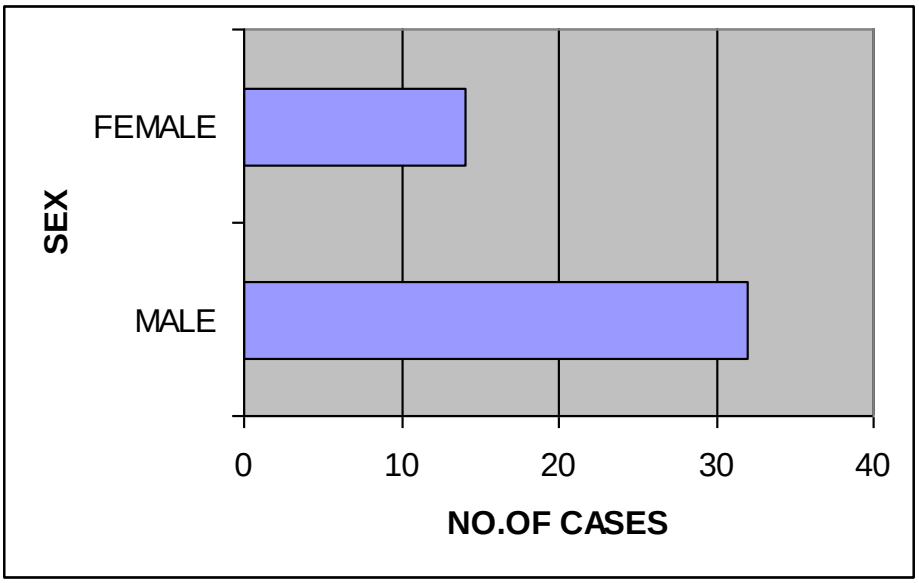

FIGURE.1 SEX RATIO

AGE

The histogram shows the distribution of the disease in different age groups are shown in figure.2

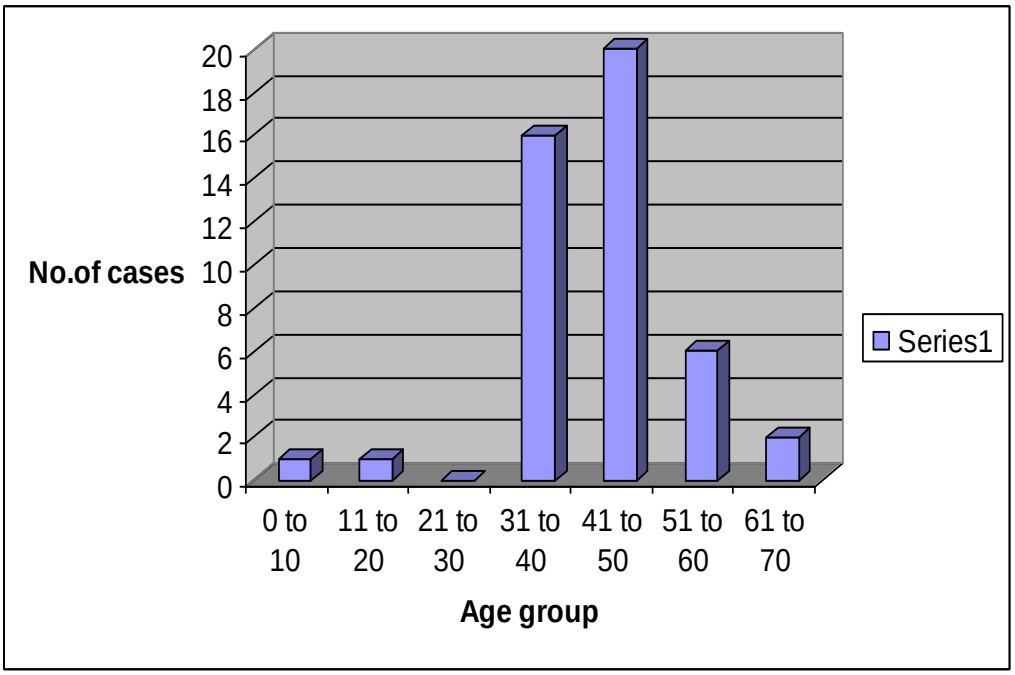

FIGURE.2 AGE GROUP

The incidence of urinary calculus was high between 41-50 age group. Next to this, the incidence was found to be high in the age group 31-40 and 51-60. The incidence was lowest among children (below 10 years) and was less in elders (above 60 years). The eldest in the series was one male and one female patient of age 65 years and the youngest was a girl of 10 years. Sex distribution in different age groups is shown in the histogram from figure from which it is clear that the incidence of stone disease is high in both sex between the age group of 41-50.

Our study in Tamil Nadu population is based on cohort study. An underlying contributing factor was found in 70% of men presenting with their kidney stone (inflammatory bowel disease 30%, hyperthyroidism 20%, hyperparathyroidism 2%, urinary tract infection 10% and prolonged immobilization 8%). In a study of women, 30% had a potentially contributing medical condition including urinary tract infection at the time of stone formation or

stone due to urinary infection (20%), hyperthyroidism (7%), inflammatory bowel disease (2%) and hyperparathyroidism (1%).

OCCUPATION

Sedentary occupations, including professional and managerial groups, are associated with a higher incidence of urinary calculi than manual jobs. Stress is also associated with stone disease.

Occupation is categorized into active (coolie, farmer, driver, businessman, housewife and Student) and sedentary are tabulated in Table.2.

TABLE.2 Occupation of the Patients

Occupation	Coolie	Farmer	Officer	Driver	Business	House wife	Student
No. of cases	21	5	3	1	5	9	2

The present study shows that all the patients are physically active, shown in figure.3

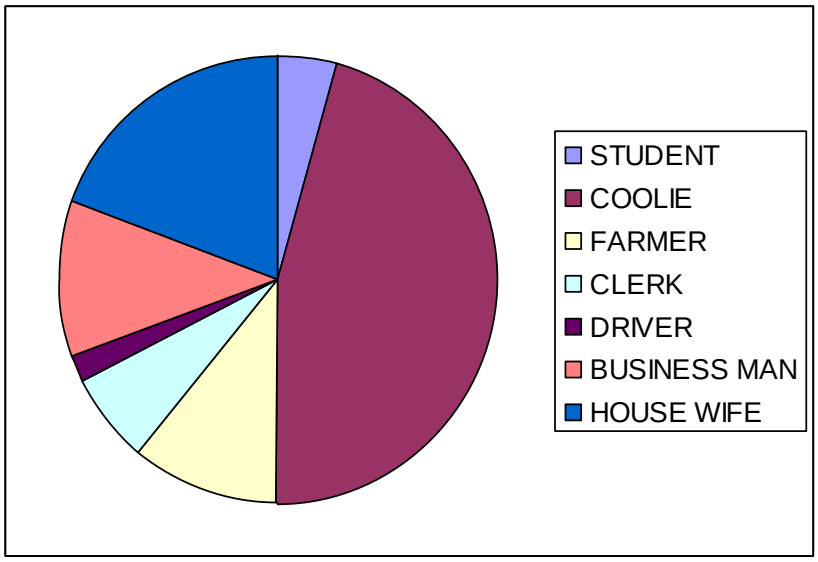

FIGURE.3 OCCUPATION

SYMPTOMS AND DURATION OF THE SYMPTOMS

In our study 63 % of the patients had the symptom of Loin Pain. Many patients had irritation, difficulty and pain while passing urine are shown in figure.4.

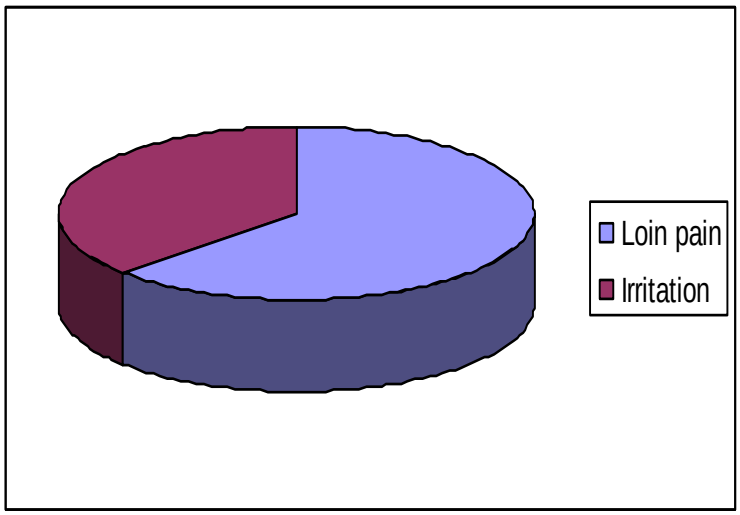

FIGURE.4 SYMPTOMS

Some had the problem of vomiting, fever, suffocation and hematuria. The average time of onset of the symptom to the time of treatment varied from within a day to last twenty years.

REMOVAL AND OBSERVATION OF THE STONES

Stones were collected from twenty cases 46% of the patient's stones in kidney, 32% in ureter and the remaining had bladder stone. One uretric stone was passed spontaneously and another uretric stone was removed by laparoscopy. In 36 cases with bladder stones, 'crushing and evacuation' method was adopted for the stone removal. The remaining ten stones were removed 'surgically'. 80% of the patient's single stone 19% had multi stones. One male patient of 28 years had stone (with sizes varying from 0.4x1x1 cm^3 to pinhead), who had his previous stones a two years back and was removed laparoscopy.

Most of the kidney stones with greater size than 1x1x1 cm^3 of kidney stones weight of the stones varied from 100 mg. to 150g. A 46 years old female patient had a biggest stone of size 6.5x4x5.5 cm^3 and weight 120g. It was a bladder stone of struvite composition

Calcium oxalate monohydrate stones were black or dark brown in colour. On the other hand, calcium dihydrates stones were light brown in colour. Calcium oxalate monohydrate kidney stones of different sizes. All the three calculi showed different external morphologies viz., the nodular surface morphology, the smooth surfaced stag horn morphology and irregular surface morphology. The cross section of a calcium oxalate monohydrate stone with radial stariation. It also shows the concentric laminations of different colours from centre to the periphery with a central nucleus. Two calcium oxalate dihydrate stone with rough surface.

Mixed composition of calcium oxalate and calcium phosphate stone with a smooth surface. Majority of the mixed (calcium oxalate and calcium phosphate) An exception of this kidney stones with highly polished surface and with some projections over the surface the cross section of two calcium oxalate and calcium phosphate mixed stones showed very different patterns one with a layered appearance with an inner linear cavity and another with an irregular pattern with a central nucleus.

A prospective study of 45,289 men in the United Stated failed to find an increased incidence of kidney stones over a 6 year period in the hotter south-eastern states; however, the prevalence of stones at baseline was higher in these states. This indicates that there was a modest increase in the risk of kidney stones in the hotter regions. Other studies performed in the United States and Isreal have indicated that the incidence of stone disease increases both in the hotter areas of the country and during the hottest months of the year.

Metabolic abnormalities

People who form kidney stones often have metabolic or other abnormalities detectable on urinary testing. The common abnormalities include low urinary volume, hypercalcuria (25-40%), hyperoxaluric (10-50%), hyperuricosuria (8-

30%) and hyperoxaluria (5-30%)[10-14]. There is, however, significant overlap with healthy controls who also often have biochemical 'abnormalities', albeit less frequently.[11,14]

OTHER ASSOCIATIONS AND RISK FACTORS

DIET

The association between diet and kidney stones has long been suspected. Populations that consume diets rich in animal protein (meat, fish and poultry) have a higher risk of stones than those with a more vegetarian diet. The risk of forming a stone is increased further by a high intake of refined sugar, salt and Animal protein foods. Sucrose increases the urinary calcium and oxalate concentrations. Lack of dietary fibre is also thought to contribute stone formation,because fibre traps and decreases the rate and extent of absorption of sucrose and animal protein.Animal protein increases urinary calcium, oxalate and uric acid along with causing a more acidic urine, contributes to calcium oxalate over-saturation and precipitation. Prospective studies show that high dietary calcium intake reduces the risk of kidney stones, possibly by reducing gut absorption of oxalate.[1,15,16] Calcium supplements, however, might be associated with an increased risk of stone disease in older women although this has not been found in younger women.[1,17]

High fluid intake is associated with a lower risk of developing kidney stones in men and women.[18,19] Certain beverages also appear to provide additional protection with coffee, tea, beer and wine consumption associated with reduced risk of kidney stones while grapefruit juice consumption was associated with an increased risk.[18-20] High quantity of water intake leads to urinary dilution of the constituents that may precipitate, as well as reducing the average time of residence of free crystal particles in urine. A high dietary intake of fruit and vegetables, a low fat dairy products, whole grains and contains only small amount of meat, sweats and sugar-containing beverages has also been associated with a lower risk of stone[21] and has other health advantages.[36]

OBESITY AND HYPERTENSION

The relative risk of developing kidney stones was greater for obesity women than it was for men. Obesity results in increased urinary excretion of uric acid, sodium, phosphate and ammonium and decreased urinary pH all of which are associated with stone crystal formation. Insulin resistance has also recently been reported to be associated with low urinary ammonium and pH and increased risk of uric acid nephrolithiasis.[22-24]

A modest association has been reported between hypertension and nephrolithiasis in both sexes.[5,25-27] In prospective studies, people with a history of nephrolithiasis are more likely to develop hypertension[5,26] and those with hypertension are more likely to develop kidney stones, especially when they are overweight.[28,29]

MEDICATIONS

Indinavir, a protease inhibitor used in the treatment of HIV-1 infection, can cause kidney stones composed mainly of the drug itself.[30] Other medications associated with stones include allopurinol, triamterene and trisilicate (silica stones).[31]

Vitamin C is metabolized to oxalate and has been shown in a small metabolic study to increase the urinary excretion of oxalate.[32] No association between vitamin C intake and the incidence of kidney stones has been demonstrated in women.[33] However, in an observational study, high vitamin C intake (>1000 mg/day) has been shown to be associated with an increased risk of stones in men, when compared with an intake of 90mg/day. [21]

STONE RECURRENCE

Two cases were treated for the stone among these cases one case had passed a stone five months before and one had removal of the stone two years back.

OTHER FACTORS

Other factors reported to be associated with an increased risk of developing kidney stones include the absence of intestinal oxalate degrading bacteria.[34,35]

SUMMARY OF THE EVIDENCE

Although data on kidney stone disease in Tamil Nadu are limited, the available studies that the epidemiology is similar to foreign countries. Of particular interest in Chennai and Thanjavur district are the Stone disease is a common significant disorder and it is important to understand the risk factors and causes to be able to manage patients effectively likelihood that climate and racial background play a role in the risk of kidney stone disease and the identification of subgroups with in the community. Preventing recurrence, after stone clearance has been achieved, is a key part of managing stone disease.

REFERENCES:

1. Curhan GC, Willett WC, Speizer FE et al. Comparison of dietary calcium with supplemental calcium and other nutrients as factors affecting the risk for kidney stones in women. Ann. Intern. Med. 1997; 126: 497-504.

2. Hiatt RA, Dales LG, Friedman GD et al. Frequency of urolithiasis in a prepaid medical care program. Am. J. Epidemiol. 1982; 115: 255-65.

3. Johnson CM, Wilson DM, O'Fallon WM et al. Rental stone epidemiology: A 25 year study in Rochester, Minnesota, Kidney Int. 1979; 16: 624-31.

4. Stamatelou KK, Francis ME, Jones Ca et al. Time trends in the reported prevalence of kidney stones in the United States; 1976-1994. Kidney Int. 2003; 63: 1817-23.

5. Madore F, Stampfer MJ, Willett WC et al. Nephrolithiasis and risk of hypertension in women. Am. J.Kidney Dis. 1998; 32: 802-7.

6. Soucie JM, Thun MJ, Coates RJ et al. Demographic and geographic variability of kidney stones in the United States. Kidney Int. 1994; 46: 893-9.

7. Sowers MR, Jannausch M, Wood C et al. Prevalence of renal stones in a population based study with dietary calcium, oxalate and medication exposures. Am. J. Epidemiol. 1998; 147: 914-20.

8. Baker PW, Coyle P, Bais R et al. Influence of season, age and sex on renal stone formation in South Australia. Med. J. Aust. 1993; 159: 390-92.

9. Gault MH, Chafe L. Relationship of frequency, age, sex, stone weight and composition in 15624 stones: Comparison of results for 1980 to 1983 and 1995 to 1988. J.Urol. 2000; 164: 302-7.

10. Van Drongelen J, Kiemeney LA, Debruyne FM et al. Impact of urometabolic evaluation on prevention of urolithiasis: A retrospective study. Urology 1998;52: 384 – 91.

11. Leonetti F, Dussol B, Berthezene P et al. Dietary and urinary risk factors for stones in idiopathic calcium stone formers compared to healthy subjects. Nephrol. Dial. Transplant. 1998; 13: 617 – 22.

12. Borghi L, Meschi T, Schianchi T et al. Urine volume: Stone risk factor preventive measure. Nephron 1999; 81 (Suppl.1): S31 – 7.

13. Trinchieri A, Ostini F, Nespoli R et al. A prospective study of recurrence rate and risk factors for recurrence after a first renal stone. J. Urol. 1999; 162: 27–30.

14. Curhan GC, Willett WC, Speizer FE et al. Twenty four hour urine chemistries and the risk of kidney stones among women and men. Kidney Int. 2001; 59: 2290 – 98.

15. Siener R, Ebert D, Nicolay C et al. Dietary risk factors for hyperoxaluria in calcium oxalate stone formers. Kidney Int. 2003; 63: 1037 – 43.

16. Curhan GC, Willett WC, Rimm EB et al. A prospective study of dietary calcium and other nutrients and the risk of symptomatic kidney stones. N. Engl. J. Med. 1993;328: 833-8.

17. Curhan GC, Willett WC, Knight EL et al. Dietary factors and the risk of incident kidney stones in younger women. Arch. Intern. Med. 2004; 164: 885 – 91.

18. Curhan GC, Willett WC, Rimm EB et al. Prospective study of beverage use and the risk of kidney stones. Am. J. Epidemiol. 1996; 142: 240 – 47.

19. Curhan GC, Willett WC, Speizer FE et al. Beverage use and risk for kidney stones in women. Ann. Intern. Med. 1998; 128: 534 – 40.

20. Hirvonen T, Pietinen P, Virtanen M et al. Nutrient intake and use of beverages and the risk of kidney stones among male smokers. Am. J.Epidemiol. 1999; 150: 187 – 94.

21. Taylor EN, Stampfer MJ, Curhan GC. Dietary factors and the risk of incident kidney stones in men: New insights after 14 years of follow up. J.Am. Soc. Nephrol. 2004; 15: 3225 – 32.

22. Pak CY, Sakhaee K, Person RD et al. Biochemical profile of idiopathic uric acid nephrolithiasis. Kidney Int. 2001: 60: 757 – 61.

23. Sakhaee K, Adams-Huet B, Moe OW et al. Pathophysiological basis for normouricousuric uric acid nephrolithiasis. Kidney Int. 2002; 62: 971-9.

24. Abate N, Chandalia M, Cabo-Chan AV et al. The metabolic syndrome and uric acid nephrolithiasis: Novel features of renal manifestation of insulin resistance. Kidney Int. 2004; 65: 386 – 92.

25. Cirillo M, Laurenzi M, Elevated blood pressure and positive history of kidney stones: Results from a population based study. J.Hypertens. 1988; 6(suppl. 4): S484 – 6.

26. Madore F, Willett WC, Stampfer MJ et al. Nephrolithiasis and risk of hypertension. Am. J. Hypertens. 1998; 11: 46 – 53.

27. Soucie JM, Coates RJ, McClellan W et al. Relation between geographic variability in kidney stones prevalence and risk factors for kidney stones. Am. J. Epidemiol. 1996; 143: 487 – 95.

28. Broghi L, Meschi T, Guerra A et al. Essential arterial hypertension and stone disease, Kidney Int. 1999; 55: 2397 – 406.

29. Cappuccio FP, Siani A, Barba G et al. A prospective study of hypertension and the incidence of kidney stones in men. J. Hypertens. 1999; 17: 1017 – 22.

30. Daudon M, Estepa L, Viard JP et al. Urinary stones in HIV – 1 positive patients treated with indinavir. Lancet 1997; 349: 1294 – 5.

31. Watts RW. Aetiological factors in stone formation. In: Davidson AM (ed). Oxford textbook of Clinical Nephrology. Orford: Oxford University Press, 1988; 1319 – 41.

32. Traxer O, Huet B, Poindexter J et al. Effect of ascorbic acid consumption on urinary stone risk factors. J. Urol. 2003; 170: 397 – 401.

33. Curhan GC, Willett WC, Speizer Fe et al. Intake of vitamins B6 and C and the risk of kidney stones in women. J. Am. Soc. Nephrol. 1999; 10: 840-45.

34. Kwak C, Kim HK, Kim EC et al. Urinary oxalate levels and the enteric bacterium oxalobacter formigenes in patients with calcium oxalate uroithiasis. Eur. Urol. 2003; 44: 475 – 81.

35. Mikami K, Akakura K, Takei K et al. Association of absence of intestinal oxalate degrading bacteria with urinary calcium oxalate stone formation. Int. J.Urol. 2003; 10: 293 – 6.

36.Taylor EN, Fung TT,Chrhan GC,Dash-style diet associates with reduced risk for kidney stones. J.Am Soc Nephrol 2009;20:2253-9.

CHAPTER -2

CHARACTERISATION OF KIDNEY STONES

INTRODUCTION:

Stone formation in renal systems is one of the oldest and the man common form of crystal deposition [1]. Analytical results show calcium oxalate (CaC2O4) to be one of the major inorganic components of renal stones and is found to be present in almost all kidney and bladder stones [2]. About 39.5% of the total composition of the calculi is found to contain purely calcium oxalate and also it occurs along with calcium phosphates and apatite's [3]. It is well known that there are three different hydrated forms of calcium oxalate such as Calcium Oxalate Monohydrate (COM), Calcium Oxalate Dihydrate (COD) and Calcium Oxalate Trihydrate (COT). COD and COT are difficult to form urinary stone because they are unstable and easy to eject from human or animal body along with urine.

Among these Calcium Oxalate Monohydrate is found to be thermodynamically stable [4]. Though a number of researchers are tackling the problem from different angles, the mechanism of the formation of the stones is not yet clearly understood and a number of questions about the promoting and inhibiting factors still remain unanswered.

Concentration of these crystals leads to the formation of urinary calculi. Calcium stones are most common, comprising 75% of all urinary calculi. They may be pure stones of calcium oxalate and calcium phosphate or a mixture of calcium oxalate and calcium phosphate [5]. Many stones are not homogeneous. Some have a nucleus of different composition from the surrounding.

Crystal formation can be caused due to several reasons [6]. In the case of insufficient intake of water or due to the decreased rate of excretion, the crystallogenic substances in the urine can be concentrated, leading to crystal formation. A change in pH value in the urine can lead to the crystal growth. The

decrease in solubility of crystallogenic substances in urine can also lead to the formation of crystals.

The morophology, composition of crystals deposits can be evaluated using Optical microscopy, UV, FT-IR, DSC and XRD. The instrument combination was successfully tried on urinary crystals and thin sections of urinary calculi. These explain the efficiency of the system in the expansion of urinary calculus analysis.

MATERIALS AND METHODS:

Urinary deposits from Forty Six samples were collected from various Hospitals in Tamil nadu. The compositions of stones are determined by various analytical techniques such as Qualitative analysis, UV, FT-IR, XRD, Optical Microscopic studies, Differential Scanning Calorimetry (DSC), Scanning Electron Microscope (SEM), Elemental analysis (ICP) and EDAX – SEM Analysis. Ten stones are removed by surgically; other stones are removed by crushing and evacuation method.

The size and morphology of the stones were examined by Optical microscopy, while their components and crystalline phases were determined by Fourier transform Infrared (FTIR) spectroscopy, Ultraviolet spectroscopy and X-ray powder diffraction.

3. RESULTS AND DISCUSSION:

3.1 QUALITATIVE ANALYSIS:

All the kidney stones are analyzed by Qualitative analysis in our Laboratory. Oxalate stones were confirmed by heating a small amount of stone with dilute sulphuric acid and MnO_2 and appearance of brisk effervescence and colourless gas turning limewater milky.

Phosphate stones are confirmed by dissolving a small amount of stone in a few drops of Concentrated Nitric acid, cooled well and adding excess of ammonium molybdate with the formation of a canary yellow precipitate.

All the stones are analyzed and through the observation and inference, are tabulated below.

Table:3 Nature of the Stone

Name of the Sample	Nature of the Sample	Colour of the Sample
US – I	Oxalate and Phosphate	Brown
US - II	Phosphate and Oxalate	White
US - III	Oxalate and phosphate	Brown
US - IV	Oxalate and Phosphate	Brown
US – V	Phosphate and Oxalate	White
US – VI	Phosphate and Oxalate	White
US - VII	Phosphate and Oxalate	White
US – VIII	Phosphate and Oxalate	White
US – IX	Phosphate and Oxalate	White
US - X	Oxalate and Phosphate	Brown

3.2 CHARACTERISATION STUDIES BY OPTICAL MICROSCOPY:

3.2.1. Analysis of Oxalate Predominant stones:

Calcium Oxalate Monohydrate (COM) and Calcium Oxalate Dihydrate (COD) stones are found to be inside the kidney (Nephrolithiasis) and the ureter (Urolithiasis) which causes increasing danger to human health.

The kidney stones are taken photograph using optical microscopy LX 400 and their size were determined. The photographic shown in Figure.5 to 8 are US-I, III, IV and X.

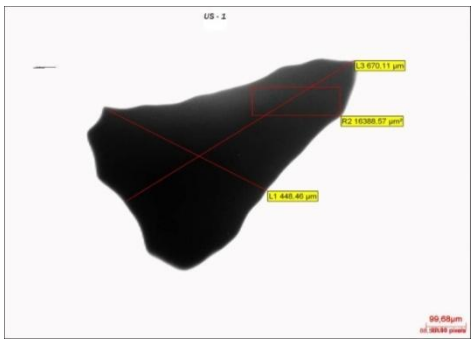

Figure: 5 Optical Microscopy of US-I

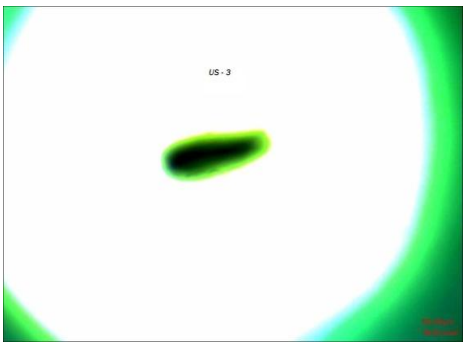

Figure: 6 Optical Microscopy of US-III

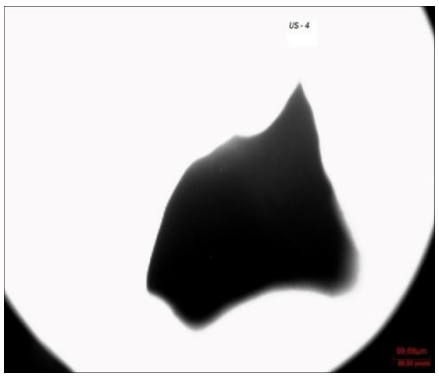

Figure:7 Optical Microscopy of US-IV

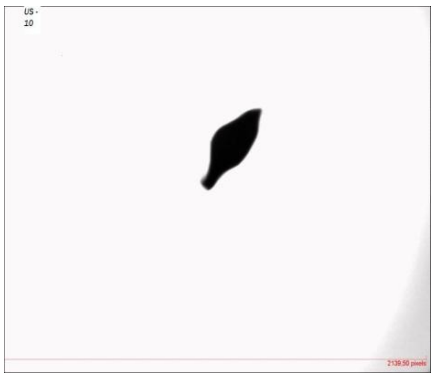

Figure:8 Optical Microscopy of US-X

The samples US – I, III, IV and X are seems to be having higher concentration of oxalate with little presence of phosphate. All the above types of stones are brown in colour smaller in size and the sizes of the stones are 99.68µm, 90.08µm, 99.68µm and 2139.5 Pixels respectively. Out of 20% are oxalate stones and size of the stones are very small.

3.2.2 Analysis of Phosphate Predominant stones:

Various studies on Urolithiasis and medical history and survey shows that the calcium phosphate is main constituent in the Phosphate stones found in Ureter (Urolithiasis) and Magnesium hydrogen phosphate is the major constituent present in inside the kidney (Nephrolithiasis) and both these stones cause danger to the livelihood.

The phosphate stones are analyzed by Optical Microscopy. The samples US – II, V, VI, VII, VIII and IX are soft in nature and white in colour. These indicate the mixture of phosphate and oxalate stones. The major composition of the stones is Phosphate. The photograph taken by the optical microscope of various phosphate predominant stones are given in Fig.9 to 13.

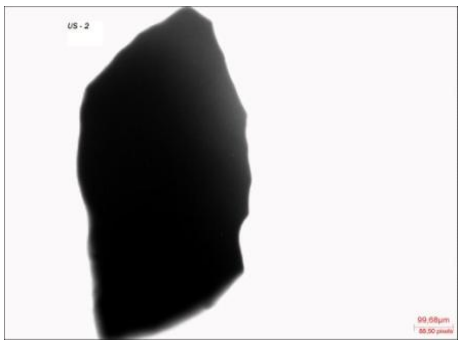

Figure: 9 Optical Microscopy of US-II

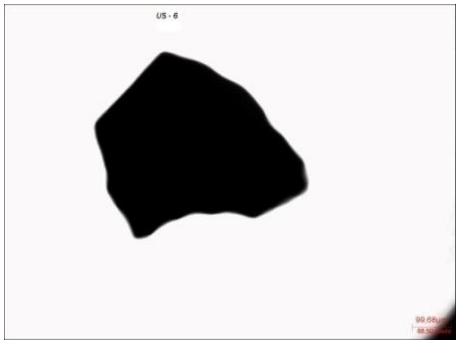

Figure:10 Optical Microscopy of US-VI

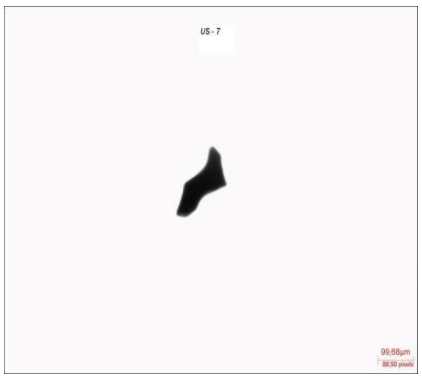

Figure:11 Optical Microscopy of US-VII

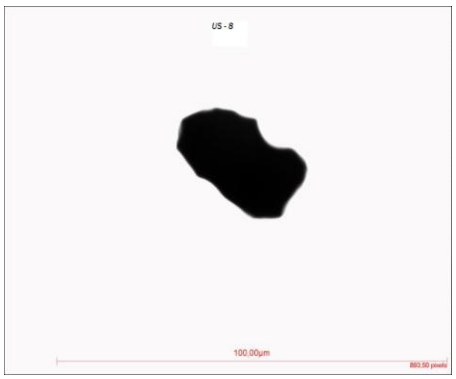

Figure:12 Optical Microscopy of US-VIII

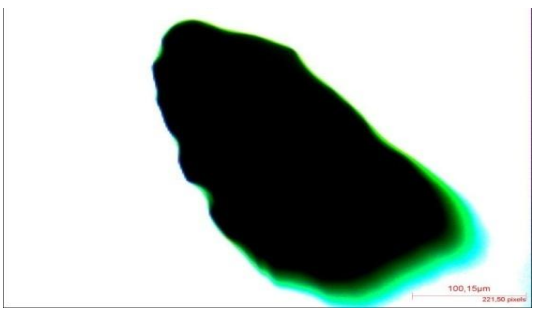

Figure:13 Optical Microscopy of US-IX

The size of the stones are 99.68µmfor US-II,VI and VII and the remaining US-VIII and IX are 100.5µm.Out of 60% are phosphate stones and sizes are big when compared to oxalate stones.

3.3. CHARACTERISATION OF STONES BY ULTRA VIOLET SPECTROSCOPY:

Absorption of UV radiation of the sample leads to electronic excitation among various energy levels within the molecule. The transition generally occurs in between a bonding or lone pair orbital and unoccupied non-bonding or antibonding orbital. The absorption spectrum of Oxalate and Phosphate predominant stones were measured in wavelength region of 190 -1100nm.

3.3.1. UV-Analysis of Oxalate Predominant Stones:

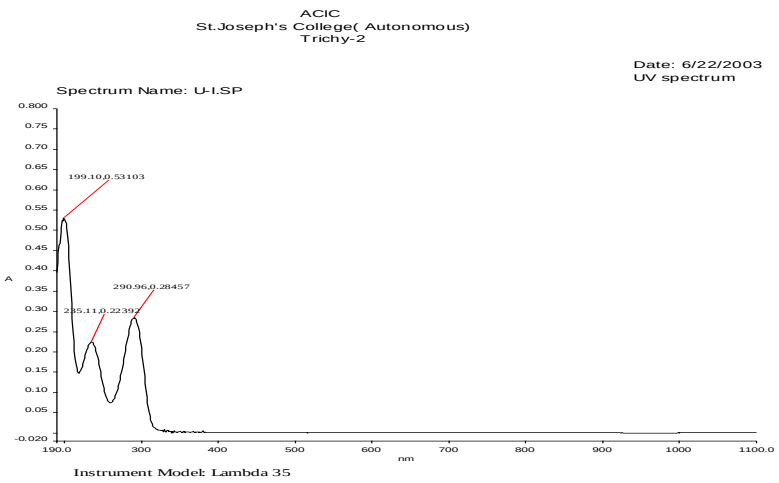

Figure. 14 UV Spectra for US-I

In Fig. 14 for US-I sample, observed λ_{max} values are 199.10nm due to σ-σ* transition. The value at 235nm and 290nm are due to π – π* and n- π* transition. A shift of absorption maximum to shorter wavelength (Hypsochromic) result shows when an auxochrome is attached to double bonds where n-electrons are available. This is due to presence of Oxalate stones.

Table: 4 UV Spectra for Oxalate Stones

US-I	US-III	US-IV	US-X	Assignment
199.1	-	-	199	σ-σ*
235.1	-	-	235.3	π-π*
290.9	348.3	290.0	291.42 and 383.3	n-π*

In Fig.15 for US-III sample, observed λ_{max} value are 348 due to n- π* transition. A shift of absorption maximum to shorter wavelength (Hypsochromic) result shows when an auxochrome is attached to double bonds where n-electrons are available. The absorption signals are very weak are due to mixed oxalate and phosphate stones.

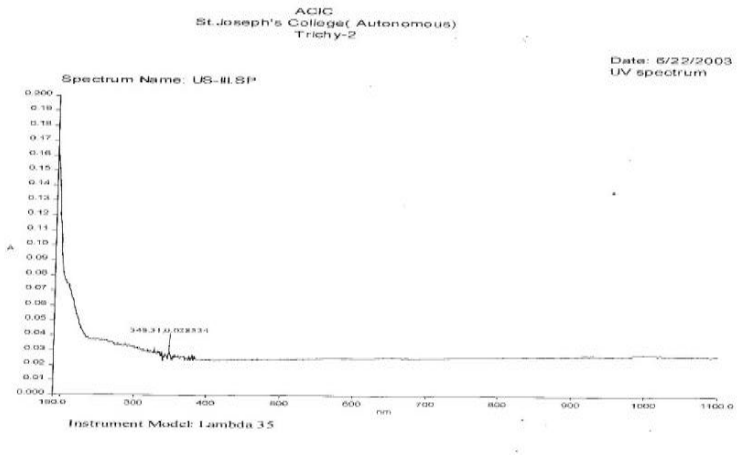

Figure.15 UV Spectra for US-III

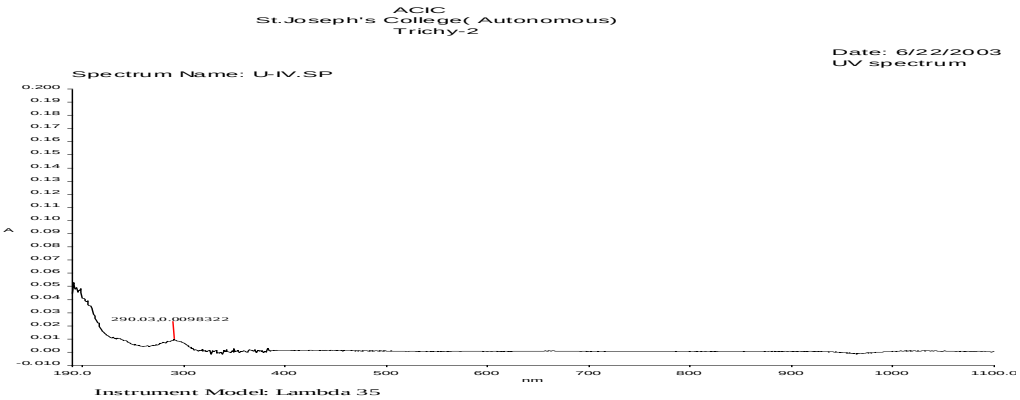

Figure.16 UV Spectra for US-IV

In Fig.16 for US-IV sample, observed λ_{max} value are 290nm due to and n-π* transition. A shift of absorption maximum to shorter wavelength (Hypsochromic) result shows when an auxochrome is attached to double bonds where n-electrons are available. This is due to presence of Oxalate stones.

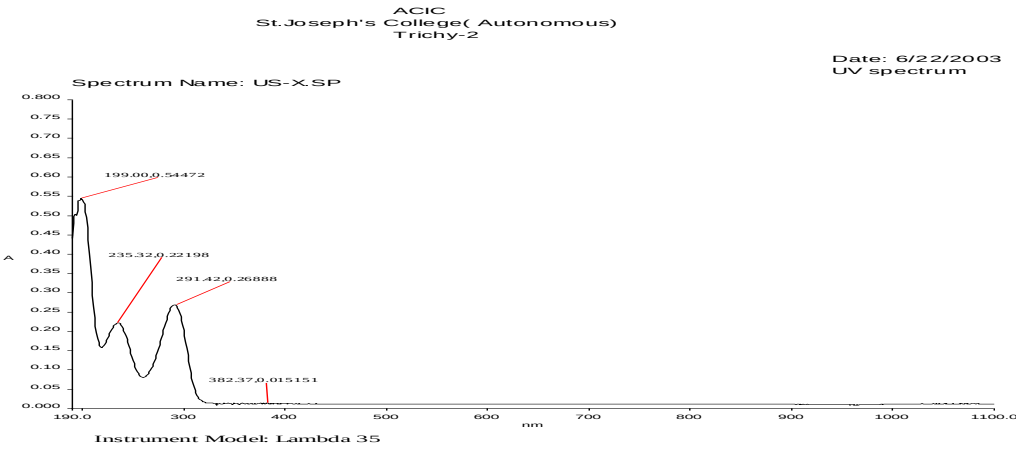

Figure : 17 UV Spectra for US-X

In Fig.17 for US-X sample, observed λ_{max} values are 199 due to σ-σ* transition. The value at 235nm, 290nm and 383 are due to π – π* and n- π* transition. A shift of absorption maximum to shorter wavelength (Hypsochromic) result shows when an auxochrome is attached to double bonds where n-electrons are available. This is due to presence of Oxalate and phosphate stones and also the phosphate concentration is higher in US – III and X when compared to others.

3.3.2. UV- Analysis of Phosphate Predominant Stones:

The absorption spectrum of Phosphate stones are analyzed in wavelength region of 190 -1100nm.

In Fig.18,19 and 20 for US-II ,V and VI sample, the observed λ_{max} value at 291nm , 331nm and 290nm are due to n-π* transition. In fig.21 is US-VII sample, observed λ_{max} values at 199nm due to σ-σ* transition. The value at 236nm and 291nm due to π- π* transition and n-π* transition.

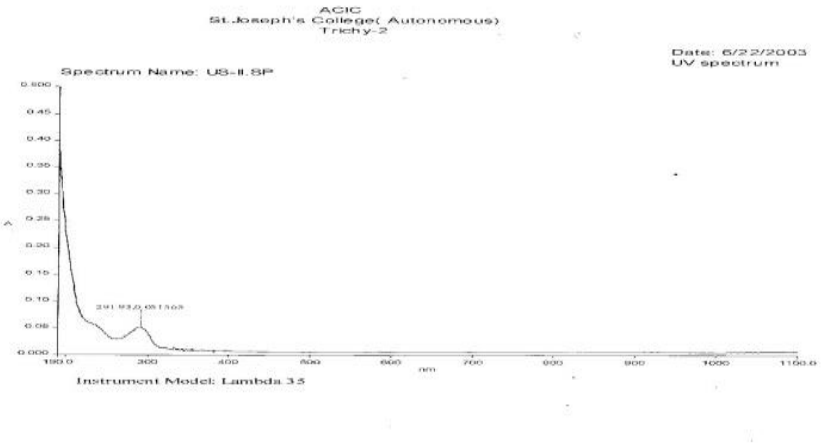

Figure .18 UV Spectra for US-II

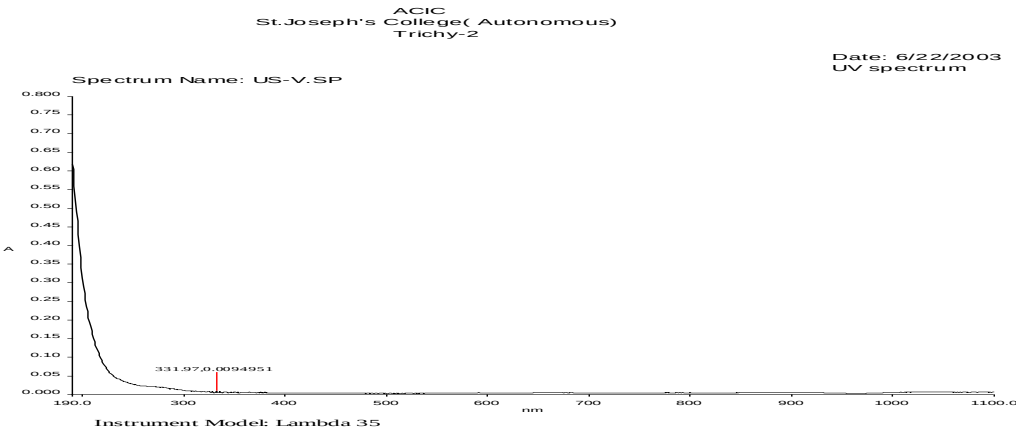

Figure:19 UV Spectra for US-V

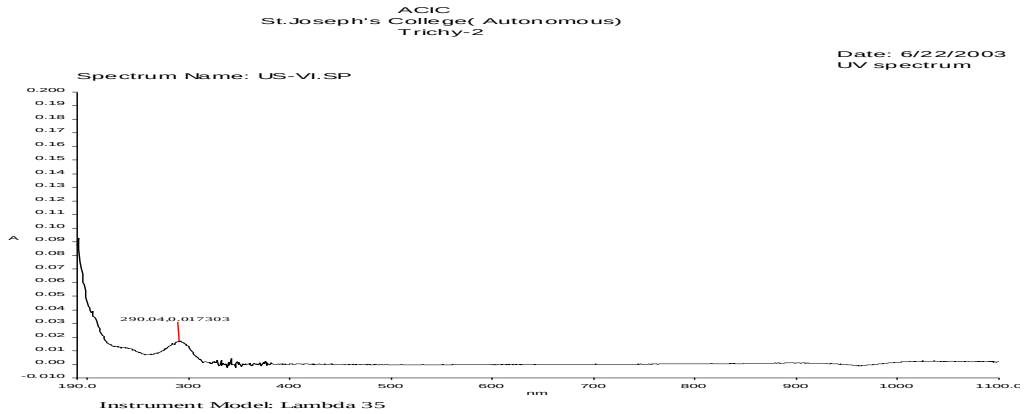

Figure:20 UV Spectra for US-VI

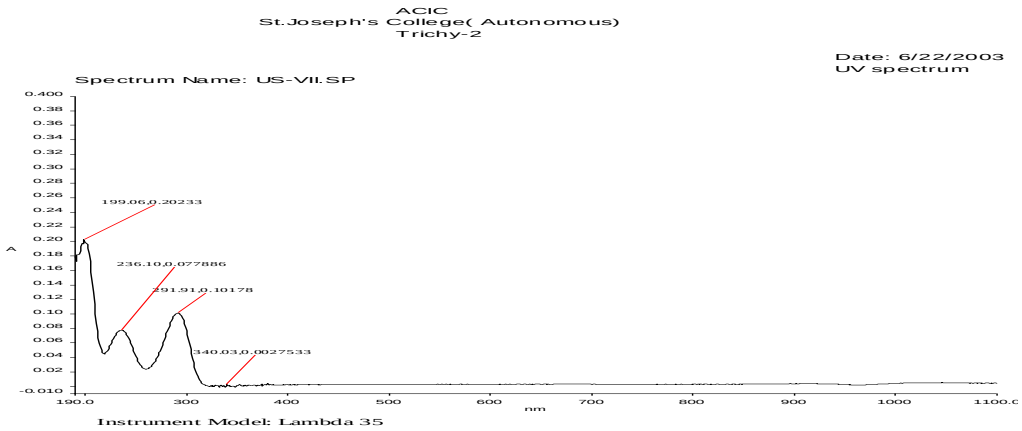

Figure. 21 UV Spectra for US-VII

Table:5 UV Spectra for Phosphate Stones

US-II	US-V	US-VI	US-VII	US-VIII	US-IX	Assignment
-	-	-	199	-	-	σ-σ*
-	-	-	236	-	-	π-π*
291.9	331.9	290.0	291 &340	291.42 and 383.3	381.9	n-π*

In fig.22and fig.23 for US –VIII and IX sample, observed λ_{max} values at 292nm,349nm and 381nm are due to n-π* transition. A shift of absorption maximum to shorter wavelength (hypsochromic) result shows when an auxochrome is attached to double bonds where n-electrons are available. The absorption signals are very weak are due to mixed Phosphate and Oxalate stones.

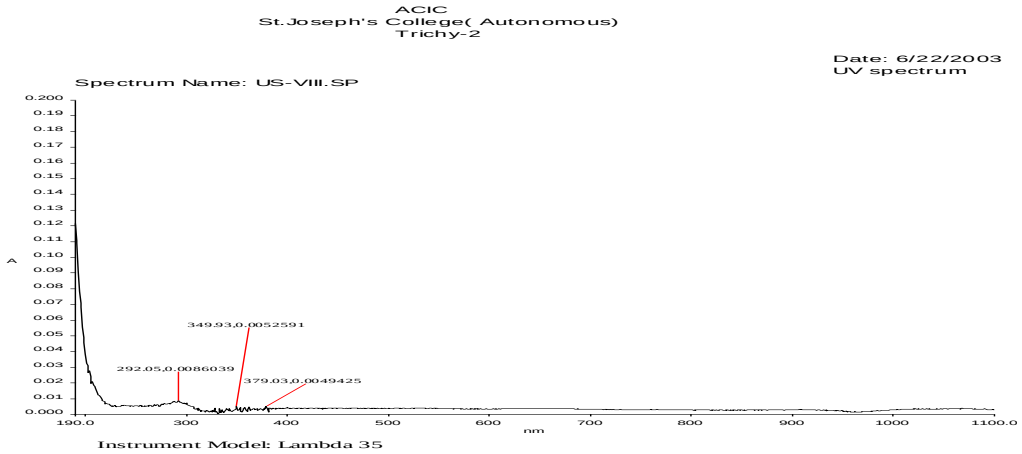

Figure.22 UV Spectra for US-VIII

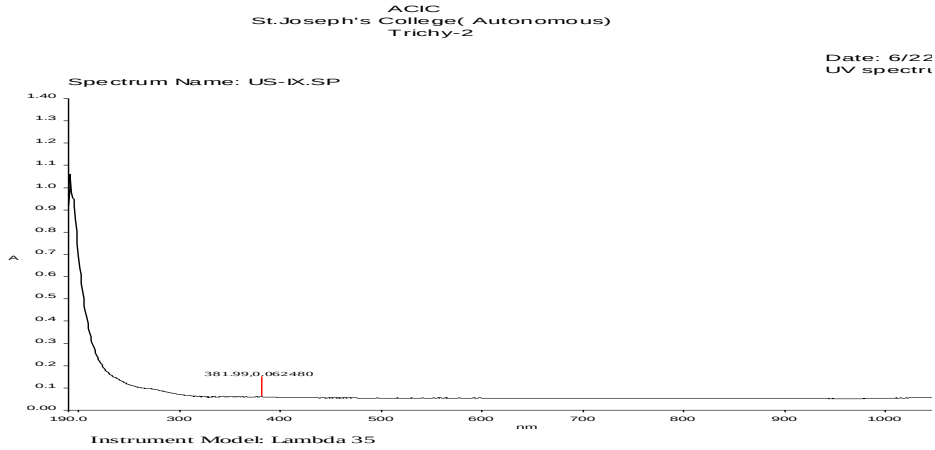

Figure.23 UV Spectra for US-IX

The UV absorption peak with λ_{max} corresponding to 199nm which is due to σ-σ* transition, 235nm corresponding to π-π* transition may be due to the presence of higher concentration of Oxalate. Generally the λ_{max} lower than 250nm corresponds to n- π* transition due to C=O bonding in oxalate stones and above 250nm corresponds to Phosphate stones. Hence whenever the λ_{max} of UV absorption is higher than 250nm, Phosphate concentration is higher

3.4. CHARACTERISATION STUDIES BY FT-IR SPECTROSCOPY:

Infrared spectroscopy gives information about the molecular vibrations or more precisely about transitions between vibrational and rotational energy levels in molecules. The oxalate and phosphate stones are characterized using FT-IR spectroscopy in the wavelength region of 400cm^{-1} to 40000cm^{-1}.

3.4.1 FT-IR – Analysis of Oxalate Predominate Stones:

FT-IR spectra of oxalate stones of US – I, III, IV and X are stones in fig.24,25,26 and 27.

Table :6 IR spectra for Oxalate stones

US-I cm^{-1}	US-III cm^{-1}	US-IV cm^{-1}	US-X cm^{-1}	Assignment
3433,3199, 3065 & 2923	3507, 3033 &3033	3482 ,3351 & 3056	3485 ,3338 & 3064	Symmetric and Asymmetric stretching of –OH group.
-	2294	2299	2300	C-H stretching
1641	1586	1630	1631	Ca – Oxa $–H_2O$ bending
1315	1324	1310	1318	Metal – Carboxylate Stretching
886&723	885&786	885&781	884&779	Asymmetric Stretching C-O-C
522	497	516	512	O-C-O in plane bending

US-I: I

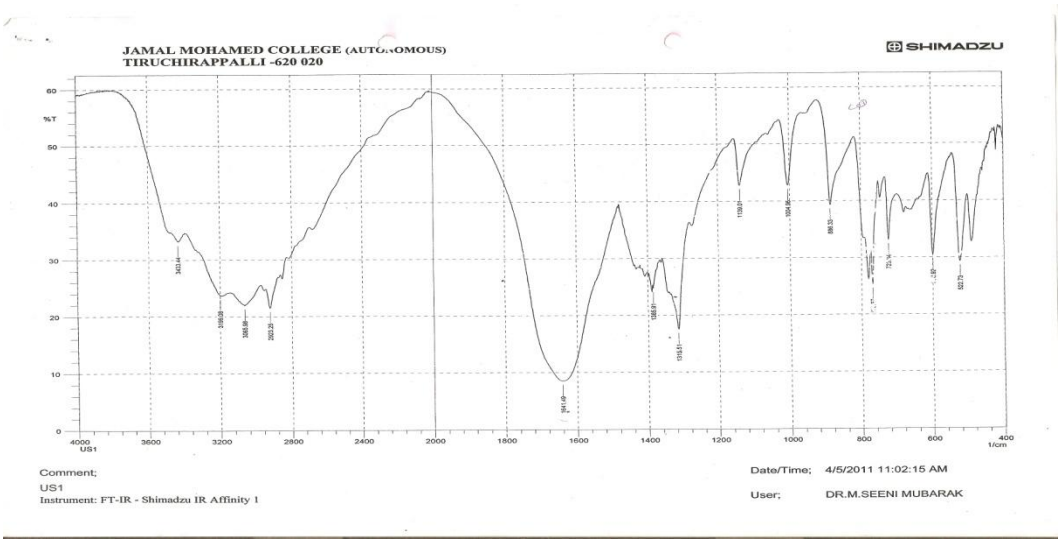

Figure:24 IR Spectra for US-I

In above spectra for the US-I, the peaks appear at 3433cm^{-1},3199cm^{-1},3065cm^{-1} and 2923cm^{-1} are due to symmetric and asymmetric hydroxyl stretching frequency of the molecules. The water molecules coordinated with the calcium oxalate molecules produce characteristic peak corresponding to the bending modes at 1641cm^{-1}. The metal –carboxylate stretch appears at 1315 cm^{-1}. The peaks at 886cm^{-1} and 723cm^{-1} are due to asymmetric stretching for C-O-C group. The peak at 522 cm^{-1} arises due to O-C-O in plane bending.

US-III:

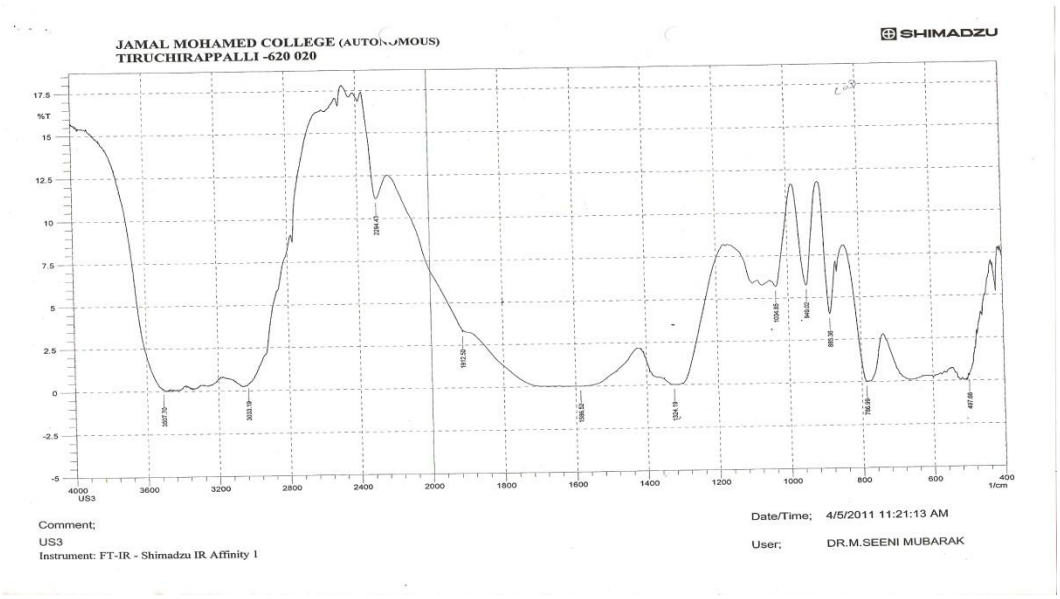

Figure:25 IR Spectra for US-III

In above spectra was US-III, the peaks appear at 3507cm^{-1} and 3033cm^{-1} are due to symmetric and asymmetric hydroxyl stretching frequency of the molecules. The peak at 2294 cm^{-1} and 1586 cm^{-1} are due to C-H stretching group in CH_2-CO group and the water molecules coordinated with the calcium oxalate molecules produce characteristic peaks corresponding to the bending mode. The metal –carboxylate stretch appears at 1324 cm^{-1}. The peaks at 885 cm^{-1} and 786 cm^{-1} are due to asymmetric stretching for C-O-C group. The peak at 497 cm^{-1} arises due to O-C-O in plane bending.

US-IV:

Figure.26 was US-IV, the peaks appear at 3482 cm^{-1} ,3351cm^{-1} and 3056 cm^{-1} are due to symmetric and asymmetric hydroxyl stretching frequency of the molecules. The peak at 2299 cm^{-1} are due to C-H stretching group in CH_2-CO group respectively. The water molecules coordinated with the calcium oxalate molecules produce characteristic peaks corresponding to the bending modes at 1630 cm^{-1} . The metal –carboxylate stretch appears at 1310 cm^{-1}. The peaks at 885 cm^{-1} and 781 cm^{-1} are due to asymmetric stretching for C-O-C group. The peak at 516 cm^{-1} arises due to O-C-O in plane bending .

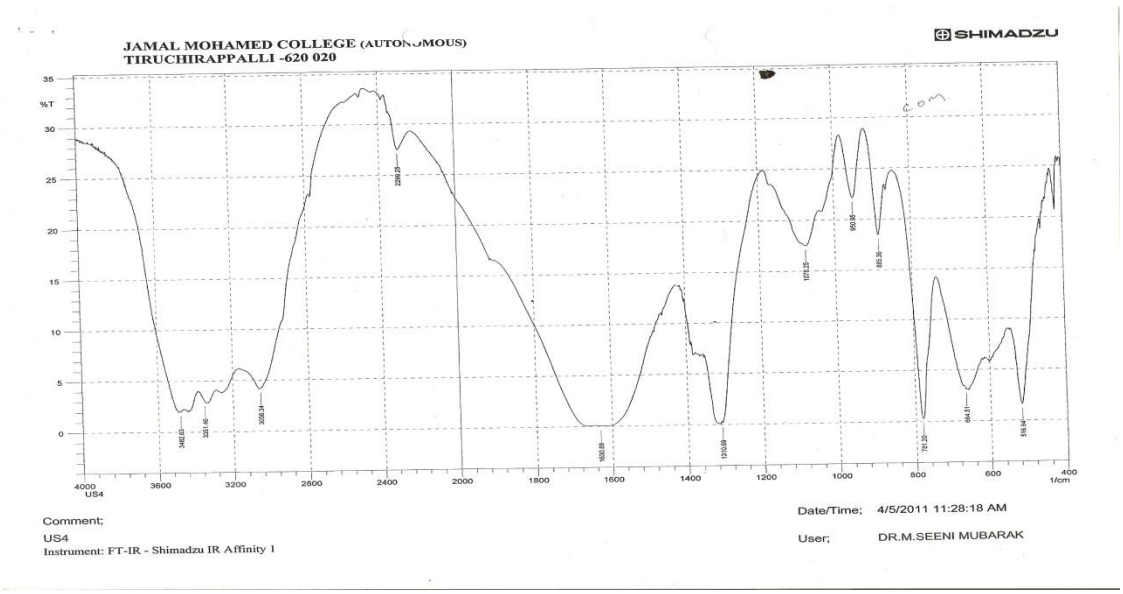

Figure:26 IR Spectra for US- IV

US-X:

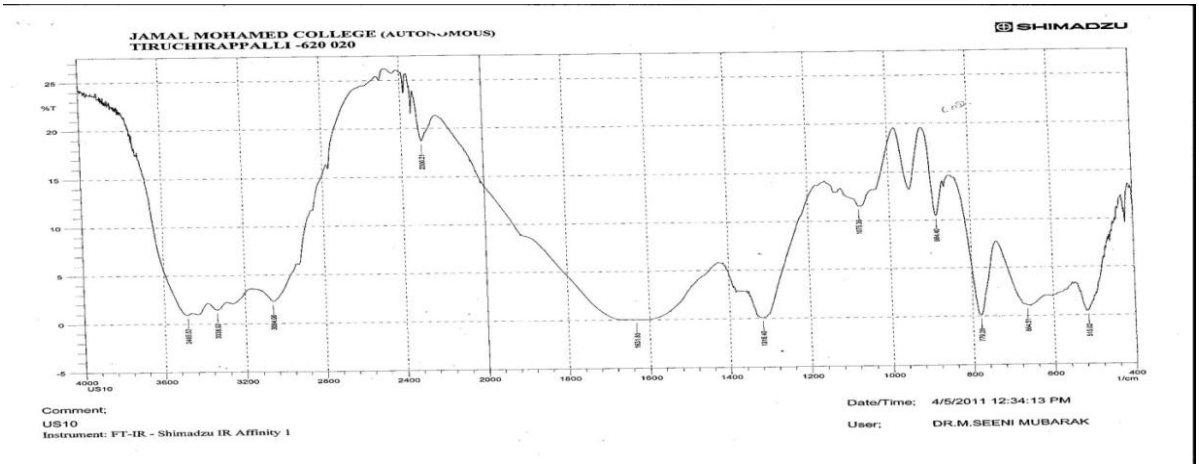

Figure:27 IR Spectra for US- X

The above IR spectra for US-X, the peaks appear at 3485cm^{-1}, 3338 cm^{-1} and 3064 cm^{-1} are due to symmetric and asymmetric hydroxyl stretching frequency of the molecules. The peaks at 2300 cm^{-1} are due to C-H stretching group in CH_2-CO group respectively. The water molecules coordinated with the calcium oxalate molecules produce characteristic peaks corresponding to the bending modes at 1631 cm^{-1}. The metal –carboxylate stretch appears at 1318 cm^{-1}. The peaks at 884 cm^{-1} and 779 cm^{-1} are due to asymmetric stretching for C-O-C group. The peak at 512cm^{-1} arises due to O-C-O in plane bending .

Generally, the symmetric and asymmetric stretching of hydroxyl group is broadened by the hydrogen bonding of oxalate group and appears in the range of 2923 – 3507cm^{-1} and also due to coupling. The C-H stretching appears in 2200-2300 cm^{-1}. The metal oxalate – water bending frequencies have been appears at 1310-1318cm^{-1}and it is shifted to higher range of 1586 cm^{-1} and 1641 cm^{-1} due to the presence of phosphate ions. The asymmetric stretching of C-O-C also varied considerably due to hyper conjugation overlapping.

3.4.2 FT-IR Analysis of Phosphate Predominant stone:

In US – II,V,VI,VII,VIII and IX for fig.28 to 33, confirms phosphate stones [8].

Table : 7 IR spectra for Phosphate stones

US-II cm^{-1}	US-V cm^{-1}	US-VI cm^{-1}	US-VII cm^{-1}	US-VIII cm^{-1}	US-IX cm^{-1}	Assignment
3117	-	3384	3194	3281	3105	Symmetric and Asymmetric stretching of –OH group.
2388	2412	2301	-	2413	-	P-H stretching
1654	1671	1638	1652	1666	1666	Carbonyl vibration
1439	1439	1315	1442&1345	1442	1439	C-H stretching
-	1237	-	1237	-	1237	P=O
1066	-	1040	-	1080	-	P-O- alkyl
882	825	-	871	760	883	HPO_4^{2-}
755 & 567	-	780 &569	736 & 568	561	-	PO_4^{3-} stretching

US-II:

In US-II are shown in fig.28 . The absorption occurred at a broad band at 3117cm^{-1} are due to stretching vibration of the molecule. The peak at 2388$cm^{-1}$are due to P-H stretching. The peak at 1654 $cm^{-1}$are due to water molecule coordinated with the calcium oxalate molecules produce characteristic peaks for carbonyl group bending mode vibration.

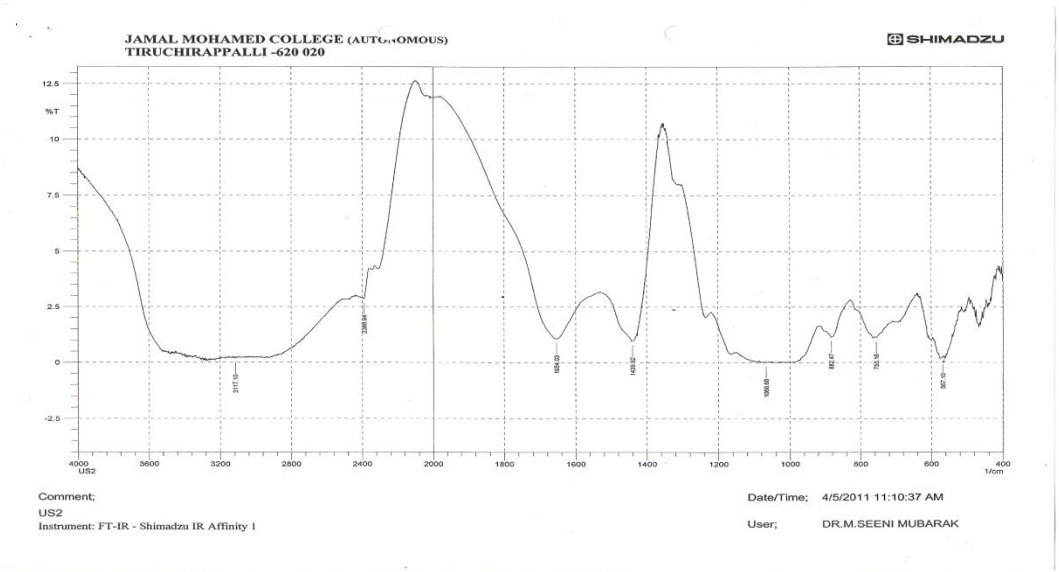

Figure: 28 IR Spectra for US-II

The peak at 1439cm^{-1}are due to C-H stretching. The P-O-alkyl peak appeared at 1066 cm^{-1}.In the spectrum the band at 882cm^{-1} are due to HPO_4^{2-}. The PO_4^{3-} bands were recorded at 567 cm^{-1} to 755 cm^{-1}.

US-V:

In below spectrum for US-V, the broading peak appeared at 3000cm^{-1} are due to stretching vibration of the molecule. The peak at 2412cm^{-1}are due to P-H stretching . The peak at 1671cm^{-1} are due to water molecule coordinated with the calcium oxalate molecules produce characteristic peaks for carbonyl group bending mode vibration. The peak at 1439 cm^{-1} are due to C-H stretching. In the spectrum the peak at 1237 cm^{-1} are due to P=O stretching. In the spectrum the bands at 825 cm^{-1} are due to HPO_4^{2-}.

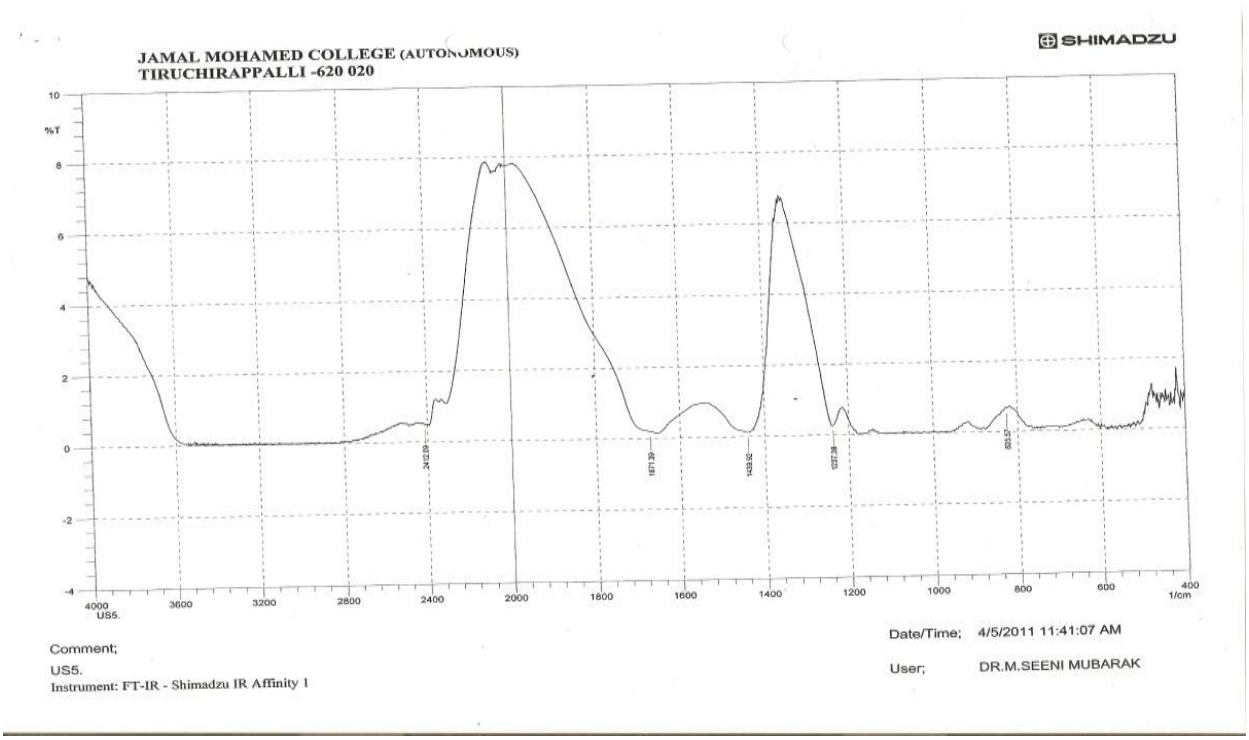

Figure:29 IR Spectra for US-V

US-VI:

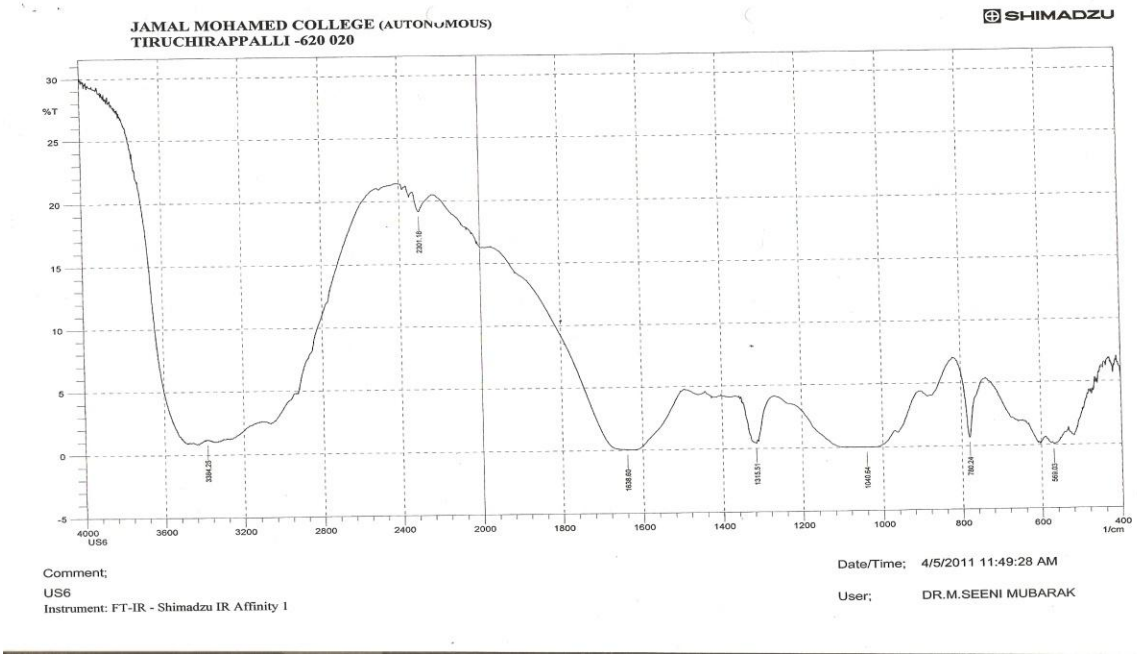

Figure : 30 IR Spectra for US-VI

Fig.30 was IR spectra for US-VI, a broad band at 3384cm^{-1}are due to stretching vibration. The peak at 2301cm^{-1} is due to P-H stretching. The peak at 1638cm^{-1} are due to water molecule coordinated with the calcium oxalate molecules produce characteristic peaks for carbonyl group bending mode vibration. The peak at 1442cm^{-1} is due to C-H stretching. The peak appeared at 1040cm^{-1} are due to stretching frequency for P-O-alkyl group. In the spectrum the bands at 780cm^{-1} are due to HPO_4^{2-}. The PO_4^{3-} bands were recorded at 569cm^{-1} .

US-VII:

The IR spectrums for US-VII are shown below. The absorption occurring a broad band at 3194cm^{-1} are due to stretching vibration. The peak at 1652cm^{-1} are due to water molecule coordinated with the calcium oxalate molecules produce characteristic peaks for carbonyl group bending mode vibration.

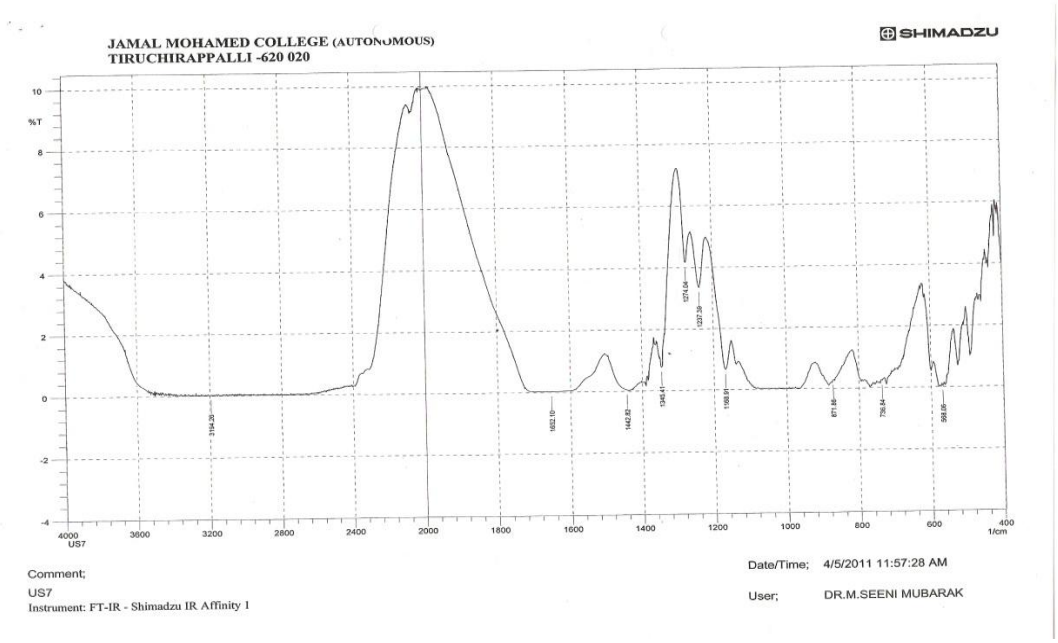

Figure:31 IR Spectra for US- VII

The peak at 1442cm^{-1} is due to C-H stretching. In the spectrum the peak at 1237 cm^{-1} are due to P=O stretching. In the spectrum the bands at 871cm^{-1} are due HPO_4^{2-}. The PO_4^{3-} bands were recorded at 568cm^{-1} to 736cm^{-1}.

US-VIII:

The fig .32 for IR spectrum for US-VIII. The absorption occurring a broad band at 3281cm^{-1} are due to stretching vibration. The peak at 2413cm^{-1}are due to P-H stretching . The peak at 1666cm^{-1} are due to water molecule coordinated with the calcium oxalate molecules produce characteristic peaks for carbonyl group bending mode vibration. The peaks at 1442cm^{-1} are due to C-H stretching. The P-O-alkyl peak appeared at 1066cm^{-1}.The PO_4^{3-} bands were recorded at 568cm^{-1} to 760cm^{-1}.

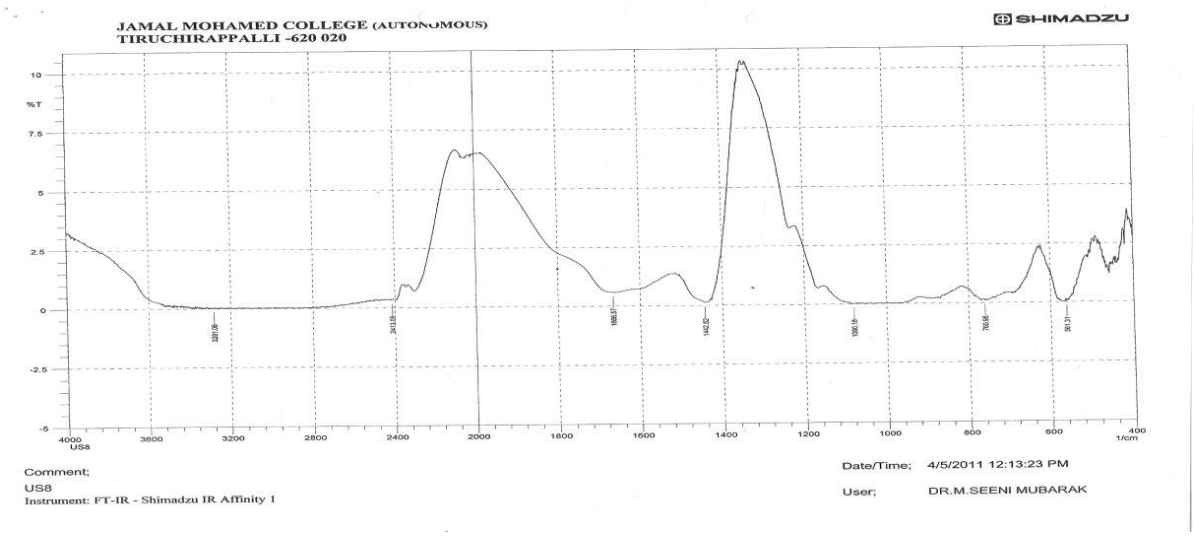

Figure:32 IR Spectra for US-VIII

US-IX:

The below fig.33 for US-IX, the peak appeared at 3105cm^{-1} was due to stretching vibration. The peak at 1666cm^{-1} are due to water molecule coordinated with the calcium oxalate molecules produce characteristic peaks for carbonyl group bending mode vibration. The peaks at 1439 cm^{-1} are due to C-H stretching. In the spectrum the peak at 1237 cm^{-1} are due to P=O stretching. In the spectrum the bands at 883 cm^{-1} to HPO_4^{2-}.

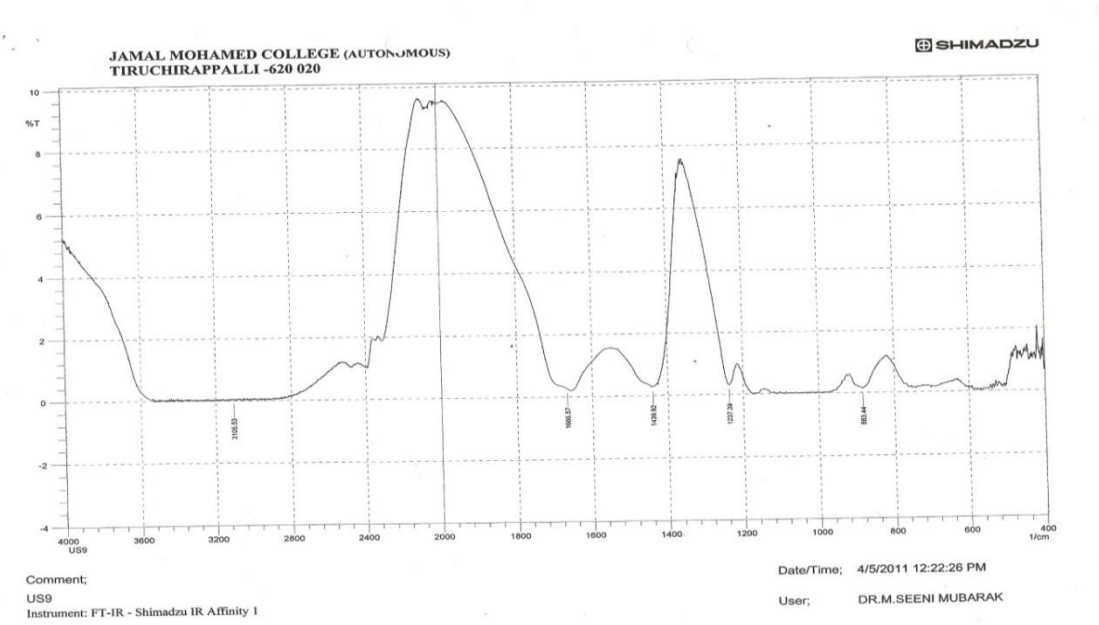

Figure:33 IR Spectra for US-IX

Generally, the symmetric stretching of -OH group is broadened by the hydrogen bonding of phosphate group appears in the range for above 3000 cm^{-1}. The P-H stretching appears in 2420-2300cm^{-1} .The Phosphate ions peak appeared at 1200 cm^{-1} to 560 cm^{-1}.

The detailed investigation of IR spectra supports the qualitative, Optical microscopic analysis and UV spectral analysis for the fact that the urinary stones of US-I,III,IV and X are oxalate predominant and US-II,V,VI,VII,VIII and IX are phosphate predominant stones. This study also shows that more broadening occurs in the hydroxyl group stretching frequency in the phosphate stones compared to oxalate stones. This may be due to increase in hydrogen bonding nature of four oxygen present in phosphate entity rather than oxalate entity contain two oxygen.

3.5. CHARACTERISATION OF STONES BY ICP:

This ICP studies analysis is confirmed the confirmative and support evidence for US-I to US- X.

3.5.1 ICP – Analysis of Oxalate Predominate Stones:

In Cations, Standard Oxalate Graph is given Fig. 34. In Fig.34,the peak appeared at 32.13min represents the oxalate, the height and area of the peak is 9.91 mV and 709.755mV*Sec respectively which corresponds to the concentration of oxalate ion in solution is 10ppm.

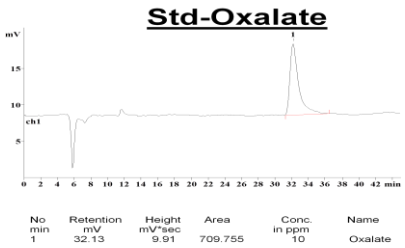

With the help of the above standard graph, the samples of urinary stones are compared and the constituents of oxalate were determined.

Figure. 34 ICP for Std. Oxalate

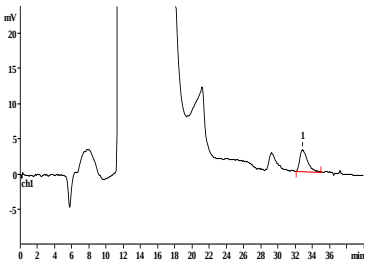

Figure.35 ICP for US – I

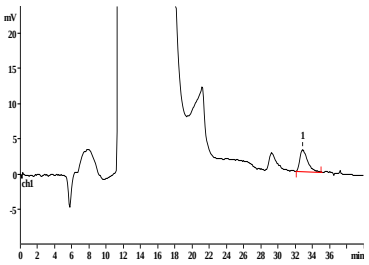

Figure.36 ICP for US-III

ICP for the sample US-I and III is given in fig.35 and 36. A characteristic peak has appeared at 32.87min and 32.13min with the height of 3.13mV and 9.10mV, area 197.158mV*sec and 716mV*Sec for the concentration of 278ppm and 10ppm respectively. When ICP for US-I and III were compared with standard ICP for oxalate it was found that the characteristic peak for oxalate were found to be same.

Table: 8 ICP Data for Oxalate Stone

Name of the sample	Retention mV	Height Mv	Area mV*Sec	Concentration ppm (Oxalate)
US-I	32.87	3.13	197.15	278
US-III	32.13	9.10	716.22	10
US-IV	33.01	3.03	197.05	278
US-X	32.80	3.23	197.25	278

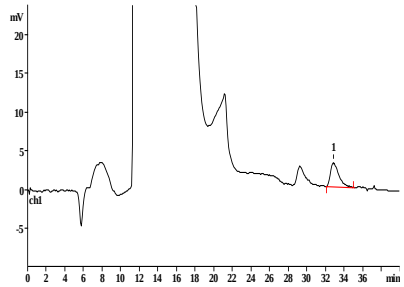

Figure.37 ICP for US – IV

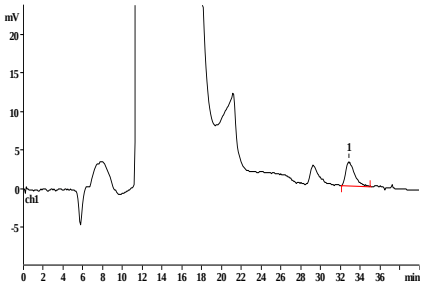

Figure.38 ICP for US – X

In Fig.37 and 38, the ICP for Samples US – IV and X, at concentration 278ppm, has a peak at 33.01min and 32.80min with the height of 3.03mV and 3.23mV and area of 197.058mV*sec and 197.25mV*sec respectively. On comparing the standard ICP for oxalate with ICP for US-IV and US-X, it was found that the major constitution was oxalate.

3.5.2 ICP – Analysis of Phosphate Predominant Stones:

ICP analysis of the stones confirms the constitution of the cations and anions. In Cations, Phosphate Graph is given by Figure.39.

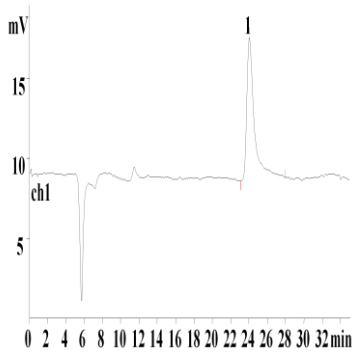

Figure.39 ICP for Std. Phosphate

In Fig.39, the retention time of the peak for the standard Phosphate is 24.04mV, the height and the area of the peak are 9.01 mV and 517.155mV*sec respectively, for concentration of 10ppm.

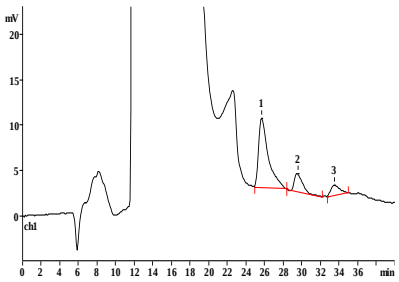

Fig: 40 ICP for US-II

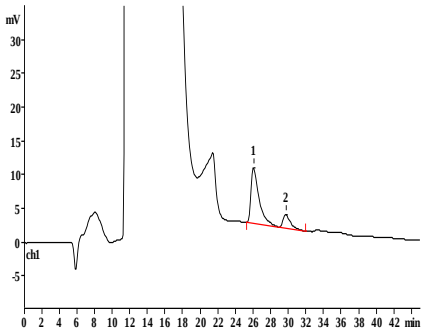

Figure.41 ICP for US – V

In Fig.40 the ICP for sample US –II, at concentration 1075ppm and 100ppm, have peaks at 25.71min and 33.52mV for phosphate and oxalate with the height of 7.68mV and 1.13mV and the area of the peaks are 556.172mV*sec and 70.749mV*sec respectively. On comparing the Standard Oxalate and Phosphate with ICP for US-II it was found that phosphate and oxalate was confirmed.

Table: 9 ICP data for Phosphate Predominant Stones

Name of the sample	Retention mV	Height mV	Area mV*Sec	Concentration ppm
US-II	25.71	7.68	556.17	1075 (Phos.)
	33.52	1.13	70.74	100(Oxalate)
US-V	26.05	8.24	519.4	1083(Phos.)
	29.69	1.98	115.79	9.2 (Oxalate)
US-VI	26.91	4.43	295.47	1118 (Phos.)
	30.68	2.26	148.70	9.5(Oxalate)
US-VII	27.07	10.1	582	1126 (Phos.)
US-VIII	27.07	13.97	15.52	1126 (Phos.)
US-IX	27.07	15.52	990.7	1126 (Phos.)

ICP for the sample US-V and VI are given in Fig.41 and 42. The characteristic peaks has appeared at 26.05min,29.69min and 26.91min,30.68min with the height of 8.24mV,1.98mV and 4.43mV,2.26mV and area 519.440mV*sec,115.792mV*sec and 295.47mV*Sec, 148.70mV*Sec for the concentration of 1083ppm and 1118ppm respectively. When ICP for US-V and US-VI was compared with standard ICP for Phosphate and Oxalate it was found that the characterisation peak for Phosphate and Oxalate were found to be same as that of the standard.

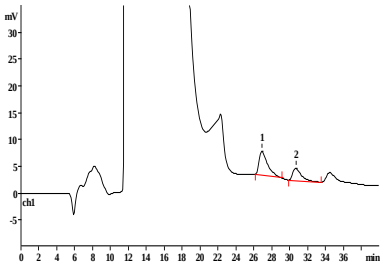

Figure.42 ICP for US – VI

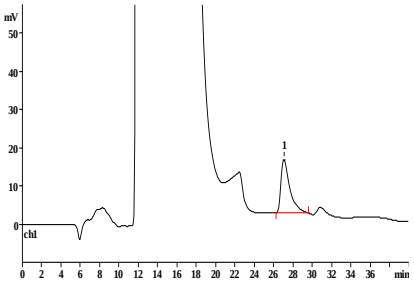

Figure.43 ICP for US – VII

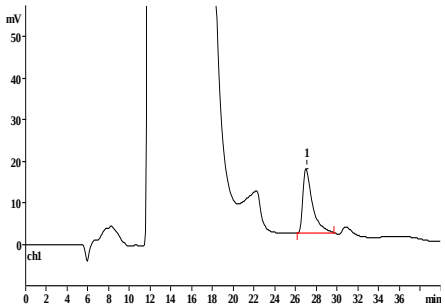

Figure.44 ICP for US – VIII

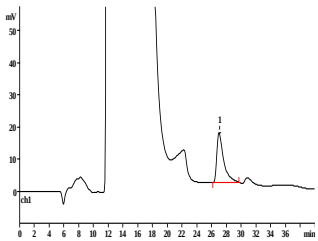

Figure.45 ICP for US – IX

Fig.43 to 45 represents the ICP for sample US – VII,VIII and IX. A characteristic peak appeared at 27.07min with the height and area of the peak of 13.97 mV,15.52mV and 889.265mV*sec, 990.7mV*sec respectively for the concentration of 1126ppm for all the three samples. Phosphate is confirmed in all these samples.

Generally in a Oxalate stone found that the characteristic peak has appeared at 33min to 33min with the height and the area of 3mV to 10mv and 197mV*Sec to 716mV*Sec and for the concentration of 278ppm to 10ppm. Phosphate stone found that concentration 1075ppm to 1126ppm, has peak 25.71min to 27.02min with the height of 4.43 mV to 15.52mV and area of 295mV*Sec to 556mV*Sec.

3.6. CHARACTERISATION STONES BY X-RAY DIFFRACTION STUDIES (XRD):

The Powder X-ray diffraction studies are analysed the purity and identification of the compound can be determined by indexing hkl values with the standard materials, standard ASTM values of the substance. Hence it gives additional supportive evidences for the samples stones.

3.6.1 XRD – Analysis of Oxalate predominate Stones:

XRD patterns of the oxalate samples for US-I,III,X and IV are in figure.46 to 49 are shown below.

Table: 10 XRD Data for Oxalate predominant stones

2Ɵ	D spacing	hkl value
14.26	5.94	200
20.01	4.49	211
24.15	3.65	002
32.17	2.78	411
37.21	2.42	103
40.00	2.21	213

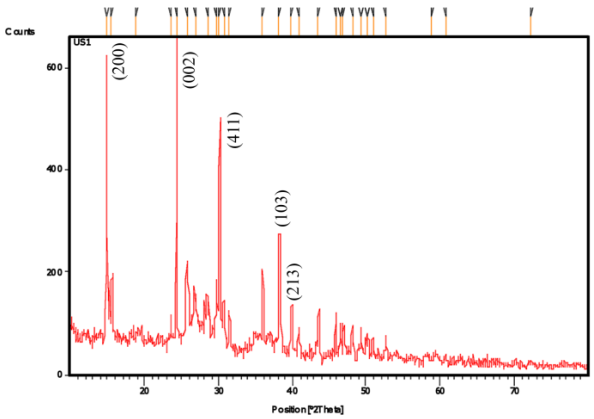

Figure: 46 XRD for US- I

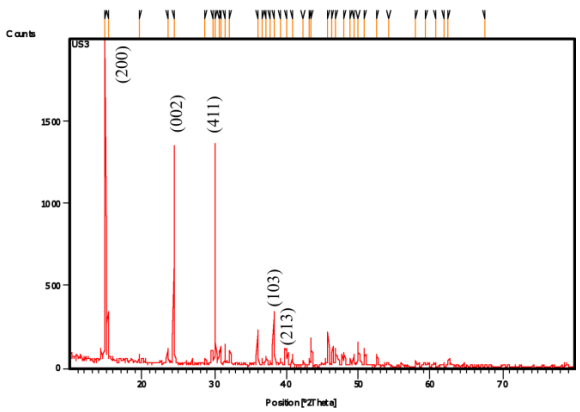

Figure: 47 XRD for US- III

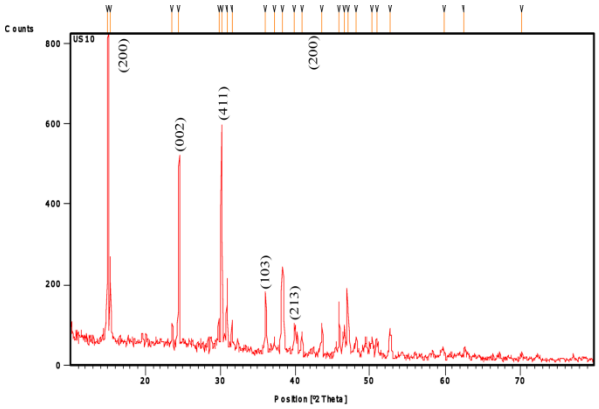

Figure.48 XRD for US- X

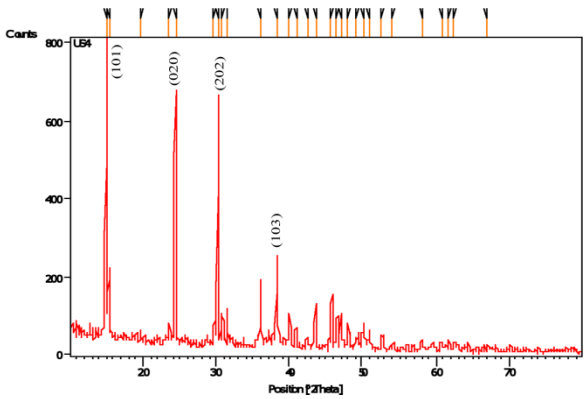

Figure.49 XRD for US- IV

In Figure.46,47 and 48 for US-I,III and X , crystal obtained the following diffraction peaks (2Ɵ):14.26,20.01,24.15,32.17,37.21 and 40.00 which can be correlated to the (hkl) indices (200),(211),(002),(411),(103) and (213) of Calcium oxalate dihydrate.

In Figure.49 for US-IV, crystal obtained the following diffraction peaks(2Ɵ): 14.95,24.39,30.12 and 38.13 which can correlated to the (hkl) indices (101),(020),(202) and (130) of calcium oxalate monohydrate.

3.6.2 XRD –Analysis of Phosphate Predominant stones:

An X-Ray diffraction study also confirms the constitution of the Phosphate stones. In figure.50 to 55 are US-II,V,VI,VII,VIII and IX . In Phosphate stones the 2Ɵ values are correlated to hkl values and d- spacing.

Table: 11 XRD Data for Phosphate predominant stones

2Ɵ		D spacing		hkl value
Std.Phos.	Sample	Std.Phos.	Sample	
10.8	10.5	8.16	8.36	100
16.8	16.5	5.26	5.39	101
21.7	21.5	4.08	4.14	200
22.8	23.0	3.88	3.85	111
25.8	25.8	3.44	3.43	002
28.9	29.0	3.08	3.07	210
31.7	31.9	2.81	2.80	211
32.9	33.3	2.71	2.68	300
32.9	33.7	2.71	2.65	202
35.4	35.8	2.52	2.50	301
42.3	42.4	2.13	2.12	302
46.7	46.3	1.94	1.95	222
50.5	50.7	1.80	1.79	321
54.4	54.6	1.68	1.67	104
57.1	57.8	1.61	1.59	313
69.7	69.9	1.34	1.34	512

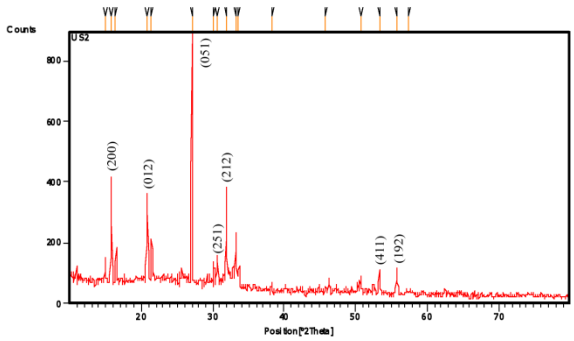

Figure:50 XRD for US- II

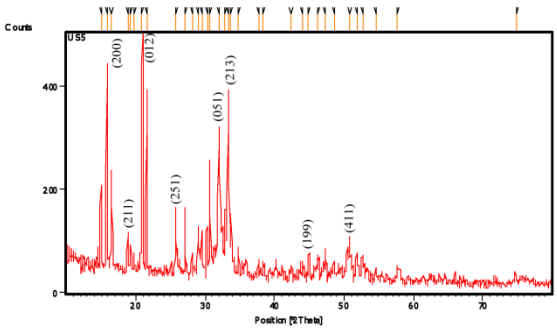

Figure:51 XRD for US- V

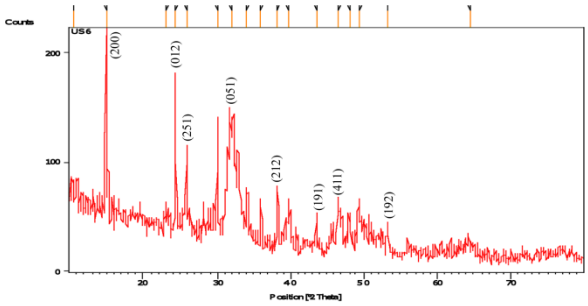

Figure:52 XRD for US- VI

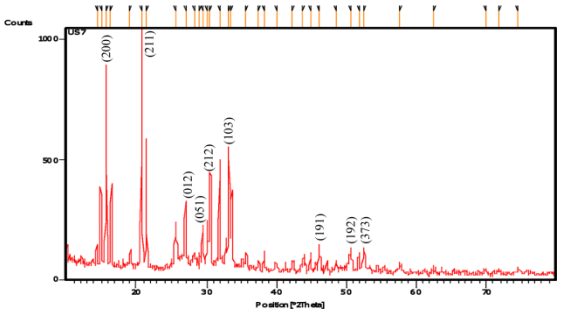

Figure:53 XRD for US- VII

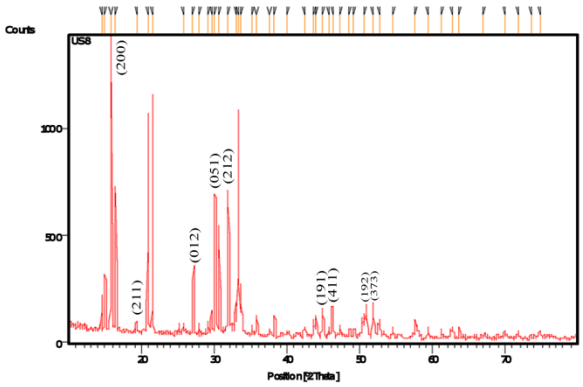

Figure:54 XRD for US- VIII

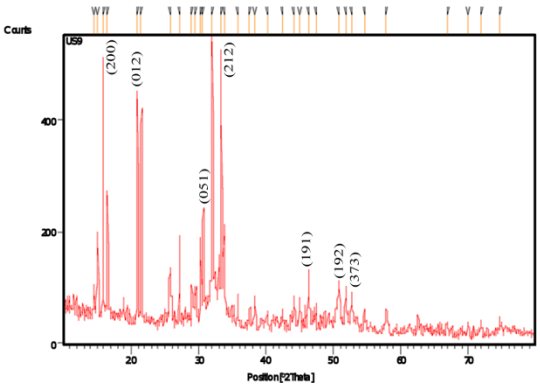

Figure:55 XRD for US- IX

The mixture of Phosphate and Oxalate crystals obtained displays the following diffraction peaks (2Ɵ): 10.5, 16.5, 21.5,23.0, 25.8, 29.0, 31.9, 33.3, 33.7, 35.8, 42.4, 46.3, 50.7, 54.6, 57.8 and 69.9 which can correlated to the (hkl) indices (100), (101),(200),(111), (002),(210),(211),(300) (202), (301),(302),(222), (321),(104),(313) and (512) of phosphate phase.

Powder XRD techniques confirmed the functional groups and crystalline phases of the Calcium Oxalate Monohydrate , Calcium Oxalate Dihydrate and Hydroxy apatite crystals in the Urinary stones.

3.7. CHARACTERSATION OF STONES BY SCANNING ELECTRON MICROSCOPY (SEM):

Present study was to perform Scanning Electron Microscopic assessment of various urinary stones. The morphology, composition, etc., of crystal deposits can be evaluated using microscopy and scanning electron microscopy (SEM) together with elemental distribution analysis. Unfortunately many of the relevant crystals are not recognized in ordinary microscopic analysis of urinary deposits performed in most of the clinical laboratories. This is because the light waves have a limited wavelength compared with that of electronics. Hence it is possible to identify the crystal, however small it may be, through SEM. SEM can produce very high resolution images of a sample surface, revealing details about 1-5 nm in size. The Urinary stones were retrieved with appropriate Pasteur pipettes, and placed on micropore filter paper discs. Thicker layers of filter paper absorbed the paraffin fluid. The dry filter papers along with invisible crystals were fixed to brass studs. These brass studs were taken up for gold sputtering, in order to make them conductive, using a sputter coater. They were gold sputtered to 100 Aº and examined under SEM (JEOL JSM 35 C microscope). In-depth analysis of urinary stone was possible using SEM as electrons were allowed to fall on the sample. When urinary stones were seen, their morphology was recorded by taking photographs at different angles. SEM could give a maximum magnification of 50000 times. Photographs were taken at different magnifications (30-5000) and were recorded.

The use of optical microscopy and SEM combined permits a more far-reaching investigation in modern research areas. The description of some findings, with the aid of examples, explains the efficiency of the system in the investigation of urinary calculus analysis.

3.7.1 SEM – Analysis of Oxalate Predominate Stones:

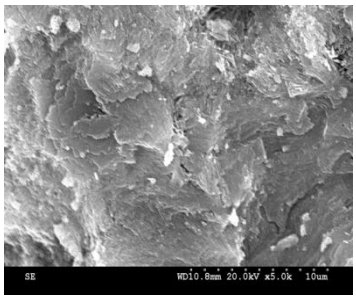

Figure.56 SEM for US- I

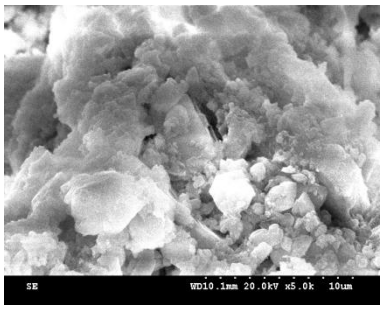

Figure.57 SEM for US- III

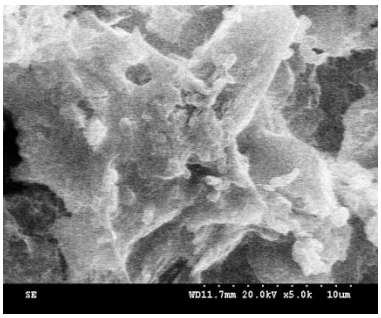

Figure58 SEM for US- IV

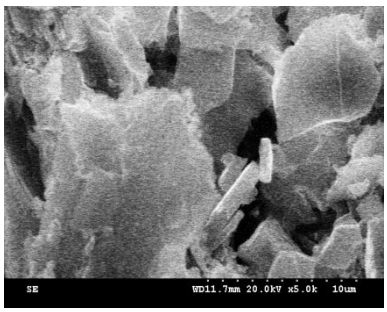

Figure.59 SEM for US- IV

Fig. 56, 57 and 59 represents the morphological analysis using SEM of the samples of urinary stones US-I,III and X respectively which are spherical and plate shape. This results shows the presence of calcium oxalate monohydrate stones.

Fig.58 represents the morphological analysis using SEM of the sample of US – IV, which has rectangular pyramidal shape. This result shows the presence of calcium oxalate dihydrate stone.

3.7.2. SEM – Analysis of Phosphate Predominant Stone:

Fig.60 and 62 represents the morphological analysis using SEM of the samples of Urinary stones US- II and VI respectively which are plate like star shaped crystals. This result shows the presence of Phosphate dihydrate stone.

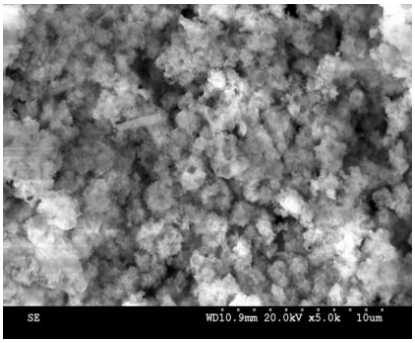

Figure. 60 SEM for US- II

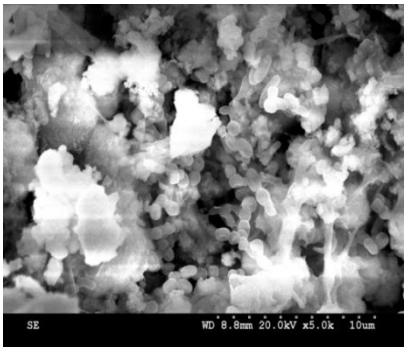

Figure.61 SEM for US- V

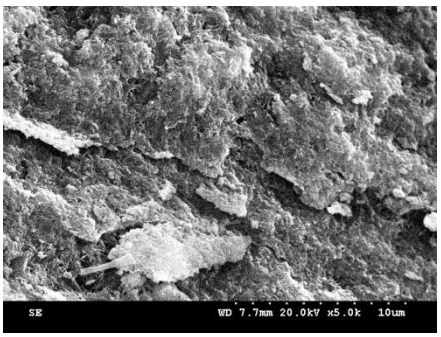

Figure.62 SEM for US- VI

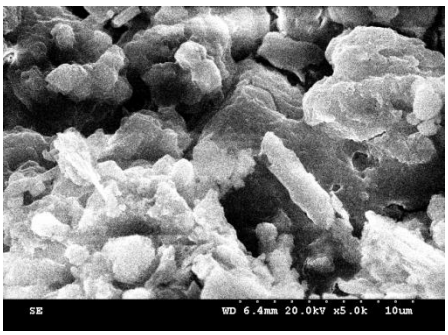

Figure.63 SEM for US- VII

Fig.61 and 63 represents the morphological analysis using SEM of the samples of US – V and VII which are spherical and star shaped crystal. This result shows the presence of oxalate monohydrate and Phosphate dihydrate stone.

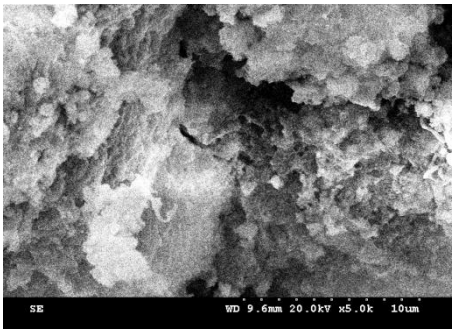

Figure.64 SEM for US- VIII

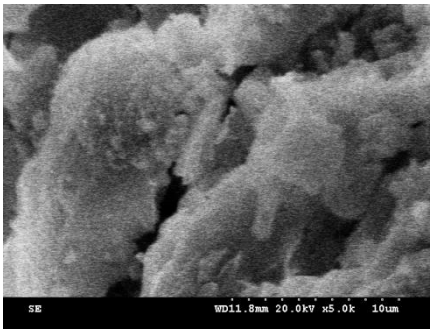

Figure.65 SEM for US- IX

Fig.64 and 65 represents the morphological analysis using SEM of the samples of Urinary stones US- VIII and IX respectively which are plate like star shaped crystals. This result shows the presence of Phosphate dihydrate stone.

Morphological studies of all the urinary stones by SEM, reveals that the Oxalate Monohydrate, Oxalate Dihydrate and Phosphate stones are having spherical shape, rectangular plate and star shaped crystals respectively. On comparison with the shape, the corresponding constituents of urinary stones of the samples US – I to US-X were depicted. The correlation from the morphology also supports that US-I,III,IV and X stones are oxalate predominant with little phosphate concentration and US-II,V,VI,VII,VIII and IX stones are phosphate predominant with less oxalate concentration.

3.8. CHARACTERISATION OF STONES BY EDAX – SEM ANALYSIS:

EDAX is a significant tool for recognizing unknown crystals not identified by ordinary light microscopy or SEM alone. The subsequent elemental distribution analysis allows the determination of mixed phases in a single crystal. EDAX probe was pointed to the crystals under study and the wave patterns were analyzed. Components of the crystals were recognized and analyzed utilizing these data. The subsequent elemental distribution analysis (EDAX) allows the determination of mixed phases.

3.8.1. EDAX –SEM Analysis of Oxalate Predominate Stones:

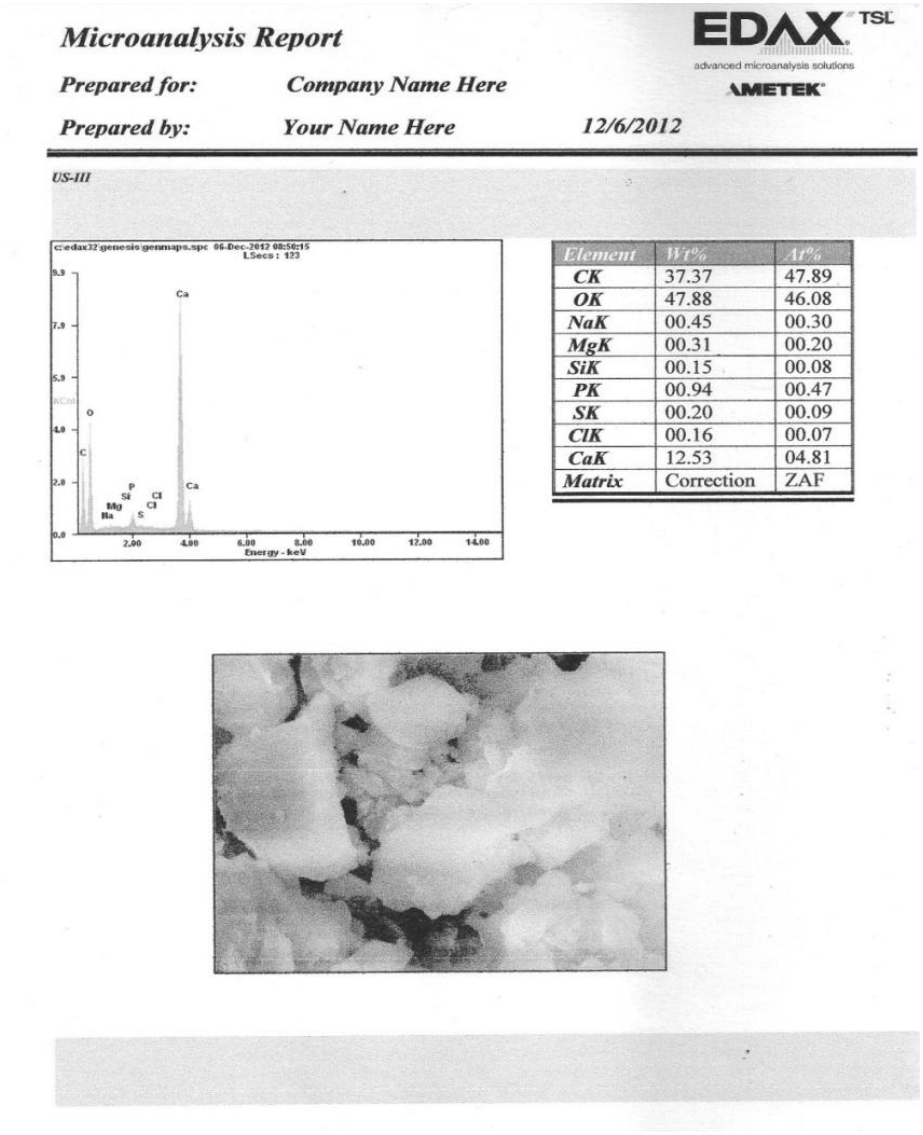

Element	Wt%	At%
CK	37.37	47.89
OK	47.88	46.08
NaK	00.45	00.30
MgK	00.31	00.20
SiK	00.15	00.08
PK	00.94	00.47
SK	00.20	00.09
ClK	00.16	00.07
CaK	12.53	04.81
Matrix	Correction	ZAF

Figure.66 EDAX with SEM for US-III

Elemental analysis using EDAX studies showed in Fig.66 for sample US – III. In SEM studies, reveals that spherical shape. From EDAX analysis predominant element was found to be Oxalate monohydrate (CK and OK – 37.37% and 47.88%). Other elements like C, Na, Mg, Cl, P, Si and O are present in traces.

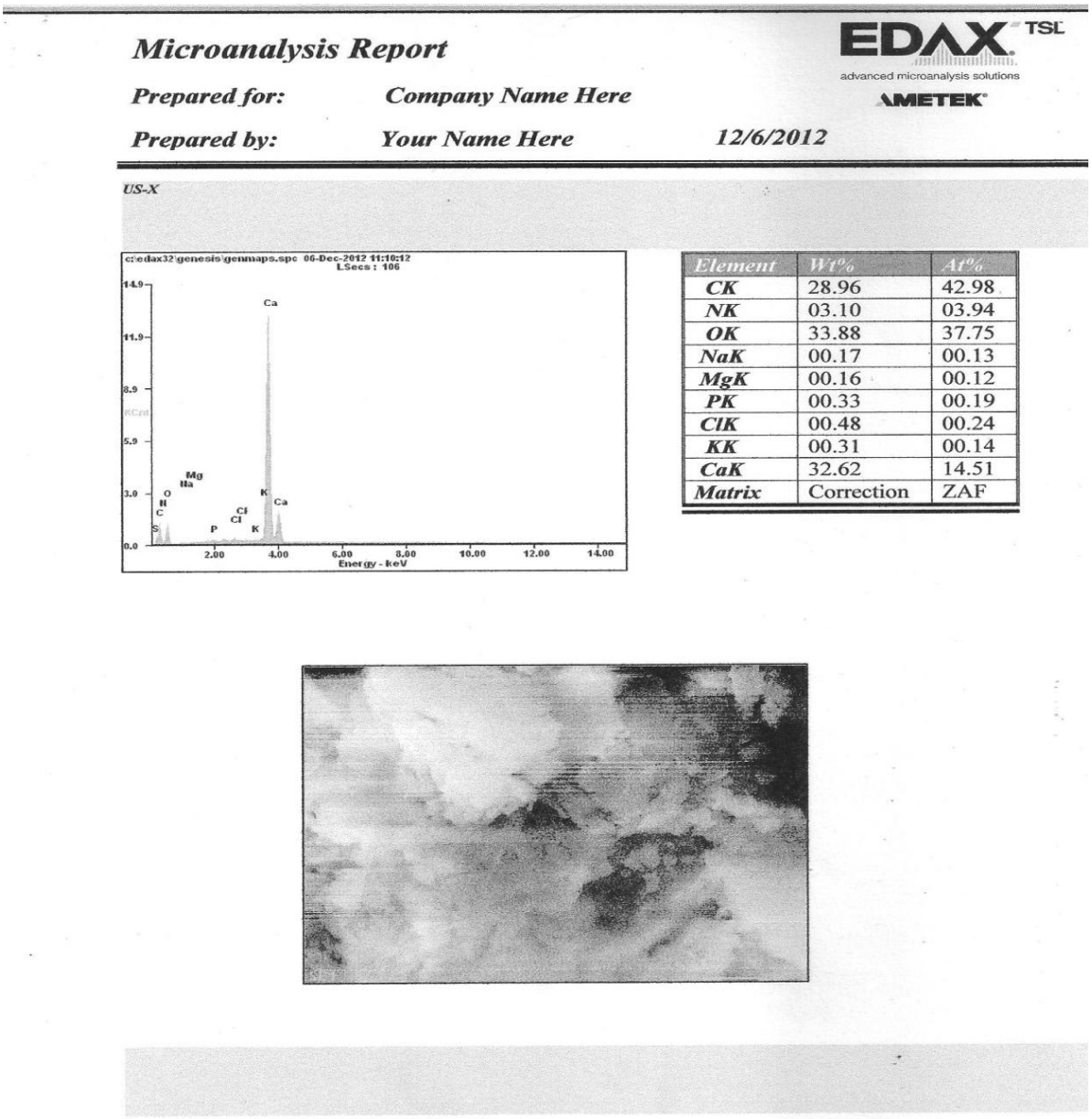

Figure.67 EDAX with SEM for US-X

Elemental analysis using EDAX studies showed in Fig.67 for sample US – X. In SEM studies, reveals that spherical and rectangular shape. From EDAX analysis predominant element was found to be Oxalate mono and dihydrate (CaK and OK -32.62% and 33.88%). Other elements like C, Na, Mg and O are present in traces.

3.9.2. EDAX – SEM Analysis of Phosphate Predominant stone:

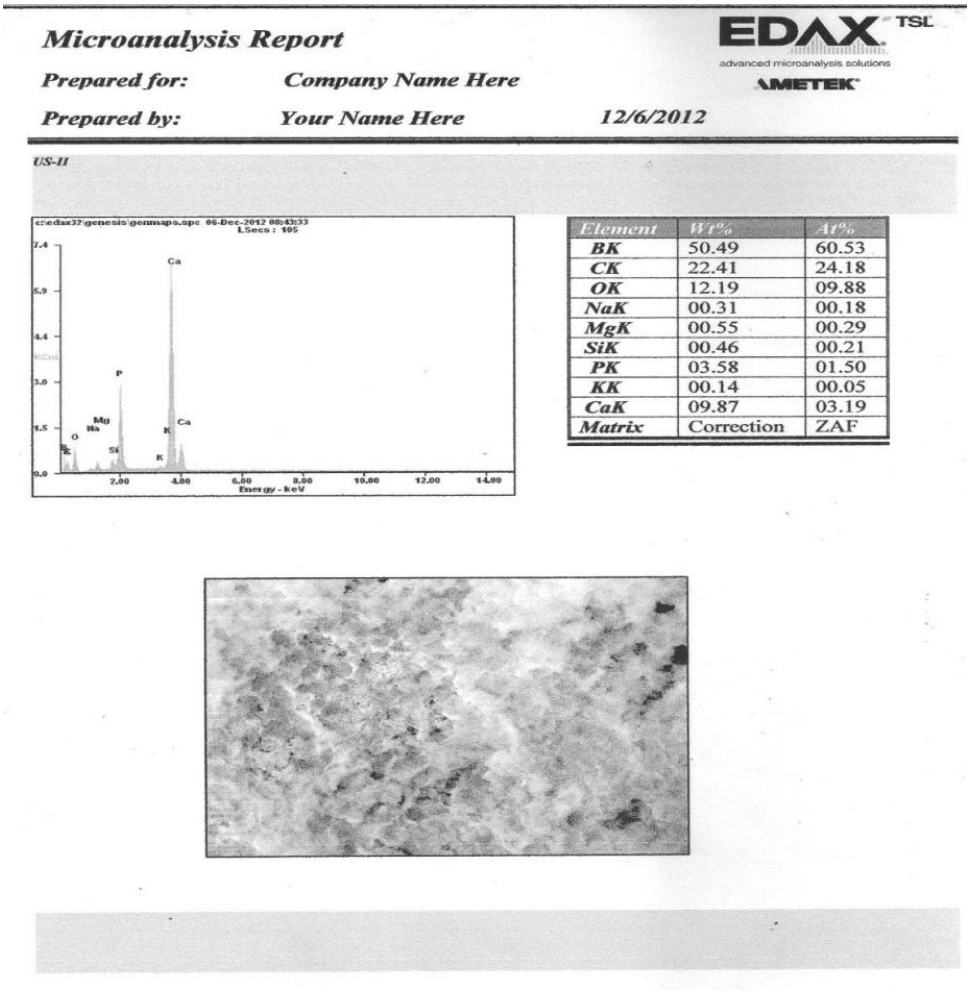

Element	Wt%	At%
BK	50.49	60.53
CK	22.41	24.18
OK	12.19	09.88
NaK	00.31	00.18
MgK	00.55	00.29
SiK	00.46	00.21
PK	03.58	01.50
KK	00.14	00.05
CaK	09.87	03.19
Matrix	Correction	ZAF

Fig.68 EDAX with SEM for US-II

Elemental analysis using EDAX studies showed in Fig.68 for sample US –II. In SEM studies, reveals that plate like and star shaped crystals. From EDAX analysis predominant element was found to be oxalate (OK - 12.19%) and phosphorous (PK-3.58%). Other elements like Na, Mg, Si and K are present in traces.

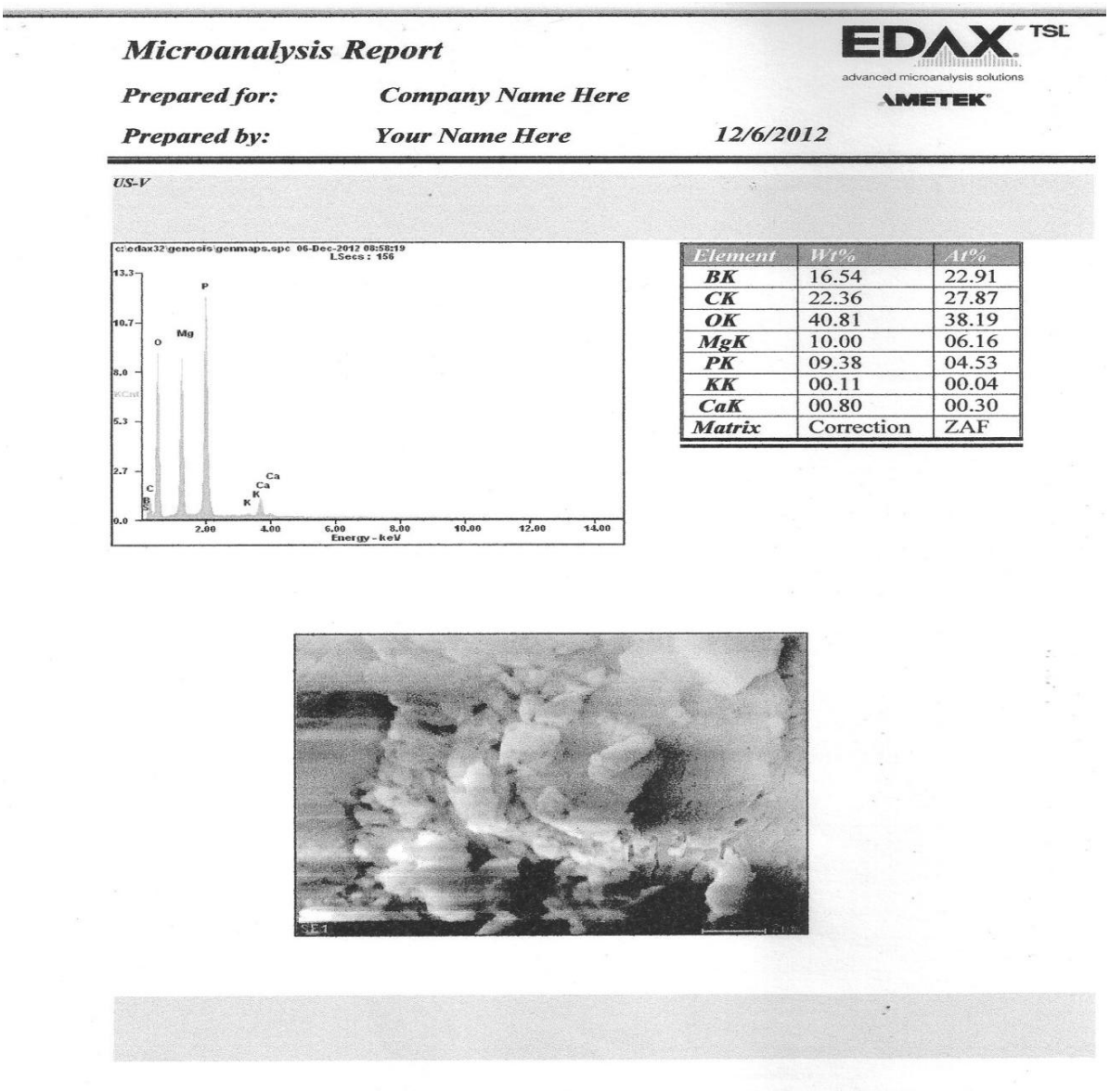

Fig.69 EDAX with SEM for US-V

Elemental analysis using EDAX studies showed in Fig.69 for sample US – V. In SEM studies, reveals that spherical and star shaped crystal. From EDAX analysis predominant element was found to be Oxalate (OK – 40.8%) and Phosphate monohydrate (9.38%). Other elements like Mg, Ca and K are present in traces.

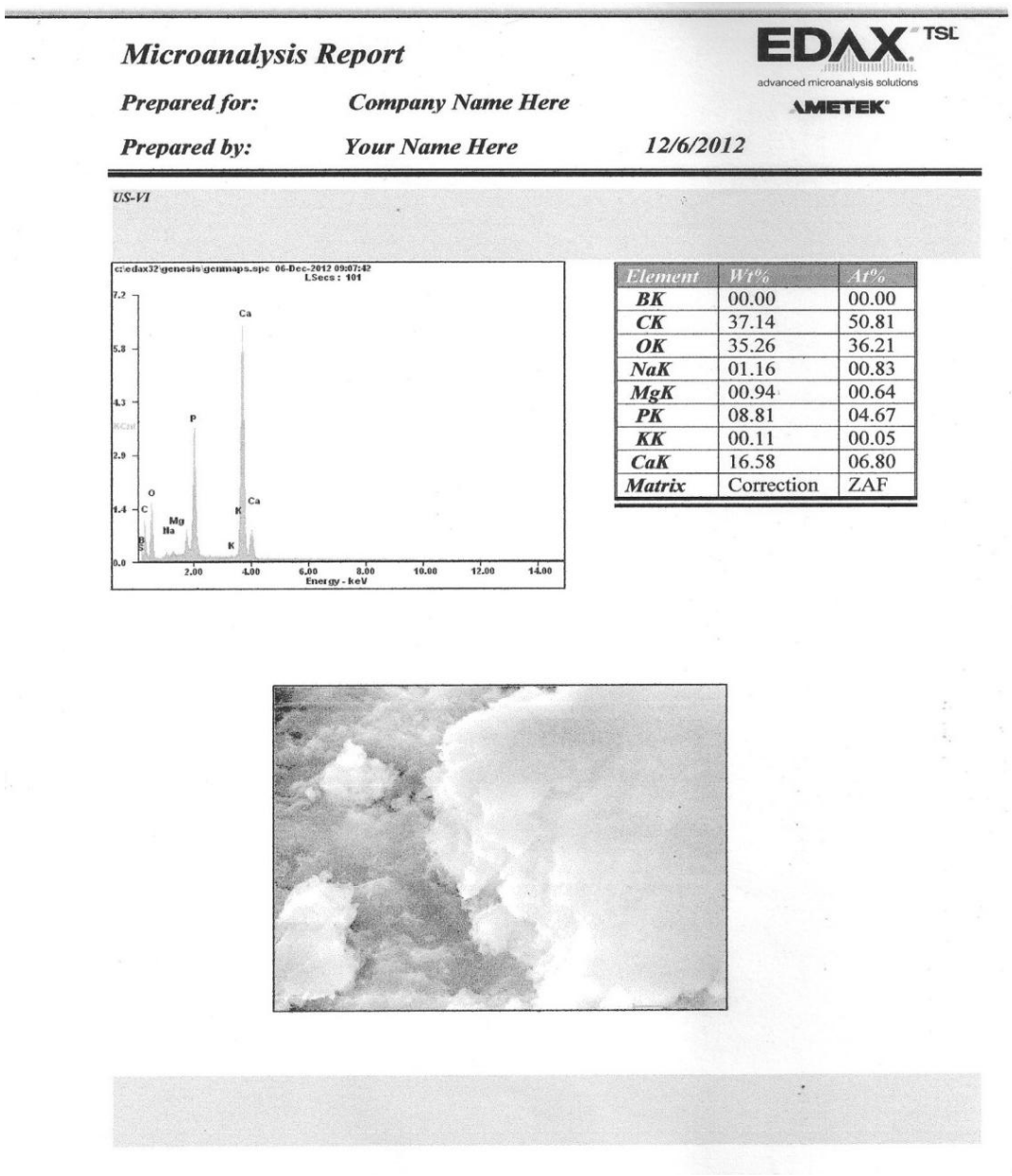

Fig.70 EDAX with SEM for US-VI

Elemental analysis using EDAX studies showed in Fig.70 for sample US –VI. In SEM studies, reveals that plate like crystals. From EDAX analysis predominant element was found to be phosphorous (PK – 8.8%) and oxalate (OK – 35.26%). Other elements like Ca, Mg, K,Na and B are found in traces.

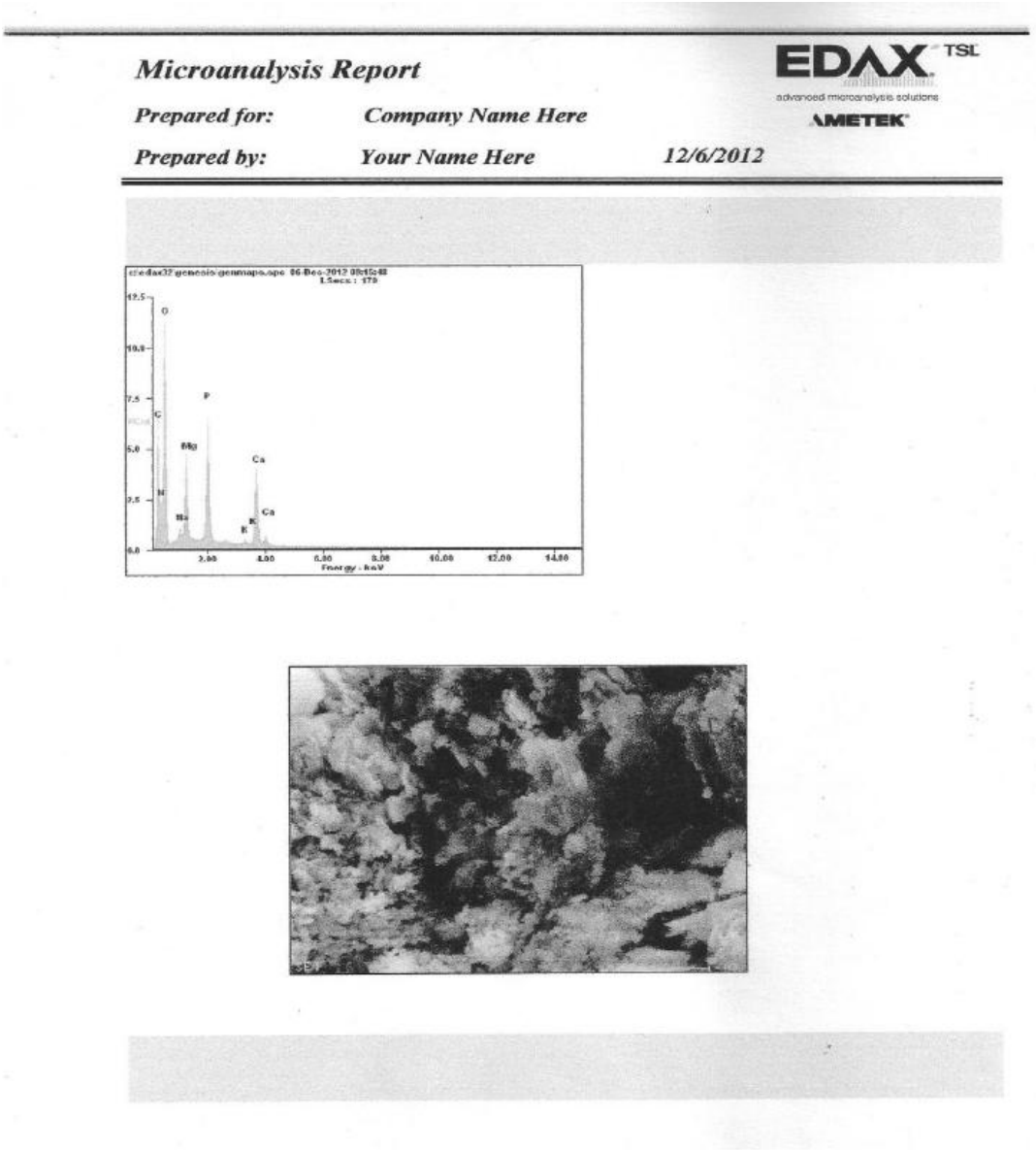

Fig. 71 EDAX with SEM for US-VII

Elemental analysis using EDAX studies showed in Fig.71 for sample US – VII. In SEM studies, reveals that spherical and star shaped crystal. From EDAX analysis predominant element was found to be Oxalate (OK- 41.8%) and Phosphate monohydrate (PK-3.08%). Other elements like Mg, Ca, Na and K are found in traces.

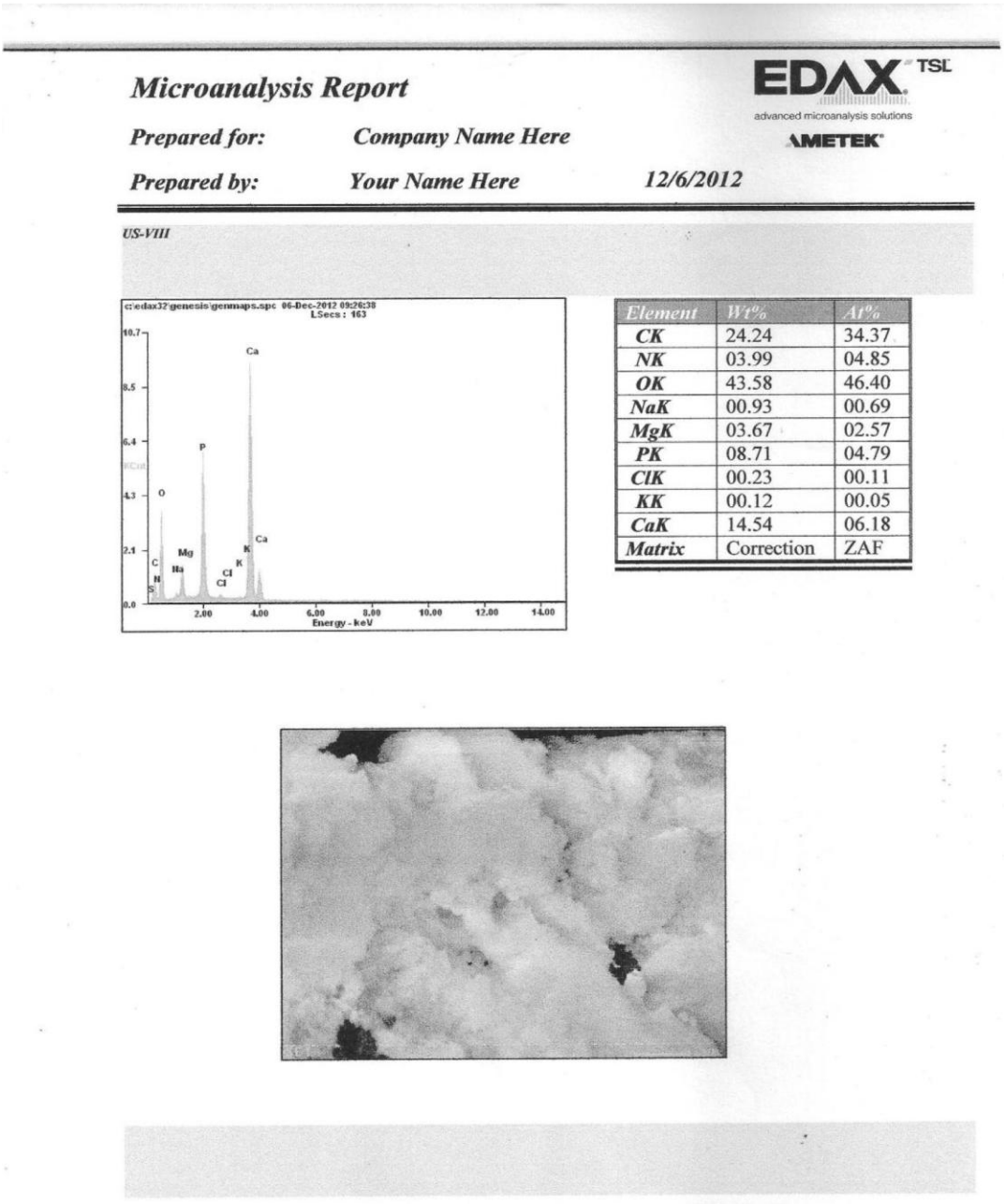

Fig.72 EDAX with SEM for US-VIII

Elemental analysis using EDAX studies showed in Fig.72 for sample US – VIII. In SEM studies, reveals that plate like star and spherical shaped crystal. From EDAX analysis predominant element was found to be Phosphate (PK-8.7%) and oxalate (OK – 43.58%). Other elements like N, Na, Mg, Cl and K are present in traces.

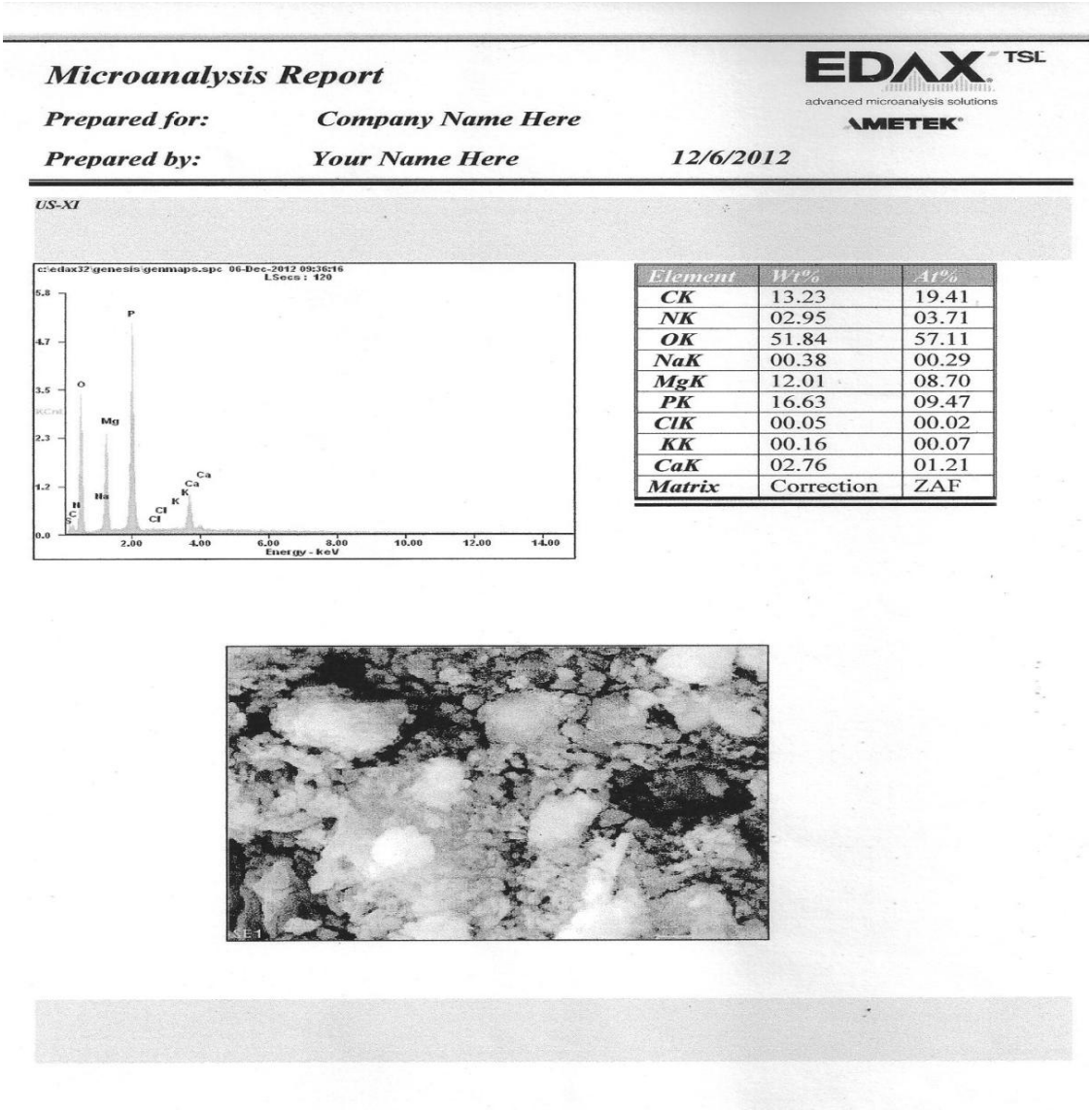

Figures.73 EDAX with SEM for US-IX

Elemental analysis using EDAX studies showed in Fig.73 for sample US – IX. In SEM studies, reveals that plate like star and spherical shaped crystal. From EDAX analysis predominant element was found to be Phosphate (PK-16.6%) and Oxalate (OK – 51.8%). Other elements like N, Na, Mg, Ca, Cl and K are found in traces.

Combination of SEM and EDAX always aids the morphology and the chemical constituents in a predictable manner. Here also for all the samples the already predicted chemical composition is further supported and confirmed by SEM and EDAX analyses. The presence of other elements like C, Na, Mg, Cl, P, Si and O are found in traces which may be due to food intake and secretion in urine and deposition along with the kidney stones.

3.9. CHARACTERISATION OF STONES BY DIFFERENTIAL SCANNING CALORIMETRY (DSC):

The thermal stability was analyzed for the stones by the Differential Scanning Calorimetry of the samples. In DSC the samples undergoes an exothermic or endothermic reaction. In exothermic peak always represents phase transition, crystalline transition, allotropic modification etc., and endothermic reaction elimination of neutral molecules decomposition of fragments etc. Hence, based on the above facts the thermal behaviors of various stones at temperature range 10 to 500ºC carried out. As the crystals decomposed above 500ºC DSC studies is performed between 10-500ºC to depict clearly the thermal transformation.

3.9.1 DSC Analysis for Oxalate Predominate Stones:

Oxalate stones are thermally stable at high temperature. In oxalate stones crystalline transition occur at 50º to 250ºC. So, these stones undergo an exothermic reaction.

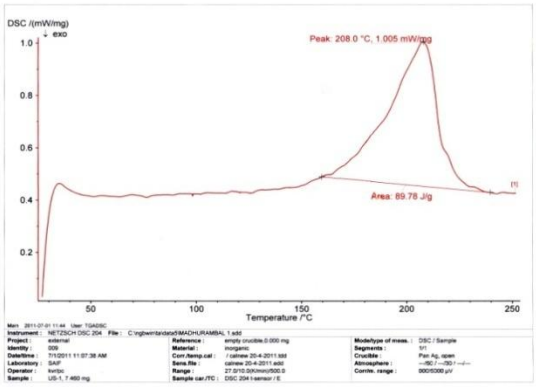

Figure:74 DSC for US-I

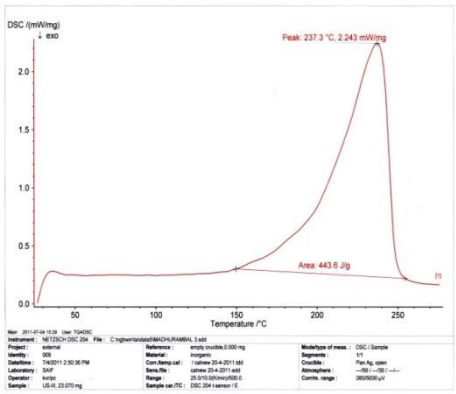

Figure:75 DSC for US-III

Fig.74 and 75 represents the DSC for US-I and US-III. the samples absorbed high temperature at 208˚C and 237˚C respectively, it undergoes an exothermic reaction. The areas of the peaks are 89.78J/g and 443.6J/g. Among the samples US-I has less peak area because the very major constitution is oxalate.

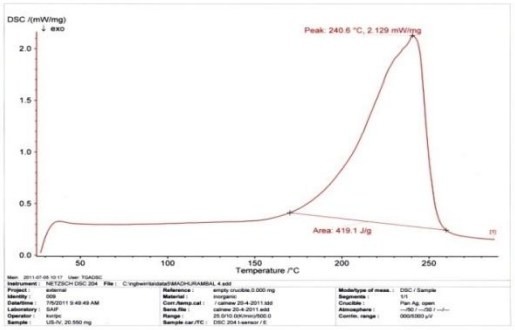

Figure:76 DSC for US-IV

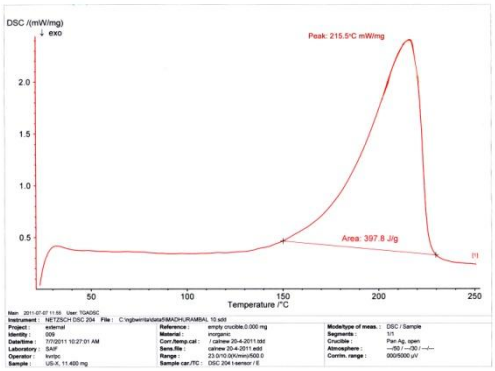

Figure.77 DSC for US -X

In above figure.76 to 77 for DSC of US- IV and X, the samples absorbed high temperature at 208˚C, 237˚C, 240.6˚C and 215˚C respectively, it undergoes an exothermic reaction. The areas of the peaks are 89.78J/g,443.6J/g,419.1J/g and 397.8J/g. Among the samples US-I has less peak area because the very major constitution is oxalate. The rest of the samples are mixture of Oxalate and Phosphate but the major constitution is oxalate. The Oxalate stones may be Lessing dissociated in the range of 150º to 250ºC to Carbon dioxide and water.

3.5.2 DSC Analysis for Phosphate Predominant Stones:

In our present study, we observed that Phosphate stones absorbed low temperature than the oxalate stones. The Phosphate stone undergoes exothermic reaction.

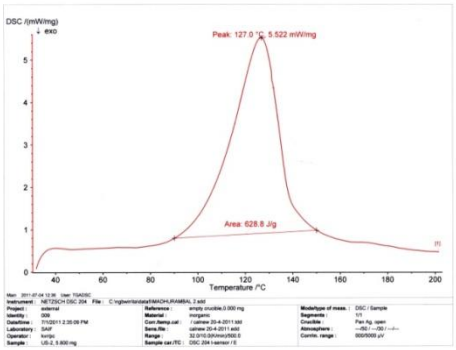

Figure:78 DSC for US-II

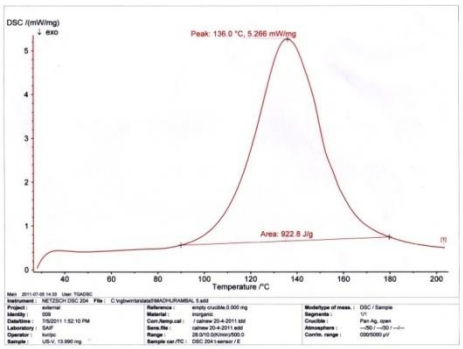

Figure:79 DSC for US-V

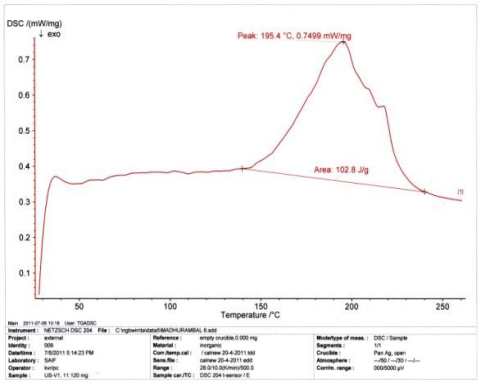

Figure:80 DSC for US-VI

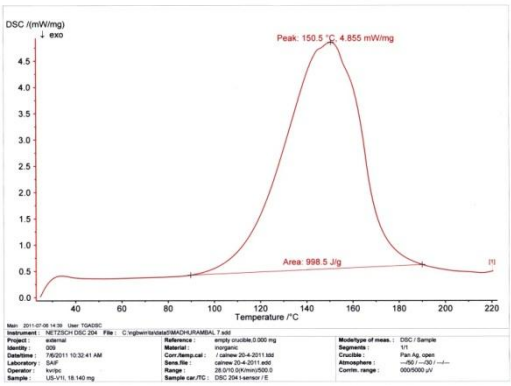

Figure:81 DSC for US-VII

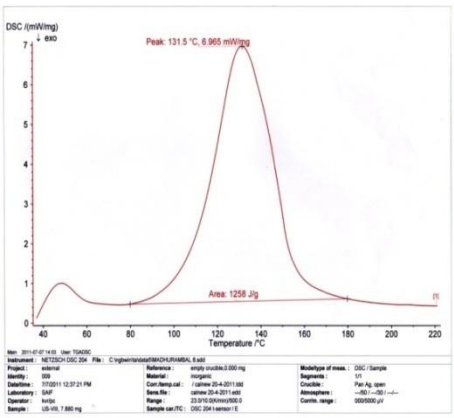

Figure:82 DSC for US-VIII

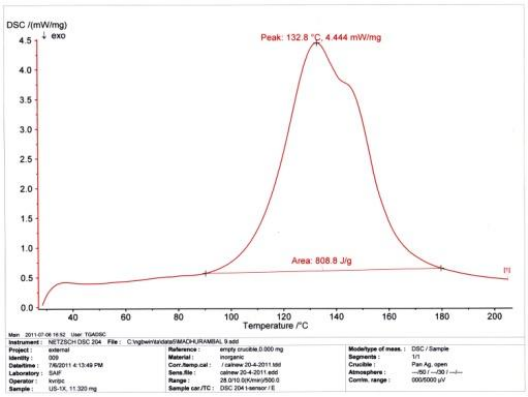

Figure:83 DSC for US-IX

In Figure.78 to 83 for the samples of US-II, V, VI, VII, VIII & IX, the samples absorbed 127˚C, 136˚C, 195˚C, 150˚C, 131˚C, 132˚C respectively. It undergoes exothermic reaction. The peak area for the samples are 628J/g, 922J/g, 102J/g, 998J/g, 1258J/g and 808J/g. These stones are dissociated in between 80˚C

to 150˚C. When compared to oxalate stones, phosphate stones are easily dissociated at low temperature. In figure.52, it dissociation at 195˚C .So, it is mixture of Phosphate and Oxalate stones, but the major constitution is phosphate. The evolution of high heat energy denotes the presence of Inorganic phosphate ion in the crystals which is more stable compound to oxalate moiety.

Conclusion:

The analysis of urinary stones its constitution are confirmed by Qualiatative, UV,XRD,DSC, FT-IR ICP,SEX and EDAX analysis. The sizes of the samples are determined by optical microscopy. FT-IR confirms the bending and stretching frequency for oxalate and phosphate stones. XRD results are in agreed with those of FT-IR. ICP results show the composition of oxalate and phosphates. EDAX analysis shows an appropriate magnification study the morphology of the stone and various elements present in the sample. Elemental distribution analysis makes it possible to confirm the SEM results and also percentage of different elements present in a single sample can be evaluated.

REFERENCES:

1. J.A.E.Wickham,Urinary calculus diseases, Churchill Livinfstone Edinburgh,1979.
2. G.H.Nancollas, G.L.Gardner, J.Cryst. Growth 21(1974)267.
3. E.J.Westbury,Br.J.Urol.46(1974)215.
4. G.L.Gardner,J.Crystal Growth 30 (1975) 158.
5. C.A.Osborne , L.S.Davis ,J.Sanna et al identification and interpretation of crystalluria in domestic animals, alight and scanning electron microscopic study. Vet Med 85:18-37.
6. P.Walther,E. Wehrli, R. Hermann, M.Miller (1995) Double layer coating for high resolutionlow temperature SEM.J. Microscopic 179:229-237.
7. E.K.Girija,S.Christic Latha, S.Narayana Kalkura, C.Subramanian, P.Ramasamy Crystallization and microhardness of calcium oxalatemonohydrate, Materials chemistry and Physics 52(1998)253-257.
8. Bharat Parekh, Mihir Joshi, ashok Vaidya, Characterization and inhibitive study of gel growth hydroxyapatite crystals at physiological temperature , J. Crystal growth310(2008) 1749-1753.

CHAPTER -3

PHYTOCHEMICAL INVESTIGATION OF TRIBULUS TERRESTRIS PLANT

Introduction :

The genus Tribulus comprise Ca 20 species which grow as shrubs in subtropical areas around the world. There are only two species distribution in China Tribulus terrestris and Tribulus cistoides. In traditional Chinese medicine the fruit of Tribulus terrestris which is known as Ci Ji Li, has been used against various diseases for a long time.

Tribulus terrestris is the scientific name of an herbal supplement. It is an annual herb of worldwide distribution. The plant is used in the folk medicine in India, China, Bulgaria and other countries against various diseases like cardiac diseases, edema, eye trouble, skin itch and impotence. It is commonly known as puncture vine or Caltrop. It is a perennial herb and it belongs to the Zygophyllaceae[1] family. It can grow in a warm, desert climate and survives even in a poor soil condition. The regions where it is most commonly found are Africa, northern parts of Australia, southern part of Europe and parts of Asia. Normally, the height of this plant is not more than one meter. The flower of the plant that are small in size and faint yellow in color. Its fruit has a five angled shape and have spines on its surface. There are medicinal properties of tribulus terrestris, due to two active components of saponins present in its leaves. These steroidal saponins are - furostanol glycosides and spirostanol glycosides[2]. In commerce and local market Tribulus is called 'Chhota Gokshru' ''Gokshru''is a famous Indian Ayurvedic Vajikarana medicine.

Material and Methods:

Aerial parts of Tribulus terrestris, collected in December 2010 in the region of Cauvery basin area, were used after drying. The air dried fruits Tribulus terrestris (10 kg) were ground to the size through mesh sieve No.10 and extracted with 60% ethanol for 2 h. The ethanol extract was concentrated under reduced

pressure to obtain a crude residue, which was chromatographed over a macroprous resin column(10×80cm), eluted successively with water -30% and ethanol-70% , glycoside, saponin, Tannnin, Flavonoide and Phenol were separated[1]. The isolated saponin and glycoside fractions are analyzed using FT-IR Spectroscopy, Nuclear Magnetic Resonance and Gas Chromatography – Mass Spectroscopy.

Thin Layer Chromatography:

Thin layer chromatography is one of the valuable and versatile methods for analysis of wide rang biomolecules. TLC is nothing but a modification of paper chromatography. Where the sheet of paper is replaced by thin layer of absorbent material. Therefore the separation in TLC is also due to the differential partition of solutes between the stationary and mobile phases.

Principle:

The general principle involved in TLC is similar to that of column chromatography, i.e., adsorption chromatography. In the adsorption process the solute competes with the solvent for the surfaces sites of adsorbent. Depending on the distribution coefficients the compounds are distributed on the surface of the adsorbent of course, in TLC the partition effect in the separation is also not ruled out. The adsorbent normally used contains a binding agent such as Calcium Sulphate which facilitates the holding of the adsorbent to the glass plate.

Procedure:

The stationary phase is prepared as slurry with water or buffer at 1:2 and applied to a glass plate or an inert plastic or aluminum sheet, as thin uniform layer by means of a spreader such as glass rod or pipette or using a TLC applicator. (0.25mm thickness for analytical separations and 2-5mm thickness for preparative separations are prepared).

Calcium Sulphate (10-15%) is incorporated to adsorbent as a binder, as it facilitates the adhesion of the adsorbent to the plate. After application of the adsorbent, the plates are air-dried for 10-15 minutes and then oven dried for 10-15 minutes at 100ºC-110ºC. This process is also known as activation of the adsorbent. The plates can be used immediately or stored in desiccators and used in separation.

FT-IR Spectroscopy:

The FTIR spectral analysis of the samples were carried out in **PERKIN ELMER FTIR** spectrometer using the KBr pelleting technique [4].All the ten samples are scanned using FTIR spectroscopy in between 400cm^{-1} to 4000cm^{-1}. The changes in the vibrational movements of the molecule are used for the detection of almost all functional groups.

Nuclear Magnetic Spectroscopy:

The NMR spectra were recorded in CH_3OD on a Brucker DRX 600 spectrometer.[5] ^{1}H and ^{13}C – spectra were obtained in a 1D and 2D NMR spectra are confirmed by chemical transformation. The homo nuclear proton-proton 2D (COSY and NOSEY) and heteronuclear proton- carbon 2D (HSQC) experiments were carried out.

Gas Chromatography-Mass Spectroscopy:

The GC-MS was carried out using a clarus 500 Perkin – Elmer Gas chromatograph equipped and coupled to a mass dector Turbo mass gold – Perkin Elmer Turbomass 5.1 spectrometer with an Elite -1 (100% Dimethyl poly siloxane), 30×0.25 mm maintained at this temperature for 2 min.[6] At the end of this period the oven temperature was rise upto 280ºC, at the rate of an increase of 5ºC/min, and maintained for 9 min. Injection voltage temperature was ensured as 250ºCand Helium flow rate as one ml/min. The ionization voltage was 70eV. The samples were injected in split mode as 10:1. Mass spectral scan range was set at 45-450(m/z).

Identification of Various Fraction by TLC:

Drawn a line lightly with a pencil about 1.5 -2.0cm from the bottom. If the thin layer was too soft to draw a pencil line, place a scale at the bottom and spot at as distance of ~1.5cm. Noted down the order. The samples were spotted using capillary tubes at ~1.5cm distances between them for preparative TLC, the sample was applied as a band across the layer rather than as a spot.

Plate Development:

The chromatographic tank was filled with developing solvent to depth of ~1.5cm and equilibrated for about 5 hrs. The thin layer plate was placed gently in the tank and allowed to stand for about 60min. made sure the spots do not touch the solvent directly capillary action caused the solvent to ascend as in paper chromatography and the separation of compounds takes place, the plate was removed, solvent front was marked with a pencil immediately and allowed to air dry placing the plate upside down.

Fig.84 TLC For Alkaloid

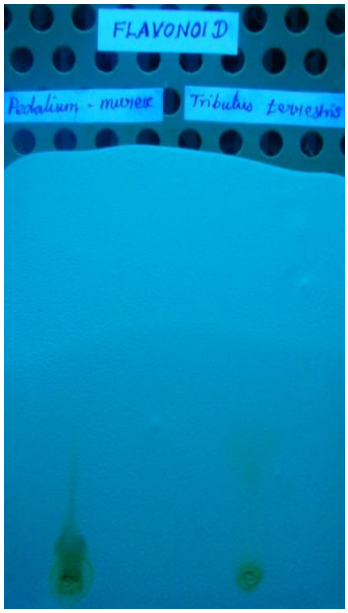

Fig.85 TLC For Flavonoid

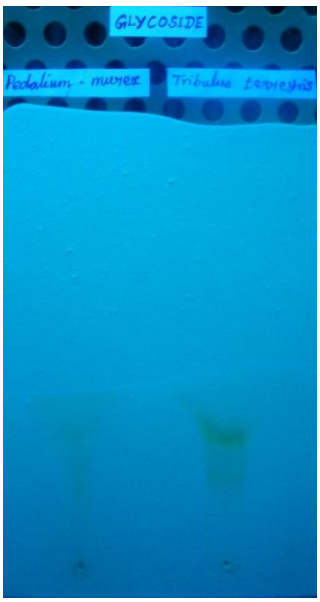

Fig.86 TLC For Glycoside

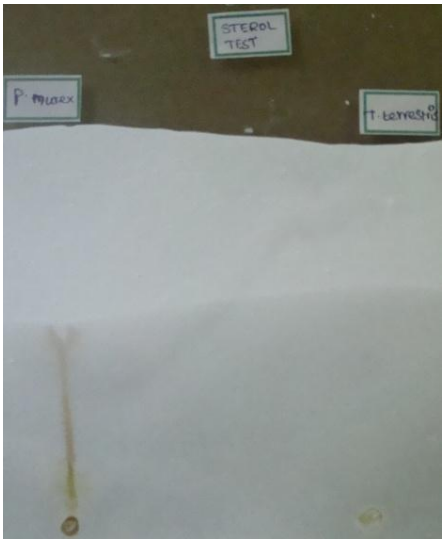

Fig.87 TLC For Phenol **Fig.88 TLC For Sterol**

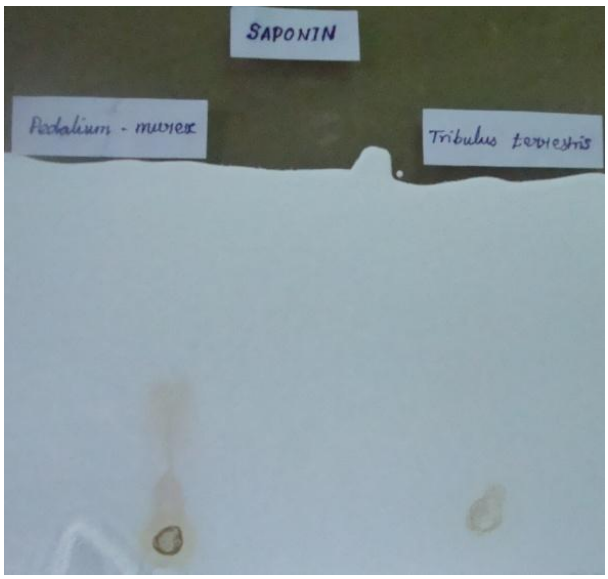

Fig.89 TLC For Tannin **Fig.90 TLC For Saponin**

Alkaloids:

The samples of P.Murex and T.Terrestris was wetted with a half diluted ammonium hydroxide and lixiviated with ethyl acetate for 24hrs at room temperature. The organic phase is separated from the acidified filtrate and basified with ammonium hydroxide. It is extracted with chloroform condensed by evaporation and used for chromatography. The alkaloid spots were separated using the solvent mixture chloroform and methanol in the ratio 15:1. The colour

and R_f value of the separated alkaloids were recorded both under Ultraviolet and visible light after spraying with Dragendroff's reagent.

Flavonoids:

The samples of P.Murex and T.Terrestris was extracted with 10ml methanol on water bath (60◦C/5min). The filtrate was condensed by evaporation, added a mixture of water and ethyl acetate in the ratio of 10:1 and mixed thoroughly. The ethyl acetate phase thus retained was used for chromatography. The flavonids spots were separted using chloroform and methanol solvent mixture in the ratio of 19:1. The color and R_f value of these spots were recorded under UV light.

Glycosides:

The samples of P.Murex and T.Terrestris was extracted with 70% ethanol on rototary shaker for 10hrs. 70% lead acetate was added to the filtrate and centrifuged at 5000rpm/10min. Then the supernatant was further centrifuged by adding 6.3% Sodium Carbonate at 10000rpm/10min. The retained supernatant was dried, redissolved in chloroform and used for chromatography. The glycosides were separated using ethyl acetate-methanol- water solvent mixture in the ratio 80:10:10. The color and R_f values of these spots were recorded by observing under UV light.

Phenols:

The samples of P.Murex and T.Terrestris was lixiviated in methanol on rototary shaker for 24h. The condensed filtrate was used for chromatography. The phenols were separated using chloroform and methanol solvent mixture. The color and R_f values of these phenol spots were recorded under visible light after spraying the plated with Folin Ciocalteu's reagents heating at 80ºC/10min.

Saponins:

The samples of P.Murex and T.Terrestris was extracted with 10ml 70% ethanol by refluxing for 10min. The filtrate was condensed enriched with saturarted n-butanol and thoroughly mixed. The butanol was retained, condensed and used for chromatography. The saponins were separated using chloroform, glacial acetic acid, methanol and water solvent mixture in the ratio of 64:34:12:8. The color and R_f values of these spots were recorded by exposing chromatogram to the iodine vapours.

Sterols:

The samples of P.Murex and T.Terrestris were extracted with 10ml 70% methanol in water bath (80◦C/15min). The condensed filtrate is used for chromatography. The sterols were separated using chloroform, glacial acetic acid, methanol and water solvent mixture in the ratio of 64:34:12:8. The color and R_f values of these spots were recorded under visible light after spraying the plates with anaisaldehyde-sulphuric acid reagent and heating at 100°C/6min.

Tannins:

The sample of P.Murex and T.Terrestris was diluted with ethyl acetate for 24hrs at room temperature. The organic phase is separated. It was extracted with chloroform condensed by evaporation and used for chromatography. The tannin spots were separated using the solvent mixture Toluene:acetone:formic acid in the ratio of 60:60:10. The color and R_f values of the separated Tannins were recorded after spraying with Butler Prussian blue reagent.

Sapogenin:

The separation of the compound Sapogenin was achieved by n-Hexane: Ethyl acetate (5:1) as the mobile phase. The ethanolic extract of aerial parts of *P. murex* was used as the sample. Kagi mischer reagent was used as a spraying reagent. Plates were subjected to visualization for band formation under UV.

Diosgenin:

The separation of the compound Diosgenin was achieved by Toluene: Ethyl acetate: Glacial acetic acid: Formic acid (2:1:1:0.75) as the mobile phase. The ethanolic extract of aerial parts of *P. murex* is used as the sample. Plates were subjected to visualization for band formation under UV.

Oleanolic acid Saponin

The Oleanolic acid saponin spots were separated using the solvent mixture Ethyl acetate and Hexane in the ratio of 2:1. The color and R_f value of the separated alkaloids were recorded both under Ultra Violet (UV 366 nm) and visible light.

Table: 12 R_f Value – P.Murex and T.Terrestris

S.No.	Name of the test	R_f – P.Murex	R_f-T.Terrestris
1.	Alkaloids	0.91	0.90
2.	Flavonids	0.64	0.66
3.	Glycoside	0.92	0.96
4.	Phenol	0.93	0.90
5.	Saponin	0.6	0.59
6.	Sterols	0.95	Absent
7.	Tannins	0.95	0.61

SEPARATION AND PURIFICATION OF SAPONIN AND GLYCOSIDE:

The separated compounds were purified using the solvents which were used to isolate the compounds in TLC. The compounds were allowed to get dissolved into in a solvent thus results the individual pure fractions of Phytocompound.[1] The combined ethanol solutions were concentrated to reduce a

volume as 3lit. and extracted in succession with Et_2O(3×24h×1.5lit.) and EtOAc (4×24h×1.5lit,). The EtOAC layer was concentrated to dryness giving the crude Glycoside residue. The residue from EtOAc fraction was taken up in a small quantity of Me_2CO left in an ice-chest for a few days. The yellow solid that separated was filtered and recrystallised from aqueous methanol, yielded yellow needles (m.p.225º). The yellow needles were analyzed using FT-IR, ^1H and ^{13}C-NMR spectra of the glycoside and their assignment to various carbon atoms were identified.

The combined ethanol solutions were concentrated to reduce a volume as 3l and extracted in succession with cholorform(3×24h×1.5l) and n-butanol (3×24h×1.5l). The n-butanol layer was concentrated to dryness giving the crude saponin extract. Again crude saponin extract is further separated by Liquid Vaccum Chromatograph (LVC) of silica gel using Chloroform-Methanol-Water (6:1:0.1 to 1:1:0.1) and the fractions F1 to F7 were obtained. The fraction F4 was subjected to Medium-Pressure-Liquid Chromatography (MPLC) with Methanol-Water (3:7 to 4:1) and for addition of eluents the fractions were collected as S1 to S7. The fraction 3-6 was repeatedly subjected to HPLC with Methanol-Water (4:1) and polyamine HPLC with Methyl Cyanide – Water (87:13) to gave three fractions (17:3;43:7;87:13) in which 17:3 gave Desgalactotigonin, 43:7 gave Gitonin and 87:13 gave terrestrosin A.

Desgalactotigonin: It is microneedles from methanol, m.p 240º, ^1H and ^{13}C NMR data :Table 14. Gitonin : It is needles from methanol, m.p 248º, ^1H and ^{13}C NMR data :Table 14. Terrestrosin A : It is needles from methanol, m.p.225º, ^1H and ^{13}C NMR data :Table 14.

FOURIER TRANSFORM INFRARED SPECTROSCOPY FOR GLYCOSIDE:

The FTIR spectral analysis of the samples were carried out in **PERKIN ELMER FTIR** spectrometer using the KBr pelleting technique[4].The Glucoside sample are scanned using FTIR spectroscopy in between 400cm^{-1} to 4000cm^{-1}.

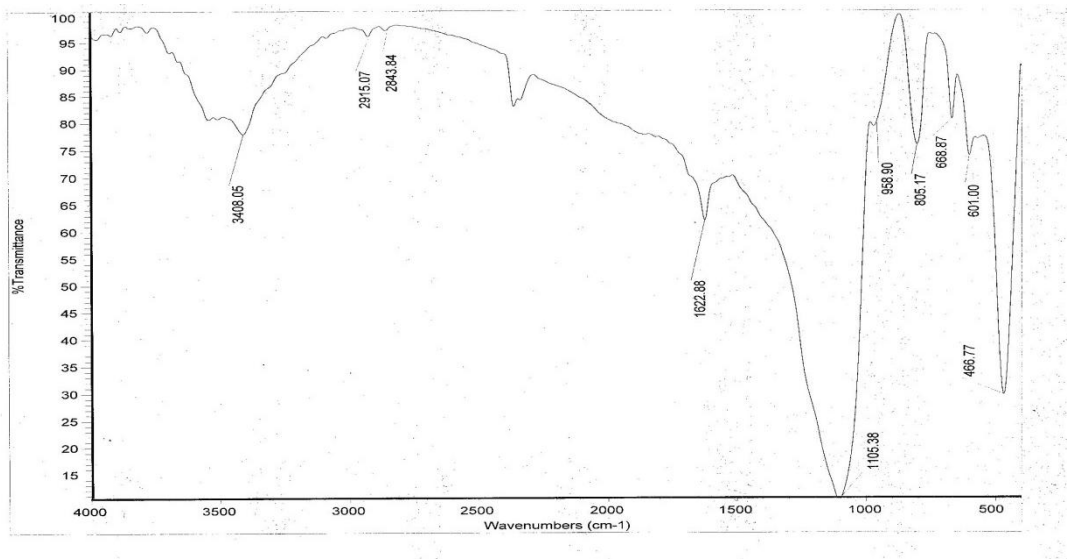

Fig.91 IR spectra for Glycoside

Table :13 FTIR Spectral Data forGlycoside

Wave Number – Glycoside cm^{-1}	**Assignments**
3408	- N-H Stretching
2915 & 2843	-C-H Stretching
1622	C=C stretching
1105	-OH stretching
958 & 805	S-O stretching
668 & 601	N-H Out of plane bending

Fig.91 represent IR spectra for Glycoside, the peak appeared at 3408 cm^{-1} are due to N-H stretching. The peaks appeared at 2915 cm^{-1} and 2843 cm^{-1} due to C-H stretching, the C=C stretching appeared at 1622 cm^{-1}. The peak appeared at 1105cm^{-1} are due to O-H stretching for secondary alcohol. The remaining peaks are C-H plane bending peaks.

NUCLEAR MAGNETIC RESONANCE SPECTRA FOR GLYCOSIDE: (NMR)

The complete assignment of all carbons and protons were achieved by 1D and 2D –NMR experiments for Glycoside are tabulated below.

Table:14 ^{1}H and ^{13}C – spectral data for Glycoside

C	^{1}H	^{13}C	C	^{1}H	^{13}C
1	1.06	47.1	24	2.67	-
2	1.71	29.3	25	2.76	-
3	2.3	76.9	26	8.32	70.0
4	2.3	29.3	27	0.44	-
5	-	134.3	1’	4.51	100.5
6	5.07	121.5	2’	-	76.7
7	1.90	28.4	3’	-	78.4
8	-	-	4’	-	-
9	0.94	47.9	5’	2.88	76.6
10	-	-	6’	3.85	61.3
11	1.48		1’’	-	103.2
12	1.36	-	2’’	3.85	72.4
13	-	-	3’’	-	73.6
14	-	61.3	4’’	-	73.9
15	2.07	28.4	5’’	-	70.6
16	-	121.2	6’’	0.45	-16.5
17	2.57	73.2	1’’’	2.88	101
18	0.70	12.9	2’’’	7.11	71.5
19	0.96	16.5	3’’’	-	72.4
20	2.67	47.2	4’’’	-	74.3
21	0.97		5’’’	-	70.0
22	3.05	93.5	6’’’	0.76	28.44
23	2.55	-		-	-

The ^{1}H-NMR spectrum[5] revealed signals for olefinic proton at δ5.07 two secondary methyl doublets at δ1.00 and 1.30 and two tertiary methyl singlets at δ1.71 and 1.24 assigned respectively to H-6,Me-27.Me-21,Me-18 and Me-19 in a Glycoside.

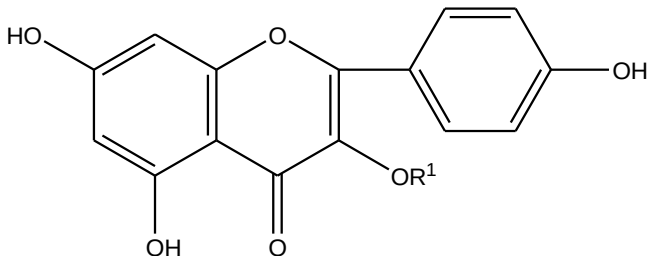

Figure : 92 Structure of Glycoside - Kaempferol 3-O-rutinoside

The ^{1}H and ^{13}C –NMR spectra showed signals for a proton at δ2.30s and quaternary C atom at121.5. The COSY correlations δ2.30 indicated a presence of a proton at C-22. In ^{13}C –NMR spectrum exhibited anomeric proton signals at 100.5 and 104.2 for sugar components. The Glycoside components having a glucose at C-26 (68.7), support a the lack of sugar moiety at C-26.

FOURIER TRANSFORM INFRARED SPECTROSCOPY FOR SAPONIN:

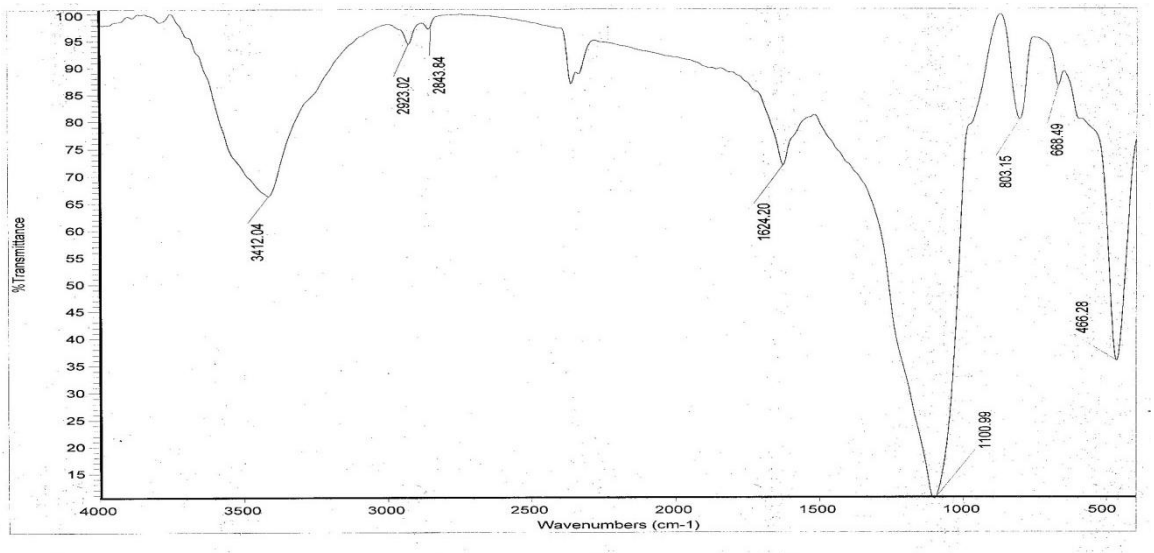

Fig. 93 IR Spectra for Saponin

Table : 15 FTIR Spectral Data for Saponin

Wave Number - Saponin cm^{-1}	**Assignments**
3412	- N-H Stretching
2923 &2843	-C-H Stretching
1624	C=C stretching
1100	-OH stretching
803	S-O stretching
668	N-H Out of plane bending

Fig.93 represent IR spectra for Saponin, the peak appears at 3412 cm^{-1} are due to N-H stretching. The peaks appeared at 2923 cm^{-1} and 2843 cm^{-1} are due to C-H stretching, the C=C stretching appears at 1624 cm^{-1}. The peak appears at 1100cm^{-1} is due to C-O stretching for tertiary alcohol. The remaining peaks are C-H plane bending peaks.

NUCLEAR MAGNETIC RESONANCE SPECTRA FOR SAPONIN: (NMR)

The complete assignment of all carbons and protons achieved[5] by 1D and 2D –NMR experiments for saponins are tabulated below.

Table:16 ^{1}H and ^{13}C – spectral data for Saponin

C	^{1}H	^{13}C	C	^{1}H	^{13}C
1	0.99	38.7	24	2.67	-
2	1.71	30.2	25	2.76	-
3	3.05	77.2	26	8.32	69.8
4	2.25	29.3	27	0.44	-
5	-	145.6	1’	4.51	100.2
6	5.43	122.0	2’	-	77.2
7	1.90	29.0	3’	-	78.8
8	-	-	4’	-	-
9	0.94	47.9	5’	2.88	76.6
10	-	-	6’	3.85	61.1
11	1.48	22.6	1’’	-	105.6
12	1.36	-	2’’	3.85	75.7
13	-	-	3’’	-	75.7
14	-	61.0	4’’	-	-
15	2.07	28.7	5’’	-	69.8
16	-	119.1	6’’	0.45	-
17	2.57	73.3	1’’’	2.88	-
18	0.70	12.9	2’’’	7.11	75.7
19	0.96	22.6	3’’’	-	-
20	2.67	47.1	4’’’	-	-
21	0.97	23.5	5’’’	-	69.8
22	3.05	94.6	6’’’	0.76	-
23	2.55	-		-	-

The ^{1}H-NMR spectrum revealed signals for olefinic proton at δ5.43 two secondary methyl doublets at δ0.94 and 1.36 and two tertiary methyl singlets at δ1.71 and 1.48 assigned respectively to H-6,Me-27.Me-21,Me-18 and Me-19 in a saponin.

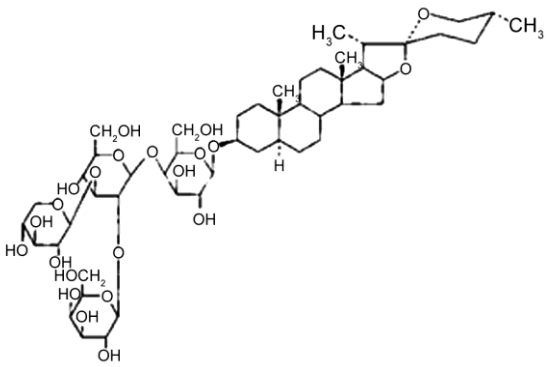

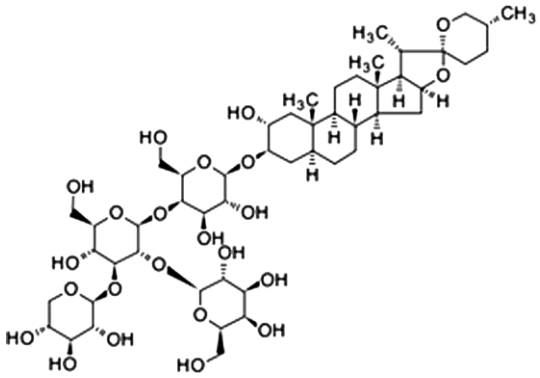

Fig .94 Structure of Desgalactotigonin **Fig.95 Structure of Gitonin**

The ^{1}H and ^{13}C –NMR spectra showed signals for a proton at δ3.85 and quaternary C atom at122.0. The COSY correlations δ2.88 indicated a presence of a proton at C-22. In ^{13}C –NMR spectrum exhibited anomeric proton signals at 100.2 and 105.6 for sugar components. The saponin components having a glucose at C-26 (δ8.32 and 69.8), support a the lack of sugar moiety at C-26.

Gas Chromatograph – Mass Spectra:

The fractions Glycoside and saponin was identified. It was confirmed by GC-MS. The GC-MS for Fractions were shown in Fig.96 The studies on the active principles in the Tribulus terrestris whole plant ethanolic extract by GC-Ms analysis clearly showed the presence of four compounds.[6] The active principles with their rentention time (RT), molecular formula, molecular weight and concentration are presented in below table. Chromatogram GC-MS analysis of the ethanolic extract of Tribulus terrestris. Showed the presence on major peaks and the components corresponding to the peaks were determined as follows, all the four minor components such as tetratricontane (19%), cinnamic acid(10.5%), Oleic acid(23%) and 1,1'-(2-tridecyl-1-3-propanediyl and cyclohexane) (2%).

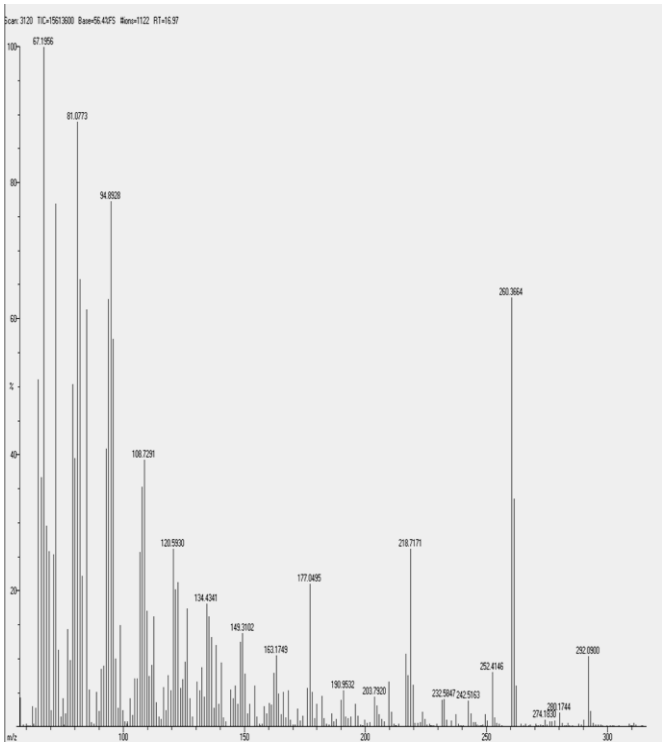

Fig .96 GC-Ms for Tribulus Terrestris

Table:17 GC-MS data of Tribulus Terrestris

S.No.	RT	Name of the Compound	Molecular Formula	MW	Concentration
1.	134.43	Tetratriacontane	$C_{34}H_{70}$	478.92	19
2.	163.17	Cinnamic Acid	$C_9H_8O_2$	148.16 g mol^{-1}	10.5
3.	177.04	Oleic acid	$C_{18}H_{34}O_2$	282.4614 g/mol	23
4.	274.18	1,1'-(2-tridecyl-1-3-propanediyl	$C_{19}H_{37}NO_2$	76.09	2
5.	280.17	Hexadecanal and cyclohexane	C_6H_{12}	84.16	2.5
6.	203.79	dihydro-4-hydroxy	-	-	5
7.	232.58	3 (+)-3,5-di-O-methyl-Zdeoxy-D-ribono-1,4-lactone;			4
8.	242.52	3,4-dianhydro-2-deoxy-a-d-lyxohexopyranose;			25
9.	218.71	Unknown	-	-	24
10.	252.41	Unknown	-	-	9
11.	260.37	Unknown	-	-	65
12.	149.31	Unknown	-	-	13.5

Four of them have a molecular formula are unknown such as dihydro-4-hydroxy (5%), 3(+)-3,5,-di-O-methyl-Zdeoxy-D-ribono-1,4-lactone(4%) and 3,4-dianhydro-2-deoxy-a-dlyxohexopyranose (25%). Many of the unknown compound, among these one of the major component (65%)

Conclusion:

As Pedalium Murex and Tribulus terrestris belong to same family (Zygophyllaceae family) and hence the active phytochemical metabolites in Pedalium Murex and Tribulus terrestris were separated by Thin Layer Chromatography. As the plant tribulus terrestris contains more amounts of saponin and glycoside which is useful for our purpose of study of therapeutic activity of nephrolothesis and urolothesis it was taken for the analysis. The saponins from the plant is separated, analysed and identified for its individual compounds through GC-MS and NMR spectral studies.

REFERENCES:

1. Wang Yan, Kazuidro Ohtani, Ryoh kasai and Kazuo Yamasaki, Pytochemistry Vol42, No.5 pp 1417- 1422 (1966).
2. Wang .Y and Lu,Y.R (1990) Xi Bei Yao Xue Za Zhi 5(4), 14.
3. Vikas Sharma, Mayank Thankur, V.K.Dixi .Journal of Ethnopharmacology 143 (2012), 201 – 206.
4. E.K.Girija,S.Christic Latha,S.NarayanaKalkura,C.Subramanian,P.Ramasamy Crystallization and microhardness of calcium oxalatemonohydrate ,Materials chemistry and Physics 52(1998)253-257.
5. J.Conrad, D.Dinchev, I.Klaiber, S.Mika, I.Kostova and W.Kraus A noval Furostanol Saponin from Tribulus terrestris of Bulgarian origin, Fitoterapia 75 (2004) 117-122.
6. P.Abirami and A.Rajendran “GC-MS Analysis of Tribulus Terrestris” Asian of plant science and research ,2011,1(4):13-16.

CHAPTER – 4

GROWTH OF COD, COM AND HYDROXYAPATITE BY GEL METHOD.

General Introduction:

Crystals play a major role in biology also. Most of the living beings form crystals. There are many minerals present in the dissolved form in the human body.[1] The body fluids contain minerals at various levels of saturation. When the body fluids get supersaturated with minerals, crystallization takes place. These crystals have both beneficial as well as pathological effects on humans. The major beneficial roles of mineralization are the formation of bones and teeth, which consist of oriented micro crystals of hydroxyapatite. Our sense of balance and acceleration is dependent upon small calcite crystal present in the inner ear. The pathological effects result in the crystal deposition disease. Crystal deposition disease may be defined as a pathological condition associated with the presence of crystals which contributes to the tissue damage and cause pain and suffering. Bone disease and caries formation; involve dissolution of hydroxyapatite under acidic condition. Atherosclerosis involves the crystallization of cholesterol and hydroxyapatite in blood vessel walls. Gallstones consist mainly of cholesterol with small quantities of calcium phosphates and calcium carbonates. Clusters of small crystals formed in the urinary systems give rise to urinary calculi which consist primarily of calcium oxalates, calcium phosphates , uric acid, urates etc.,. The three major mineral phases associated with joint disease are monosodium urate monohydrate, calcium pyrophosphate dihydrate and hydroxyapatite. The increasing incidence of crystal deposition disease are the result of a complex sequence of events that give rise to disease through simple mechanical effects such as blocking ducts or by hardening or weakening of the flexible tissues. Crystal deposition occurs in a variety of tissues including kidneys, eyes, thyroid glands and bone marrow.

Carr (1953) and Iwata et al (1986) had shown that the urinary stones grow in a gel like medium, which is probably one of the reasons for the radially striated growth of crystals found in urinary calculi. Achilles et al (1995) suggested that crystallization experiments which are intended to understand urinary stone formation should be carried out in a gelatinous medium rather than in solutions or suspensions. Thus gel growth seems to be an ideal medium to study the crystallization of urinary stone components (biomolecules) as its viscous nature provides simulation of biological fluids in which it grows.

Introduction:

A large number of people in this world are suffering from problems due to urinary stones.[2] There are many areas of high incidence of urinary calculi which include British Isles, Scandinavin Countries, northern Australia, central Europe, northern India and Pakistan and Mediterranean Countries[3]. It has also an economic impact on the society. [4]

Calcium-containing stones are the most common comprising about 75% of all urinary calculi, which may be in the form of pure calcium oxalate (50%) or calcium phosphate (5%) and a mixture of both (45%). Calcium Oxalate stones are found in two different varieties, Calcium Oxalate Monohydrate(COM) or Whewellite, and Calcium Oxalate Dihydrate (COD) or Weddellite.[3] The Chemical compositions of various calcium phosphates are roughly equivalent to that of the inorganic matrix of the human bone and they are found to be the most suitable as implant materials.[5] The major phase found in bone is hydroxyapatite (HA) or basic calcium phosphate(BCP) and the other commonly known phases are octacalcium phosphate, tricalcium phosphate, dicalcium phosphate dihydrate and dicalcium phosphate.[6] Hydroxyapatite has been used to study the hard tissue calcifications such as bone, teeth and many undesirable cases of pathological mineralization of the articular cartilage[7,8], cardiac valves[9,10] and kidney stones[11].

The present investigation deals with the growth of Calcium oxalate and Hydroxyapatite crystals by gel method. The slow and controlled diffusion of nutrients to the growing crystals in the gel medium is very useful to study the

growth and inhibition of Calcium Oxalate crystals in vitro. Hydroxyapatite crystals are grown in the silica gel medium in the Lieseganag rings. These crystals were characterized by various experimental techniques.

Materials and Methods:

The Chemicals used for the experiments were of AR grade. Single and double diffusion growth techniques were employed for the growth of calcium oxalate monohydrate crystals.

In a single diffusion method, gel was set by mixing sodium meta silicate solution of density 1.03gcm^{-3} was adjusted to a pH of 6.3 by adding 5% acetic acid[12]. Calcium chloride, one of the reactants was incorporated inside the gel. After the gel was set, 0.5 M oxalic acid solution was slowly added over the gel as the supernated solution and the experiments were conducted at room temperature. Within a day, a white column of tiny crystals of microscopic sixes were formed. The depth of the column was found to increase with increase in time and there was no change in the size of the crystals.

The double diffusion gel growth technique was used to grow calcium oxalate crystals. The crystallization apparatus used was glass U-tubes with 2.5cm internal diameter, 16mm limb lengths and the separation between two limbs approximately 12cm. The nucleation of COM crystals was due to the calcium chloride and oxalic acid in the silica hydro-gel medium. The neutral gel was prepared by hydrated sodium meta-silicate solution of specific gravity 1.03gcm^{-3} was adjusted to a pH of 6.3 by adding 5% acetic acid. It was then allowed to gel in U-tubes. It took about 48h to gel. After gelling, equal volume of 1M Calcium chloride solution was added to one limb of the U-tube and 0.5M Oxalic acid was added to the other limb. The tubes were kept at room temperature. In 24h, a disc of tiny single and twinned prismatic crystals appeared exactly at the centre of the gel column and in due course, the thickness of the disc increased. In some tubes the number of crystals formed in the disc was found to be high and in some other tubes it was found to be less.

CALCIUM OXALATE CRYSTALLIZATION-INITIAL PROCESS

Fig.97 Single Diffusion - Calcium Oxalate Crystals

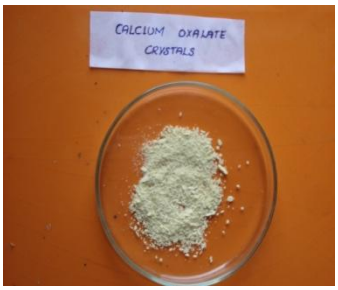

Fig. 98 Calcium Oxalate Crystals

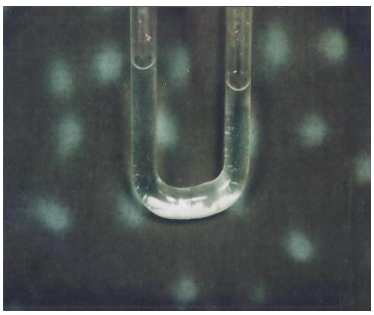

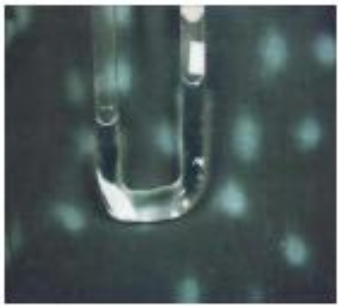

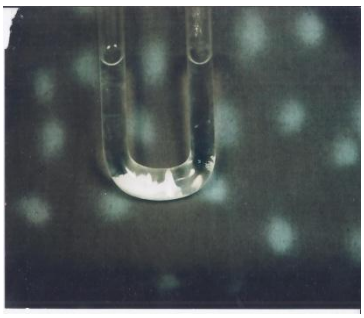

Fig.99 Double Diffusion – Calcium Oxalate

Table. 18 Growth of Calcium Oxalate Crystals at different pH and different concentration.

S.No	Volume of Oxalic acid (ml)	Volume of Calcium Chloride (ml)	pH	Duration of Crystal formed	Quality and Nature of the Crystal
1.	0.5	0.5	5.5	24hr.	Many tiny crystals
			6.0	24hr.	Many tiny crystals
			6.3	24hr.	Large size crystals
			6.5	24hr.	White column of tiny crystals
			6.7	24hr.	White column of tiny crystals
			7.0	24hr.	White column of tiny crystals
2.	1.0	1.0	5.5	24hr.	Many tiny crystals
			6.0	24hr.	Many tiny crystals
			6.3	24hr.	Large size crystals
			6.5	24hr.	White column of tiny crystals
			6.7	24hr.	White column of tiny crystals
			7.0	24hr.	White column of tiny crystals
3.	1.5	1.5	5.5	24hr.	Many tiny crystals
			6.0	24hr.	Many tiny crystals
			6.3	24hr.	Large size crystals
			6.5	24hr.	White column of tiny crystals
			6.7	24hr.	White column of tiny crystals
			7.0	24hr.	White column of tiny crystals

4.	2.0	2.0.	5.5	24hr.	Many tiny crystals
			6.0	24hr.	Many tiny crystals
			6.3	24hr.	Large size crystals
			6.5	24hr.	White column of tiny crystals
			6.7	24hr.	White column of tiny crystals
			7.0	24hr.	White column of tiny crystals
5.	2.5	2.5	5.5	24hr.	Many tiny crystals
			6.0	24hr.	Many tiny crystals
			6.3	24hr.	Large size crystals
			6.5	24hr.	White column of tiny crystals
			6.7	24hr.	White column of tiny crystals
			7.0	24hr.	White column of tiny crystals
6.	3.0	3.0	5.5	24hr.	Many tiny crystals
			6.0	24hr.	Many tiny crystals
			6.3	24hr.	Large size crystals
			6.5	24hr.	White column of tiny crystals
			5.7	24hr.	White column of tiny crystals
			7.0	24hr.	White column of tiny crystals

In hydroxyapatite crystals were grown by single diffusion technique.[13] Sodium Meta silicate solution of specific gravity 1.03 was acidified by 1N orthophosphoric acid so that the pH of the mixture could be set within 6-6.5. This mixture was transferred into different test tubes and allowed to set into the gel form. After setting the gel, 1M Calcium chloride solution was poured gently on

the set gel. Good quality and very small hydroxyapatite crystals were grown in the form of Liesegang ring. The crystals in the Liesegang rings are of micrometer size and hence are not observasble in the photograph as separate crystals. In a spencer method we can also prepare the hydroxyapatite crystals. These experiments were repeated for different densities 1.03,1.04 and 1.05 and pH 5.5 -7.

Fig.100 Double Diffusion – Hydroxyapatite.

Table. 19 Growth of Hydroxy Apatite Crystals at different pH and different concentration.

S.No	Volume of Oxalic acid (ml)	Volume of o-Phosphoric Acid (ml)	pH	Duration of Crystal formed	Quality and Nature of the Crystal
1.	0.5	5	5.5	24hr.	Indistinguishable Liesegang rings are formed.
		5.8	6.0	24hr.	Indistinguishable Liesegang rings are formed.
		6.5	6.3	24hr.	Distinguishable Liesegang rings are appeared
		7.2	6.5	24hr.	Coagulant appearance
		7.8	6.7	24hr.	Coagulant appearance
		8.3	7.0	24hr.	Coagulant appearance

2.	1.0	5	5.5	24hr.	Indistinguishable Liesegang rings are formed.
		5.8	6.0	24hr.	Indistinguishable Liesegang rings are formed.
		6.5	6.3	24hr.	Distinguishable Liesegang rings are appeared
		7.2	6.5	24hr.	Coagulant appearance
		7.8	6.7	24hr.	Coagulant appearance
		8.3	7.0	24hr.	Coagulant appearance
3.	1.5	5	5.5	24hr.	Indistinguishable Liesegang rings are formed.
		5.8	6.0	24hr.	Indistinguishable Liesegang rings are formed.
		6.5	6.3	24hr.	Distinguishable Liesegang rings are appeared
		7.2	6.5	24hr.	Coagulant appearance
		7.8	6.7	24hr.	Coagulant appearance
		8.3	7.0	24hr.	Coagulant appearance
4.	2.0	5	5.5	24hr.	Indistinguishable Liesegang rings are formed.
		5.8	6.0	24hr.	Indistinguishable Liesegang rings are formed.
		6.5	6.3	24hr.	Distinguishable Liesegang rings are appeared
		7.2	6.5	24hr.	Coagulant appearance
		7.8	6.7	24hr.	Coagulant appearance
		8.3	7.0	24hr.	Coagulant appearance

5.	2.5	5	5.5	24hr.	Indistinguishable Liesegang rings are formed.
		5.8	6.0	24hr.	Indistinguishable Liesegang rings are formed.
		6.5	6.3	24hr.	Distinguishable Liesegang rings are appeared
		7.2	6.5	24hr.	Coagulant appearance
		7.8	6.7	24hr.	Coagulant appearance
		8.3	7.0	24hr.	Coagulant appearance
6.	3.0	5	5.5	24hr.	Indistinguishable Liesegang rings are formed.
		5.8	6.0	24hr.	Indistinguishable Liesegang rings are formed.
		6.5	6.3	24hr.	Distinguishable Liesegang rings are appeared
		7.2	6.5	24hr.	Coagulant appearance
		7.8	5.7	24hr.	Coagulant appearance
		8.3	7.0	24hr.	Coagulant appearance

Calcium oxalate crystals were obtained for the conditions of gel density 1.03 with pH 6.3. The hydroxyapatite crystals were appeared as Liesegang rings in silica hydrogel density 1.06 with pH 6.3. The harvested crystals are subjected to FT-IR, XRD and TGA.

Result and Discussion:

In order to confirm the grown crystals to be Calcium oxalate monohydrate [12], Dihydrate and Hydroxyapatite, the crystals were characterized by Fourier Transform Infra-Red Spectroscopy and X-Ray Diffraction. Thermogravimetric analyses can be carried out monohydrate crystals.

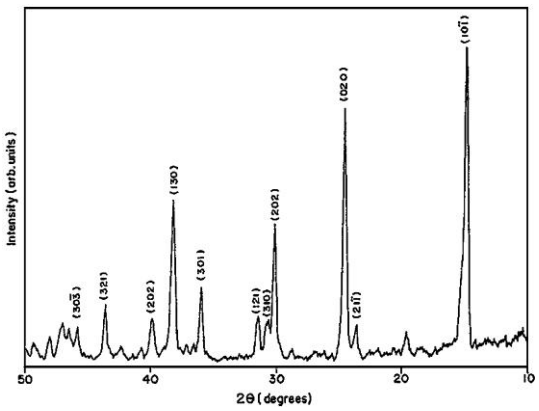

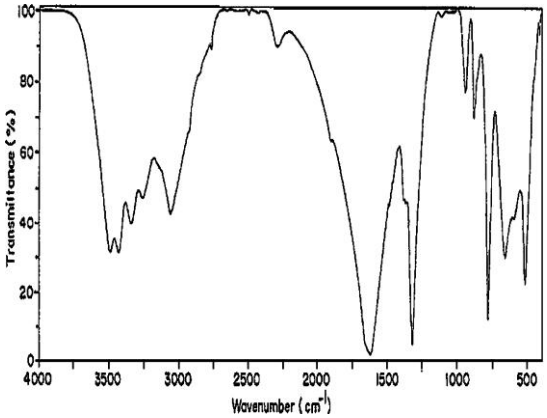

Fig.101 XRD for COM **Fig.102 IR for COM**

A bruker IFS 66v FTIR spectrometer was used to record the IR spectrum using KBr pellets and the spectrum is shown Fig.102. The peak at 519cm^{-1} arised due to o-c-o in plane bending. The metal – carboxylate strectch appears at 1316cm^{-1}. The water molecules coordinated with the calcium oxalate molecules produce characteristic peaks corresponding to the bending modes at 1621cm^{-1}. The peaks for asymmetric and symmetric stretch of the coordinate water molecule is shown by the broad spectrum of peaks above 3000cm^{-1}.

The XRD pattern of the grown crystal was obtained from a diffractometer[14] instrument using CuKα radiation was shown in Fig.101. The following diffraction peaks (2θ) 14.95, 24. 39,30. 12 and 38.13 which can be correlated to the indices (101),(020), (202) and (130) of Calcium Oxalate Monohydrate phase.

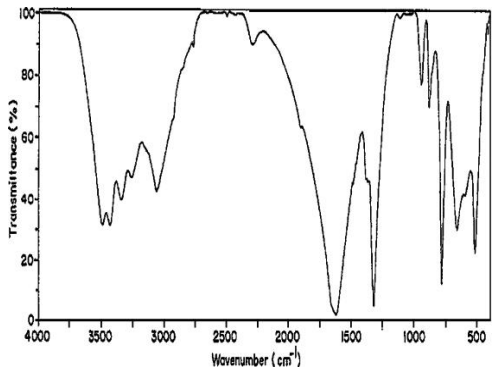

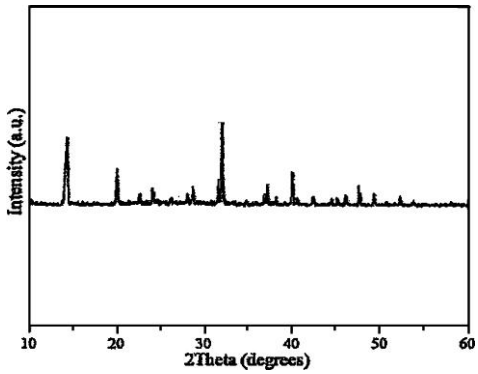

Fig.103 IR for COD **Fig.104 XRD for COD**

A bruker IFS 66v FTIR spectrometer was used to record the IR spectrum using KBr pellets and the spectrum is shown Fig.103. The two peaks are at 915 and 615cm^{-1} arised due to o-c-o in plane bending. The metal – carboxylate strectch appears at 1318cm^{-1}. The water molecules coordinated with the calcium oxalate molecules produce characteristic peaks corresponding to the bending modes at 1652cm^{-1}.

The XRD pattern of the grown crystal was obtained from a diffractometer instrument using CuKα radiation was shown in Fig.104. The following diffraction peaks (2θ) 14.26, 20.01, 24.15, 32.17, 37.21 and 40.00 which can be correlated to the indices (200),(211), (002), (411), (103) and (213) of Calcium Oxalate dihydrate phase.

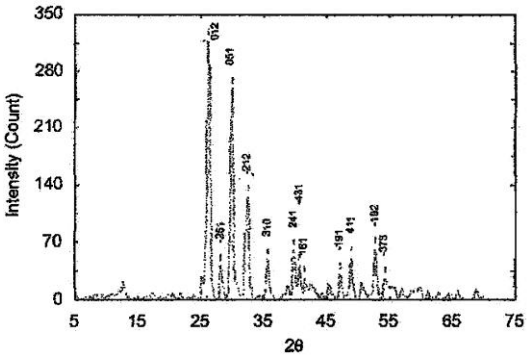

Fig.105 XRD for HA

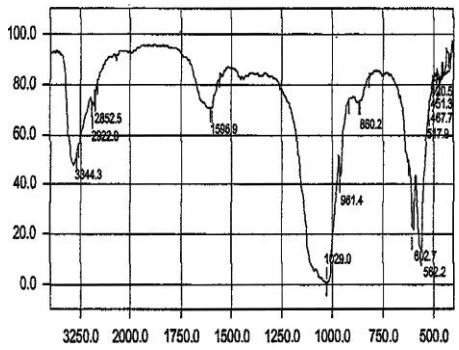

Fig.106 IR for HA

The XRD pattern of the grown crystal was obtained from a diffractometer instrument using CuKα radiation was shown in Fig.105. The following diffraction peaks (2θ) 25.00, 27.13, 32.19, 34.25,35.09, 47.87 and 54.00 which can be correlated to the indices (012),(251),(051), (212),(310),(191) and (102) of Hydroxyapatite phase.

A bruker IFS 66v FTIR spectrometer was used to record the IR spectrum using KBr pellets and the spectrum is shown Fig.106. The absorptions occurring at 3344.3 and 1596.9cm^{-1} are due to O-H stretching and O-H plane bending vibrations. The PO_4^{3-} bands were appeared at 467cm^{-1},562.2 cm^{-1}, 602.7 cm^{-1} , 961.4 cm^{-1} , and 1029 cm^{-1}.

Conclusions:

The Oxalate crystal are very good yield at 6.3 pH with density 1.03 and Phosphate rings density 1.06 with 6.5 pH at low concentration. The grown crystals are characterized found to be pure and these crystals used for dissolution studies.

REFERENCES:

1. P.Sanathana Raghavan, P.Ramasamy- Crystal Growth Processes and Methods.
2. V.S.Joshi, B.B.Parekh,M.J.Joshi and A.B.Vaidya " Herbal Extracts of Tribulus terrestris and Bergenia ligulata inhibit growth of calcium oxalate monohydrate crystals in vitro" J.of crystal growth 275 (2005) 1403 -1408.
3. M.D. Menon, BG.Parulkar, G.W. Drach, Campbell's Urology, seventh ed., W.B. Saunders company, New York, 1988.
4. J.Y.Clerk, I. M.Thomson, S.M.Optenberg, J.Urol.154 (1995) 2020-2040.
5. J.C.Merry,I.R.Gibson,S.M.Best,W.Bonfield,J.Mater.Sci.Mater,Med.9 (1998)779.
6. L.C.Clapham, R.J.C.McLeam, J.C.Nickel,J.Downey,J.Crystal Growth 104 (1990) 475.
7. G.V.Gordon,T.Villaneva,H.R.Shumacher,V.J.Gohel,rheumatology11 (1984)861.
8. A.L.Boskey,P.G.Bullogh,Scanning Electron Microsc,28 (1984)511.
9. F.J.SchoenR.J.Levy, Cardiol. Clin 2 (1984)713.
10. M.Valente, U.Bortloli, G.Thiene, Am.J.Patholo.119 (1985) 12.
11. G.H.Nancollas, J.Crystal Growth 42 (1984) 185.
12. E.K.Girija,S.Christic Latha,S.Narayanan Kalkura, C.Subramanian, P.Ramasamy-J. Material Chemistry and Physics 52 (1998) 253-257.
13. Bharat Parekh, Mihir Joshi, Ashok Vaidhya , Journal of Crystal Growth 310 (2008) 1749-1753.

Chapter – 5

Dissolution of Kidney Stones

Introduction:

Humankind is known to be affected by urinary stone disease, which was first noted in Egyptian mummies dated to 4800 BC.[1] Hippocrates in the 4th century BC noted renal stones together with a renal abcess and wrote in the Hippocratic Oath, " I will not cut for stone,'' although he was not a urologist.[1] The physician Galen (129 to 200CE) also mentions the use of Judaean stone to treat bladder stones and the Roman Emperor Septimius Severus (193 to 211CE) used to visit the Hissarya baths in Bulgaria often because of his renal stones.[2]

Urinary stone disease has always been a common disease. Currently urinary stone formation affects 10% to 12% of the population in industrialized countries and the peak incidence seems to be at ages 20 to 40 years.[3] Although historical treatment modalities were not so successful, many milestones have passed since that time to the current modern technology used to treat urological disease. Until the 1980s urinary stone disease was a major health problem with a significant percent of patients undergoing severe surgical procedures for disease, in contrast to Hippocrates. Because of the morbidity and mortality of these surgical procedures, some oral drugs are used to treat this disease but adverse effects compromise their long- term consumption. On the other hand, some herbal remedies have long been used to treat urinary stone disease, although scientific principles have been lacking. Today with the understanding of many path physiological features underlying urinary stone disease and the mechanism of herbal remedies that can have a role in the formation and treatment of urinary stones phytotherapy might be an alternative treatment with an effective, safe and culturally acceptable nature.

Many inhibitors on the growth of Calcium oxalate monohydrate (COM), Calcium oxalate dihydrate (COD) and hydroxy apatites (HA) were studied. Several authors have attempted to grow these crystals by gel technique. The slow and controlled diffusion of nutrients to the growing crystals in the gel medium is

very useful to study the growth and inhibition of calcium oxalate crystals in vitro. This also helps to develop inhibition conditions, which can be extended to urinary calculi. In the present investigation, COM, COD and HA crystals were grown by the gel growth technique. The Phytochemical separation of Tribulus terrestris gave Saponin, Flavonoids, Glycosides, Tannin and Phenolic compounds. Hence the effect of the above metabolites on the growth of COM, COD and Hydroxy apatite by gel method was investigated. By studying the effect suggestion in the Nephrolthesis and Urolothesis may be formulated.

Materials and Methods:

The double diffusion gel growth technique was used to grow COM and COD crystals. The growth of hydroxy apatite crystals was carried out by using single diffusion gel growth technique in silica hydro gel method. The grown crystals were used for dissolution studies. As the plant tribulus terrestris contains Saponin, Glycoside, Flavonoid, Tannin and Phenolic compound which is useful for our purpose of study of therapeutic activity of nephrolothesis and urolothesis it was taken for the analysis and dissolution studies.

Results and Discussion:

There has been a long-standing quest for potent inhibitors of calcium oxalate growth. Many components have been identified as inhibitors of calcium oxalate growth, for example, tartrates in natural and artificial urine media, some amine acids, citrate and polyhydroxycarboxylic acids.

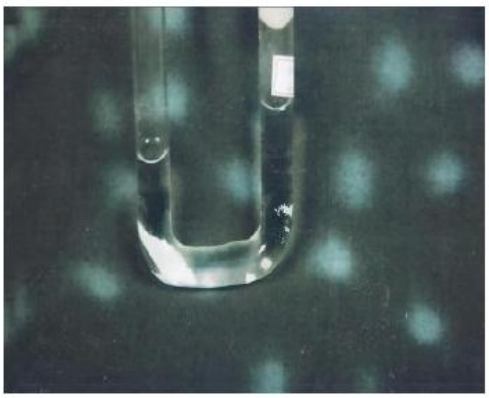

Fig.107 Growth of Oxalate Crystal

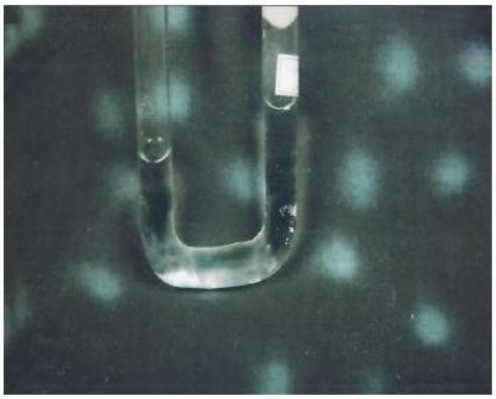

Fig. 108 Dissolution of oxalate crystal Saponin

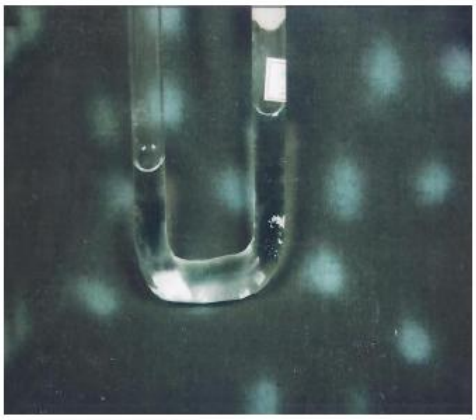

Fig. 109 Dissolution of oxalate crystal Glycoside

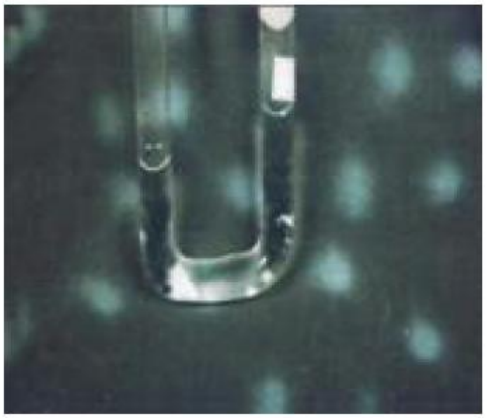

Fig.110 Dissolution of oxalate Crystal – Phenolic

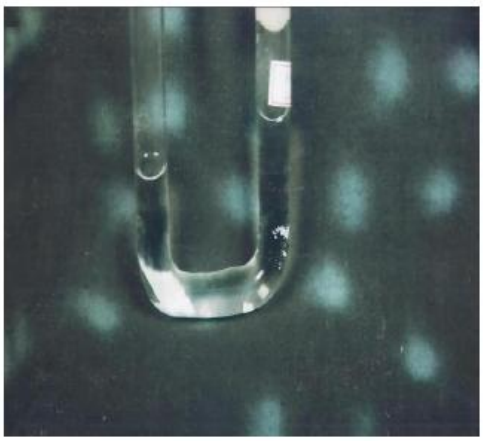

Fig. 111 Dissolution of oxalate Crystal - Tannin

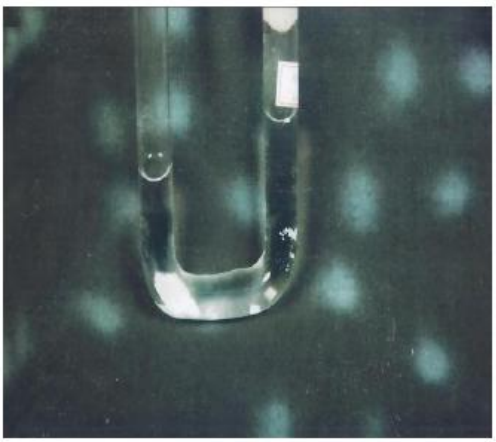

Fig.112 Dissolution of oxalate Crystal – Flavonid

The various fractions in the plant extract such that Saponin, Glycoside, Phenol, Tannin and Flavonoid are isolated. These fractions are added 2ml of 1% solution in the grown oxalate crystal. The average apparent length of grown crystals decreases when solution b,c,d,e and f are added as supernatant solution are shown in figure. 108 to112. The inhibition studies of oxalate crystals are tabulated in table.20

Table:20 Dissolution of Oxalate Crystal.

Time (Hrs)	**Growth of Oxalate crystal (a)**	**Saponin (b)**	**Glycoside(c)**	**Phenol (d)**	**Tannin (e)**	**Flavonid(f)**
0	-	-	-	-	-	-
20	0.46	0.13	0.15	0.16	0.2	0.29
40	0.5	0.18	0.23	0.29	0.35	0.37
60	0.55	0.27	0.3	0.34	0.39	0.42
80	0.6	0.35	0.39	0.4	0.46	0.49
100	0.6	0.39	0.43	0.45	0.52	0.55
120	0.65	0.45	0.49	0.52	0.59	0.62
140	0.65	0.52	0.54	0.59	0.63	0.65
160	0.7	0.55	0.6	0.63	0.67	0.7
180	0.75	0.6	0.65	0.68	0.7.	0.72
200	0.75	0.6	0.7	0.75	0.79	0.75
220	0.8	0.6	0.7	0.75	0.79	0.8
240	0.82	0.6	0.7	0.75	0.79	0.8
260	0.87	0.6	0.7	0.75	0.79	0.8

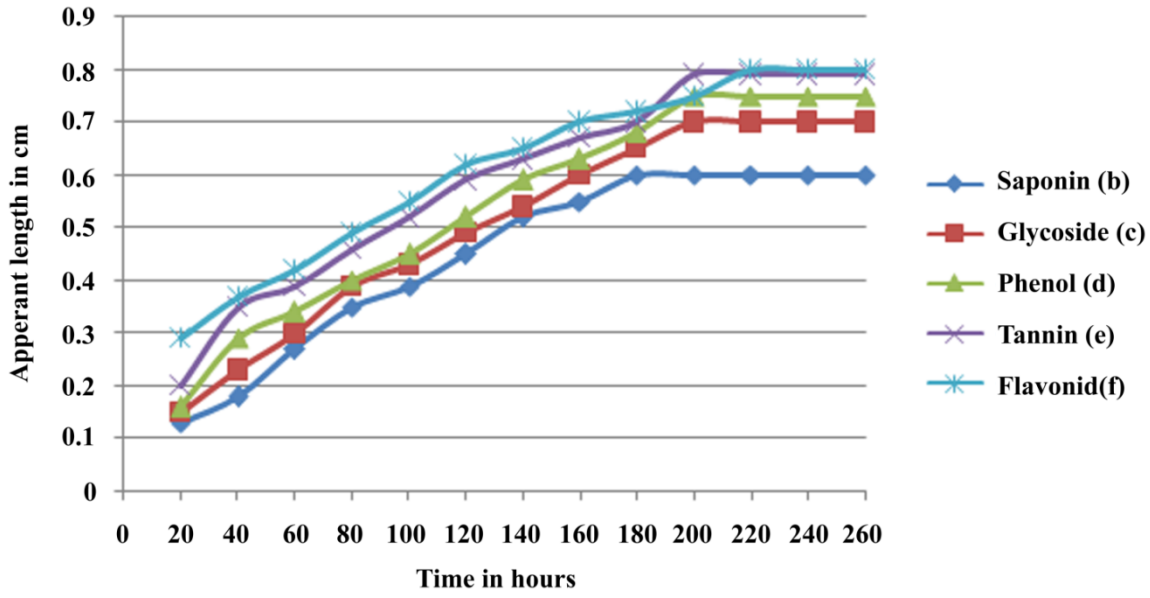

Table. 21 Dissolution of Hydroxyapatite Crystal.

Time (Hrs)	Growth of Hydroxy Apatite crystal (a)	Saponin (b)	Glycoside(c)	Phenol (d)	Tannin (e)	Flavonid(f)
0	-	-	-	-	-	-
20	1.9	1.5	0.9	0.6	0.6	0.6
40	2.5	1.9	1.4	0.9	1.2	1.5
60	2.5	2.4	1.9	1.5	1.9	2.2
80	3.2	2.9	2.2	2.3	2.4	2.9
100	3.5	3.2	2.7	2.9	3.2	3.5
120	3.9	3.7	2.9	3.3	3.7	3.9
140	4.2	3.9	3.4	3.9	4.2	4.5
160	4.9	4.3	3.7	4.4	4.6	4.9
180	5.2	4.7	3.9	4.8	5.2	5.5
200	5.2	4.7	4.2	5.4	5.7	5.9
220	5.2	4.7	4.9	5.9	6.2	6.5
240	5.2	4.7	4.9	5.9	6.2	6.5
260	5.2	4.7	4.9	5.9	6.2	6.5

Figure:113 Leisegang Ring

Figure: 114 Dissolution of Leisegang Ring-Saponin

Figure:115 Dissolution of Leisegang Ring Glycoside

Figure: 116 Dissolution of Leisegang Ring-Phenolic

Figure:117 Dissolution of Leisegang Ring Tannin

Figure: 118 Dissolution of Leisegang Ring-Flavonid

The hydroxyapatite crystals are formed a Liesegang rings. All the fractions are added 2ml of 1% solution in the grown Liesegang ring. The average apparent length of rings decreases when solution b,c,d,e and f are added as supernatant solution are shown in figure.114 to 118. The inhibition studies of Hydroxy apatite crystals are tabulated in table.21.

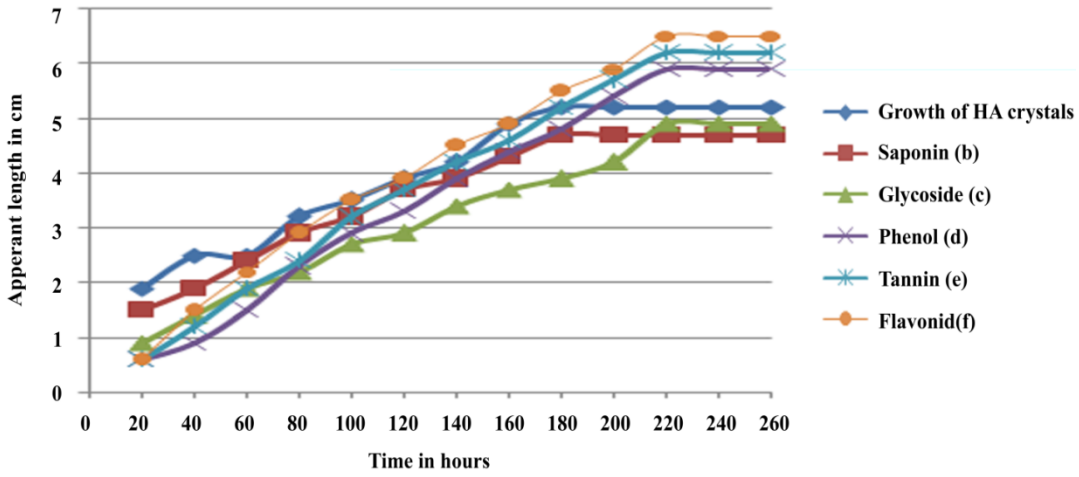

The grown Oxalate and Hydroxy apatite crystals undergoes inhibition by the addition of the metabolites such as Saponin, Glycoside, Phenol, Tannin and Flavonoid. The average apparent length of grown crystals decreases due to the addition of the metabolites are shown as b, c,d,e and f extracted and separated from the extract of the plant tribulus terrestris are added. The apparent length of the crystal decreases to the maximum extract in saponin addition compared to other metabolites the order of dissolution is found to be Saponin > Glycoside> Phenolic Compound> Tannin >Flavonoid. .

The effect of Ayurvedic drug Sveta Parpati with Tribulus terrestris in the management of Urolithiasis is reported[5]. The major constituents of tribulus terrestris include steroidal saponin.e.g., terrestrosins- A,B,C,D and E, Desgalactotigonin, F-gitonin, desglucolanatigonin, gitonin and the minor constituents also include alkaloids common phytosterols, viz, β-sitosterol, stigmasterol.[6] These biomolecules play an important role in the inhibition of COM & HA crystals. This in vitro study provides useful information for in vivo studies as well as prevention and inhibition stones in human body. The saponin fractions

contain many micro biomolecules and the roles of these molecules are very important in the growth and inhibition study.

Conclusion:

The order of dissolution is found to be Saponin > Glycoside> Phenolic Compound> Tannin >Flavonid. Hence Saponin was taken and the individual composition was identified by spectral studies. The metabolite saponin present in Tribulus terrestris is having promising effect in the treatment of both Nephrolothesis and Urolothesis.

References:

1. Clendening.L: Source Book of Medical History,New York:Dove Publications,pp.14-18,1942.
2. Lev,E and Dolev,E: Use of natural substances in the treatment of renal stones and other urinary disorders in the Medieval Levant.Am J Nephrol, 22: 172, 2002
3. Pak,C.Y.C.: Citrate and renal ca;culi.Miner Electrol Metab,13:257,1987.
4. B.N.Sand,A.Kumar,N.Kumar,JRAR 32 (1993) 98-114.
5. K.K.Purashothaman, S. Chandraseknaran,K.Balkrishna, J.Res.Indian Med. Yogo and Homeopathy 11 (1976)121.

Chapter – VI

Summary and Conclusion

The epidemiology studies throw light on the occurrence symptoms and also the other factors concerning age, sex, geographical region and the food habits of the people. Forty six stones were collected in Stanly medical college, Chennai and SP Hospital, Thanjavur along with questionnaire to analyze all the above factors. Most of the samples were very small in size, powdered in nature and ten samples which were of moderate size have been taken for characterization studies.

The compositions of the stones are determined by various analytical techniques such as Qualitative analysis, UV, FT-IR, XRD, Optical Microscopic studies, Differential Scanning Calorimetry (DSC), Scanning Electron Microscopic (SEM), Elemental analysis (ICP) and EDAX – SEM Analysis. In UV spectroscopy, the λ_{max} value corresponding to 199nm which is due to $\sigma\sigma^*$ transition. The λ_{max} value lower than 250nm corresponds to Oxalate stones and above 250nm corresponds to Phosphate stones. The IR spectroscopy study also shows increase in hydrogen bonding nature of four oxygen present in phosphate rather than oxalate contains two oxygen. Combination of SEM and EDAX always aids the morphology and the chemical constituents in a predictable manner. Here all the samples predicted chemical composition is further supported and confirmed by SEM and EDAX analysis. The presence of other elements like C,Na,Mg,Cl,P,Si and O are found in traces which may be due to food intake and secretion in urine and deposition along with the kidney stones. The DSC analysis reveals that the kidney stones emit high heat energy and denotes the presence of Inorganic phosphate ion in the crystals which is a more stable compound to oxalate moiety.

In Phytochemical studies, Tribulus terrestris is a herbal supplement and an annual herb of worldwide supplement. All the parts of the plant are used as medicine. The herbs were separated and purified by Thin layer Chromatography. The saponins and glycoside from the palnt are separated, analysed and identified for their individual compounds through GC-MS and NMR spectral studies. .

Most of the samples were very smaller in size and powdered in nature. The urinary stones grow in a gel like medium, which is probably one of the reasons for the radically striated growth of crystals found in urinary calculi. So, we chose to grow the oxalate and phosphate crystals in a double diffusion and single diffusion gel growth method in our laboratory. The grown crystals are characterized and all the parameters are correlated with the available analysis of urinary stone and found to be more or less identical and these crystals were used for dissolution studies.

The inhibition of growth of COM and HA crystals by 2ml of 1% solution of all the metabolites in tribulus terrestris. A highly significant correlation of data was shown in the statistical analysis. The order of dissolution is found to be saponin>glycoside>tannin>phenols. The maximum inhibition of COM crystals growth followed by the aqueous extract of saponin in Tribulus terrestris in vitro conditions. This study is useful to formulate the necessary dosages to prevent and cure Nephrolothesis and Urolothesis.

SUGGESTIONS FOR FURTHER STUDIES:

1. By adding different types of Saponin, the dissolution rate are to be investigated and suitable drug formulation can be made.

2. After suggesting that the metabolites supporting evidence with respect to urine rate flow technique in the Nephrolithasis and Urolithiasis can be diagonised.

3. The presence of same type of saponin and glycoside in other type of plants can be investigated by trial and error method.

Paper Publication